博士学位論文

Study on the corrective abrasive finishing of workpiece surface using magnetic abrasive finishing process

磁気研磨法による工作物表面の修正研磨に関する研究

指導教員:　鄒　艶華

宇都宮大学大学院 工学研究科

博士後期課程　システム創成工学専攻

張　玉龍

2022 年 2 月

CONTENTS

SUMMARY

This thesis discusses the corrective abrasive finishing of workpiece surface using magnetic abrasive finishing process. The overview of each chapter of the paper is as follows:

In chapter 1, the research background and some research on MAF process are introduced. In addition, the research purpose of this article is explained and the content of each chapter is summarized.

In chapter 2, first introduced the processing principle of traditional MAF. Secondly, that is the processing principle of the corrective abrasive finishing. In addition, the method and steps of data processing are also given out.

In chapter 3, the experimental setup is described in detail. First, the block diagram of the system is described. The connection mode and control mode of the electrical control part are introduced. Secondly, the magnetic field analysis software used to simulate the magnetic field distribution of magnetic pole is introduced. Through the software simulation, the reference data for analyzing the magnetic pole design and experimental results are provided. The magnetic field strength measuring device is introduced. Through the comparison between the measurement results and the simulation results, it is helpful to analyze the experimental results. The pressure measuring device is introduced and the pressure on the workpiece during magnetic brush movement was measured. Finally, the parameters of magnetic particles and abrasive particles used in this study are introduced.

In chapter 4, the investigation on correction MAF with 23 mm magnetic pole application of SUS304 steel plate is carried out to prove the feasibility of this method. First, the magnetic field distribution near the processing

area is simulated and measured. Secondly, the experiment at a fixed position is carried out, the section curve of the trace after finishing is measured, and the average value of the height change of the working surface after finishing per unit time is calculated. Thirdly, SUS304 stainless steel plate is used for previous processing and correction processing experiments, and the experimental results are measured. Fourthly, in order to prove the feasibility and effectiveness of modified finishing, the experimental results are analyzed and discussed. The experimental results show that the finishing of shape correction can be realized. However, the effect of the outer edge of the processing range is obvious, and the middle part has no effect.

In chapter 5, the investigation on correction MAF with 1 mm magnetic pole for application of aluminum alloy plate is discussed. Firstly, according to the different shapes of the magnetic pole, the magnetic field distribution of the front end of the magnetic pole is analyzed by the magnetic field analysis software of "magnet 7", and the magnetic field distribution of the front end of the magnetic pole is studied. According to the simulation results, a magnetic pole with a front diameter of 1mm is designed. The magnetic field distribution at the front end of the 1mm magnetic pole and the pressure distribution of the magnetic brush were measured and recorded. Then, the proportion of abrasive and finishing gap are tested, and the appropriate magnetic brush is selected. Thirdly, the previous finishing and correction finishing experiments are carried out with 5052 aluminum alloy plate, and the experimental results are measured. Fourthly, the experimental results show that the modified finishing method is feasible and effective.

In chapter 6, the application of correction MAF with 1mm magnetic pole

to plane surface is discussed when the workpiece to the aluminum alloy plate. First design the processing trajectory and program the control circuit board. Then carry out processing experiments according to different moving steps. The influence of the translation step length on the plane quality and processing efficiency is discussed, and the optimal processing method is obtained. Third, it is compared with the experimental results of conventional processing. The experimental results are analyzed and discussed from different attitudes. It is proved that this method can correct the workpiece in the plane range.

In chapter 7, the main conclusions of this thesis are summarized.

NOMENCLATURE

Symbols	Explanation
F_x	Magnetic force at x direction.
F_y	Magnetic force at y direction.
H	Magnetic field intensity.
$H_0(S_i)$	Initial height at position S_i.
$H(S_i)$	Initial height at position S_i after filtered.
$h(x, y)$	Removal depth at (x, y).
$h(S_i)$	Removal height sequence.
h_0	Height of The target finishing line.
k	Removal factor.
L	Chord length of the magnetic brush passing through a point.
M_R	Amount of material removal.
m	Number of data to be averaged filtered.
n	Number of loops for processing.
$P(x, y)$	Pressure at The point (x, y)
ΔS	Displacement change.
S_i	Abscissa of The i-th sampling point.
t	The finishing time.
t_1	Finishing time for any point in a single processing.
$\Delta t(S_i)$	Finishing time in segment S_i.
V	Velocity of the tool relative to the workpiece.
$V(x, y)$	Velocity of the tool relative to the workpiece at point (x, y).
$v(S_i)$	Feed speed at each segment.
V_p	Volume of magnetic particle.
η	Finishing efficiency, .
μ_0	Magnetic permeability of vacuum.
χ	Susceptibility of magnetic particles.

Chapter I Introduction

1.1 Research background

Magnetic abrasive finishing (MAF) is an unconventional precision finishing process that utilizes magnetic abrasives for finishing process [1]. Magnetic abrasives are mainly composed of ferromagnetic particles and abrasive particles. Under the action of the magnetic field [2], the magnetic particles form a flexible magnetic abrasive brush (FMAB) along the direction of the magnetic force lines [3, 4]. MAF is a precision finishing technology that achieves material removal through the relative motion of the magnetic brush and the workpiece. By using the formed flexible magnetic brush as a finishing tool, various cylindrical, inner surfaces, outer surface, and free-form workpieces can be finished [5]. The MAF process has attracted extensive attention of many researchers due to its technical advantages of gentle tool and self-adaptability. Early researchers developed numerous experimental setups based on the MAF process, realized the finishing of different workpieces, explored the mechanism of the process, and studied the basic characteristics in detail. Through continuous development, this process has been widely used in aerospace, medical, electronics and molds [6].

The researchers designed different experimental devices using magnetic abrasive finishing technology to achieve the purpose of processing different workpieces, and analyzed the processing mechanism. In Figure 1.1, the current development status and main research results of magnetic abrasive finishing technology are shown.

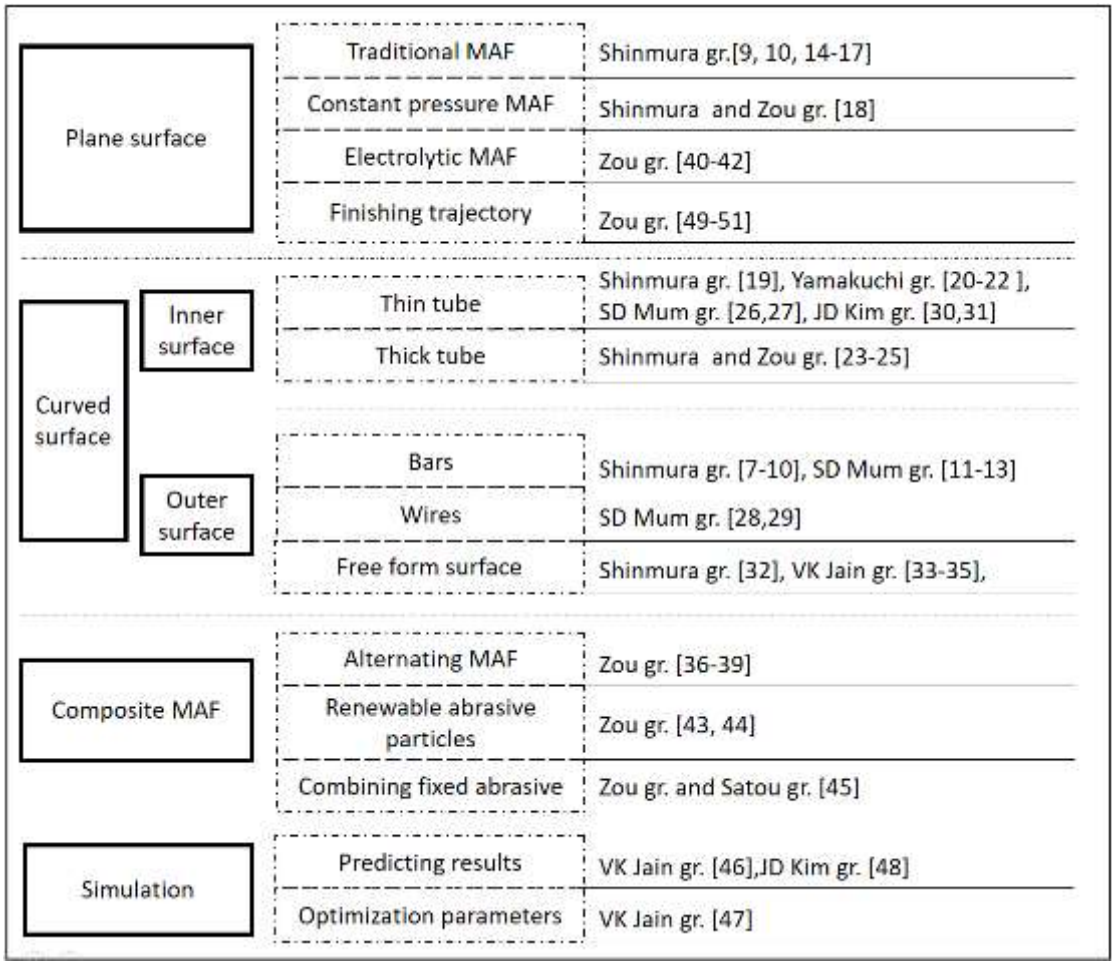

Fig.1. 1 Main researches of magnetic abrasive finishing technology

As shown in Fig.1.1, it mainly includes five aspects: plane magnetic abrasive finishing, curved surface magnetic abrasive finishing, inner surface magnetic abrasive finishing, simulation, etc.

In the 1980s, Shinmura et al. [7-10] proposed to use MAF process to finish the outer surface of the cylinder, and analyzed the influence of processing conditions such as magnetic pole shape, magnetic flux density, working speed, vibration frequency, vibration amplitude, working gap and mean diameter of magnetic abrasive on the finishing performance. SD Mum et al. [11-13] used this technology to process ZrO2 ceramic bars, Microscale-diameter zirconia ceramic bars, and AISI 304 bars, and achieved good results. Shinmura et al. [14-17] also proposed the basic principle of plane MAF, developed the plane MAF device using

electromagnets, and discussed the effects of process parameters such as finishing fluid and magnetic abrasives supply weight on the finishing depth and surface roughness.

In order to improve the shape accuracy of the workpiece, Zou et al. [18] proposed a planar magnetic polishing method using a new constant pressure magnetic brush, and described its feasibility and characteristics. The experimental results show that this new plane magnetic abrasive finishing process can remove burrs and improve the shape accuracy of the workpiece better than the traditional magnetic brush processing. Shinmura and Yamaguchi [19-22] proposed a method of finishing the inner surface of circular pipe by magnetic abrasive finishing. They found that the finishing pressure distribution of magnetic abrasives was affected by the magnetic field distribution over the finishing area, and the magnetic field distribution controlled the finishing characteristics. However, if the pipe wall is thick, the efficiency of this processing method will be greatly reduced. Therefore, Zou et al. [23-25] proposed a new magnetic field assisted finishing process using a magnetic finishing jig. By using this process, the finishing of the inner surface of thick barrel (5-30 mm thick) can be realized, which is very effective. The experiment on SUS304 stainless steel pipe (10 mm thickness) verifies the applicability of improving the inner surface roughness and inner thickness of the pipe. SD Mum et al. [26, 27] applied this method to improve the smoothness of the inner surface of oval-shaped tubes and cone pipes. And recently, they also studied the technology of finishing the surface of wire by MAF. This technology is used to finishing a 316L SUS wire as a biomaterial, which is commonly used in medical applications (such as coronary stent, orthodontics, and implantation) [28, 29]. Kim et al. [30, 31] also studied

the inner surface processing method of the tube. They analyzed the magnetic flux distribution and magnetic flux density in the working area under two driving modes by using the finite element method, and from which the desirable mode for efficient polishing was determined. Shinmura et al. [32] realized the magnetic abrasive finishing of processing free-form surface by using NC machine tools. It is proved that this method shortens the processing time and has high processing accuracy. VK Jain et al. [32-35] finished free-form surfaces with ball joint tools, and the force and surface roughness of magnetic abrasive finishing ware analyzed.

In order to further improve the performance of MAF, Zou et al. have carried out many innovative and improved research on magnetic abrasive finishing technology. Zou et al. proposed electrolytic magnetic abrasive finishing, magnetic abrasive finishing of recyclable abrasive and so on, and studied the magnetic abrasive finishing technology of alternating magnetic field in detail. They found the influence of magnetic particle size and magnetic field frequency on magnetic cluster changes, and analyzed the relationship between finishing force and alternating magnetic field [36-39]. Zou also proposed an effective method combining electrolysis and magnetic abrasive finishing (EMAF). Through the EMAF process, the surface roughness can be reduced from the original 393.08 nm RA to 30.94 nm RA in 40 minutes [40]. Moreover, they further studied the relationship between electrolytic current and finishing efficiency, and refined the surface of a5052 aluminum alloy [41, 42]. In the traditional MAF process, with the finishing process, the magnetic brush will be squeezed and worn. This is not conducive to continuous and stable finishing. So Zou et al. proposed a magnetic abrasive finishing process using the circulatory system to renew magnetic abrasive slurry [43]. The experimental results

show that the process can realize the stable processing of the material surface, and the surface roughness of polytrifluoroethylene chloride resin plate can be improved from 274 nm RA to 34 nm RA in 15 minutes [44]. Recently, Zou et al. proposed a finishing process combining magnetic abrasive finishing process and fixed abrasive polishing process (MAF-FAP). Using this method, the surface roughness of alumina ceramic plate is improved from 202.11 nm RA to 3.67 nm RA in 30 minutes [45].

In order to predict the results of magnetic grinding and better optimize the finishing parameters, VK et al. [46] carried out modeling, simulation and analysis. A series of numerical experiments were carried out on the process by using finite element method and surface roughness model. The effects of magnetic flux density, working gap height, magnetic abrasive particle size and magnetic pole speed on surface quality were studied. VK et al. [47] also established the theoretical model of abrasive particle removal and surface roughness. The effects of process parameters such as magnetic flux density, map size, tool speed, finishing time, initial surface roughness and abrasive particle shape on finishing characteristics were studied. In order to better understand the influence of the above process parameters on surface roughness, try to determine the surface roughness index. JD Kim et al. [48] have also predicted the surface roughness as a function of finishing time through the model derived from the material removal volume. According to the surface roughness model, the time of complete removal of existing scratches can be predicted.

However, planar MAF also has some technical difficulties. For example, due to the edge effect of the magnetic field distribution of the circular magnetic pole, the magnetic field strength at the edge of the magnetic pole is high, while the magnetic field strength at the center position is weak,

which leads to uneven distribution of magnetic particles, so that the pressure on the workpiece is different at each point of the magnetic brush. This increases the difficulty of increasing the shape size progress. In order to improve the geometrical accuracy of the plane, the influence of the finishing trajectory on the geometrical accuracy of the workpiece was investigated. Zou et al. [49, 50] proposed a processing method to change the trajectory of the magnetic brush. On the basis of the rotation of the magnetic brush, the movement of revolution is added to improve the uniformity of the polishing surface. They conducted further studies on this method and proved that the revolution radius is an important factor affecting the surface flatness, and proposed an effective method for evaluating the surface profile [51].

1.2 Research purposes

With the continuous development of science and technology, the requirements for the surface accuracy of components are getting higher and higher. For example, in modern optical systems, the requirements for performance indicators such as shape accuracy, surface quality, sub-surface quality, and residual stress of optical components are increasing [49, 50]. For many optical workpieces, the shape accuracy of the surface has a great influence on the refraction and reflection of light, so high geometric accuracy is required. When the surface of the workpiece is uneven, can we efficiently process it into a uniform plane? The basic shape of the workpiece does not change much after a period of time using the method of uniform processing. Although I believe that long-term processing can definitely process it into a flat surface. But it may take longer. So can we increase the speed of correction by changing the processing strategy? This

is the main purpose of this research.

In order to further solve the problem of processing uniformity, this article proposes a method of using 1mm diameter magnetic pole to form a small-sized magnetic brush. According to the initial profile of the surface, control the processing of different positions at different feed speeds. Through the analysis and processing of the collected surface profile data, and according to the processing rate characteristics of the magnetic brush, the distribution of the feed speed during the processing is planned, so that the effective processing time at different positions is different, thereby the surface flatness is improved rapidly.

Chapter II Processing principle

2.1 Introduction

The surface accuracy of the machined surface, such as reducing the surface roughness, can be improved by using the traditional magnetic finishing. Since the magnetic brush in magnetic abrasive finishing is a flexible processing tool, it can finish some irregular workpieces. It can finish the workpiece on the basis of basically not destroying the shape of the workpiece. In the previous research, detailed research has been carried out on the experimental device, as well as the finishing slurry, etc., and good results have also been achieved. So, now we think about the problem in reverse, whether we can also use magnetic finishing, while polishing the workpiece, can also carry out a certain degree of damaged workpiece morphology correction. This is also the problem we have to solve next. This chapter will analyze it in principle.

2.2 Conventional plane MAF process

Figure 2.1 shows the processing principle of the conventional plane MAF process. The basic principle of the conventional plane MAF process is to fill the magnetic abrasive or compound magnetic finishing fluid between the magnetic pole and the workpiece. Magnetic abrasives are made of iron powder and abrasives through sintering or chemical or other techniques [52]. However, sintering requires both high temperature and pressure within an inert gas atmosphere. Subsequently, the sintered material should be crushed mechanically and then sieving is required to sort it into a specific particle size. Obviously, due to the complex

production process, additional production costs will increase [53]. Therefore, more and more researches have focused on the use of unbound magnetic abrasives [10, 54]. The compound magnetic finishing fluid is obtained by uniformly mixing a certain proportion of magnetic particles, abrasive particles and finishing fluid. In the magnetic field, the magnetic particles are attracted by the magnetic poles and arranged along the lines of magnetic force to form a magnetic brush. The relative movement between the magnetic brush and the workpiece is generated through the feed movement and the rotation movement, thereby realizing the material removal on the surface of the workpiece.

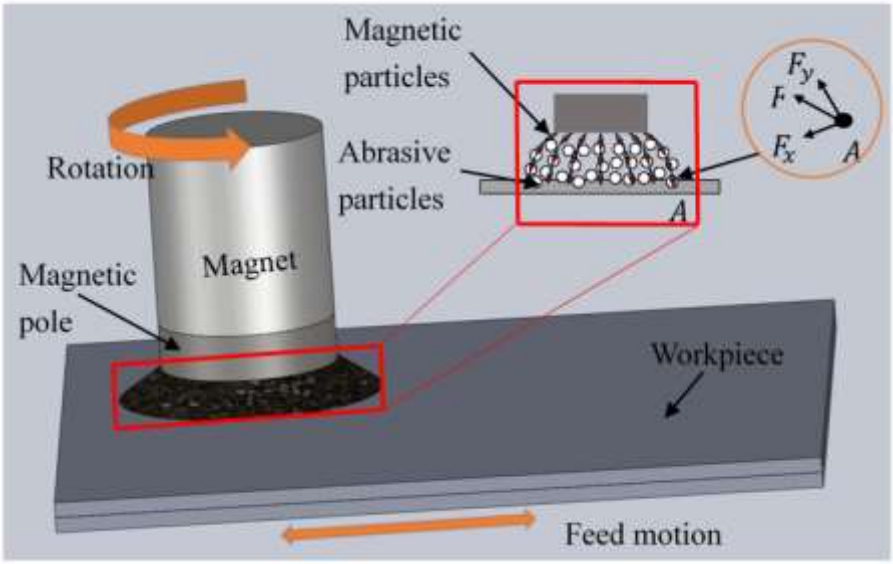

Fig.2. 2 The magnetic force acting on a magnetic particle

Figure 2.1 shows the schematic diagram of magnetic force acting on a magnetic particle in magnetic field. F_x and F_y can be calculated by Eqs. (2.1) and (2.2) [55],

$$F_x = V_p \chi \mu_0 H \left(\frac{\partial H}{\partial x}\right) \tag{2.1}$$

$$F_y = V_p \chi \mu_0 H \left(\frac{\partial H}{\partial y}\right) \tag{2.2}$$

where x is the direction of the line of magnetic force, y is the direction of the magnetic equipotential line, V_p is the volume of magnetic particle, χ is susceptibility of particles, $\mu_0$is the magnetic permeability of vacuum, H is the magnetic field intensity at point A, $\partial H/\partial x$ and $\partial H/\partial y$ are gradients of magnetic field intensity in x and y directions, respectively.

2.3 Processing principle of the corrective abrasive finishing

As shown in the Fig.2.2, the process of the corrective abrasive finishing is described. In order to improve the plane quality, first, the surface shape is measured by a measuring device and a database is constructed. Next, the finishing section is subdivided according to the initial surface profile of the workpiece, the finishing speed of each part is calculated, and the finishing experiment is performed at different feed speed.

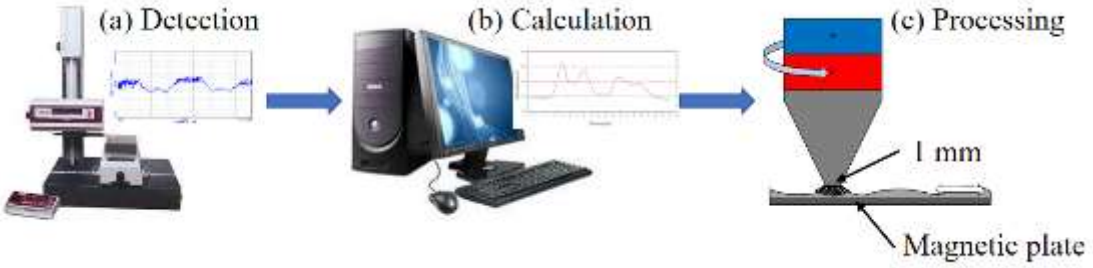

Fig.2. 3 Principle of corrective abrasive finishing

The schematic of the principle of finishing is shown in Fig.2.3. The X-Y Stage is used to achieve precise control of the processing position. The linear slide realizes the motion control of the workpiece feed. It is filled with mixed magnetic abrasive particles (magnetic particles and abrasive particles) and abrasive fluid between the workpiece and the magnetic pole. The magnetic particles are arranged along the lines of magnetic force to

form a flexible magnetic brush. The magnetic pole can rotate under the driving of the motor, and the material is removed due to the relative friction between the magnetic brush and the work piece. The distance between the magnetic pole and the work piece can be changed by changing the height of Z-adjustment, thereby changing the pressure and friction.

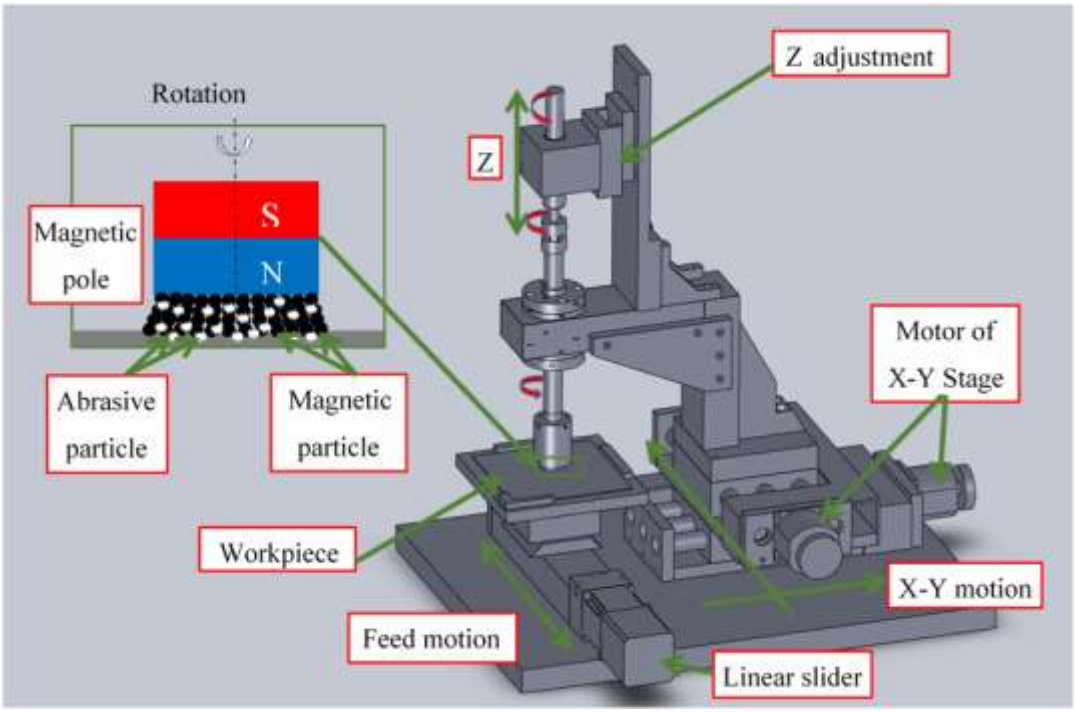

Fig.2. 4 Schematic of mechanical principle

The rotation of the magnetic poles is driven by a DC motor, and the speed of the magnetic pole rotation is controlled by a power control device to adapt the needs of the experimental conditions. The control of the processing position is realized by inputting the control instructions in the computer to control the movement of the X-Y stage. The work piece is placed on a linear slider to linearly move the work piece. Linear sliders can be used to move at different speeds in different region.

As shown in the Fig.2.4, when the surface profile of the workpiece has ups and downs, according to the changes of the surface profile, it is

necessary to reasonably allocate the finishing time of each area to reduce the height difference.

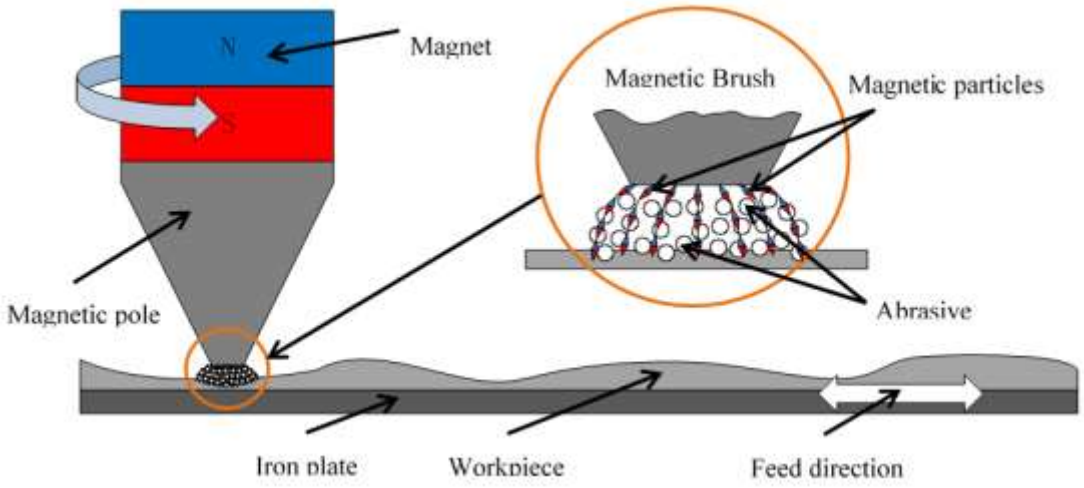

Fig.2. 5 Schematic of correction processing principle

The material removal amount satisfies the following formula:

$$dM_R = kP(x,y)V(x,y)dt, \tag{2.3}$$

where, M_R is the amount of material removal, k is the removal factor, $P(x,y)$ is the pressure, $V(x,y)$ is the speed of the relative to the workpiece, and t is the processing time. When the magnetic field strength, the composition of the abrasive, and the finishing gap are constant, the amount of material removal depends on $V(x,y)$ and t [50, 56].

In the finishing process, the movement of the particles consists of circular movement and movement relative to the workpiece. As shown in Fig.2.5, ω is the angular velocity of circular motion, r is the distance between the particle and the axis of rotation, that is, the radius of the circular motion, so the linear velocity of the particle circular motion is equal to ωr, and v is the speed of the particle relative to the workpiece in the feed direction, and θ is the angle between the two velocity vectors, therefore, the composite velocity of the particle V is:

$$\omega r - v < V = \sqrt{(\omega r)^2 + v^2 - 2\omega r v \cos(\pi - \theta)} < \omega r + v \qquad (2.4)$$

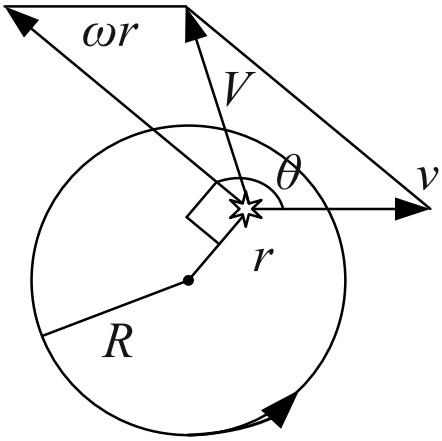

Fig.2. 6 Schematic of the abrasive particle velocity vector

In the process of finishing, the feed speed *v* is very small, generally about 1mm/s, or even smaller. Relative to the feed speed, the rotating speed of the magnetic brush is very large. The rotating speed of the experiment part of this paper is set to 400rpm. The brush radius is about 2.5mm, so the linear velocity component of the circular motion of the particles on the outer edge of the magnetic brush is：

$$\omega r = 400 \times 2.5 \times 2\pi / 60 = 104.7 \text{ mm/s}.$$

When the feed speed is very small, and much smaller than the linear velocity of the circular motion, that is $v \ll \omega r$, the velocity of the particle relative to the workpiece can be approximately equal to the linear velocity of the circular motion. In order to simplify the model, this article ignores the influence of the feed speed component on the particle velocity. It is considered that the velocity of the particle relative to the workpiece is approximately equal to *ωr,* as shown in Equation 2.5. Therefore, it can be considered that when the feed speed is changed, the processing efficiency does not change.

$$V \approx \omega r \tag{2.5}$$

Therefore, when the rotation speed ω is constant, V is unchanged. From formula 2.3, it can be known that the amount of material removal only depends on the processing time t. In a single processing process, the effective processing time for any point (except for the point at the edge) on the workpiece is the elapsed time of the magnetic brush at that point, represented by t_1, it should be equal to:

$$t_1 = L/v \tag{2.6}$$

Where L is the chord length of the magnetic brush passing through that point. When the point is located in the center line of the processing trajectory, L gets the maximum value $2R$. Where R is the radius of the magnetic brush. And v is the speed of the particle relative to the workpiece in the feed direction. Therefore, in order to process the undulating surface of the workpiece shown in Fig.2.4 into a flat surface, the key is to process at different feed speeds on different positions. The specific principles of variable speed finishing will be explained.

First of all, the initial profile data of the workpiece needs to be measured. In this paper, the initial data $H_0(S_i)$ is obtained by Surftest SV-624-3D. $H_0(S_i)$ is the initial height at position S_i. Then, it is needed to calculate the feed speed $v(S_i)$ at different positions. In order to facilitate the division of regions, the original data is filtered. The width of the filtered data is m, so it is the mean filtering of m data, and the data $H(S_i)$ is obtained after filtering.

$$H(S_i) = \frac{\sum_i^{i+m-1} H_0(S_i)}{m} \tag{2.7}$$

Where, S_i is the position of the i-th sampling point, and m is the number of data to be averaged filtered. Then, it is necessary to set the height h_0 of the target processing line. The filtered data is processed as follows formula

(2.7) with respect to the target processing line. So removal height sequence $h(S_i)$ of each position is calculated according to the following formula (2.8).

$$h(S_i) = H(S_i) - h_0 \tag{2.8}$$

Thereby, the processed height transformation sequence is obtained. Assuming the processing efficiency is η μm/min, then the processing time $\Delta t(S_i)$ for each segment is:

$$\Delta t(S_i) = \frac{h(S_i)}{\eta} \tag{2.9}$$

Then, assuming that it needs n loops for processing, the displacement change is ΔS, the speed of each segment is:

$$v(S_i) = \frac{2n\Delta S}{\Delta t(S_i)} \tag{2.10}$$

Because the movement speed of the particles is the vector sum of the speed and the feed speed, and the speed is much higher than the feed speed, the influence of the feed speed on the finishing effect is ignored here. The feed speed change only changes the processing time. Then at high places, $v(S_i)$ speed is slow, $\Delta t(S_i)$ time is long, and in low-lying places, $v(S_i)$ speed is fast, $\Delta t(S_i)$ time is short. Reorganize the above formula to get:

$$v(S_i) = 2n\Delta S/(h(S_i)/\eta) = 2n\eta\Delta S/h(S_i) \tag{2.11}$$

It can be seen that when the processing parameters are unchanged, η is a constant. Therefore, $v(S_i)$ is inversely proportional to $h(S_i)$.

$$v(S_i + 1)h(S_i + 1) = v(S_i)h(S_i) = 2n\eta\Delta S \tag{2.12}$$

This is:

$$v(S_i + 1) = v(S_i)h(S_i)/h(S_i + 1) \tag{2.13}$$

In order to facilitate the calculation, $v(S_1)$ can be obtained first, and then all regional velocity array $v(S_i)$ can be solved according to the above recurrence formula 2.13.

Here is an example to illustrate the calculation process of obtaining the velocity curve. The curve shown in Fig.2.6 (a) is the contour curve of the workpiece surface obtained by instrument measurement. Sample 100 points per mm. It can be seen that the height of the contour curve is positive or negative. Therefore, we shifted the contour curve upward by 5um in this example according to Formula (2.8) to obtain the curve as shown in Fig.2.6 (b). As the surface of the workpiece is rough, the contour curve fluctuates greatly, so the calculated speed will change frequently, which is not conducive to the control of the motor. Therefore, Formula (2.7) is used to filter the curve and the filtered curve shown in Fig.2.6 (c) is obtained. Here we can also filter first, shift the curve, and it doesn't matter.

Then, the theoretical processing time curve required by each point can be calculated according to Formula (2.9), as shown in Fig.2.7. By comparing the time curve and the contour curve, we can see that the high place corresponds to the processing time required is longer, while the low place corresponds to the processing time is shorter, which is consistent with our assumption. The time here is an ideal processing time, because we cannot realize that the processing time of two points near each other is significantly different.

Similarly, we can calculate the feed velocity of the workpiece at each point according to Formula (2.10), so as to obtain the change curve of the feed velocity as shown in Fig.2.8. By comparing the speed curve with the time curve and the contour curve, we can see that the high part corresponds to the long processing time and slow feed speed, while the low part corresponds to the short processing time and fast feed speed, which is also in line with our assumption. Therefore, in theory, we can realize the modification of the workpiece surface topography.

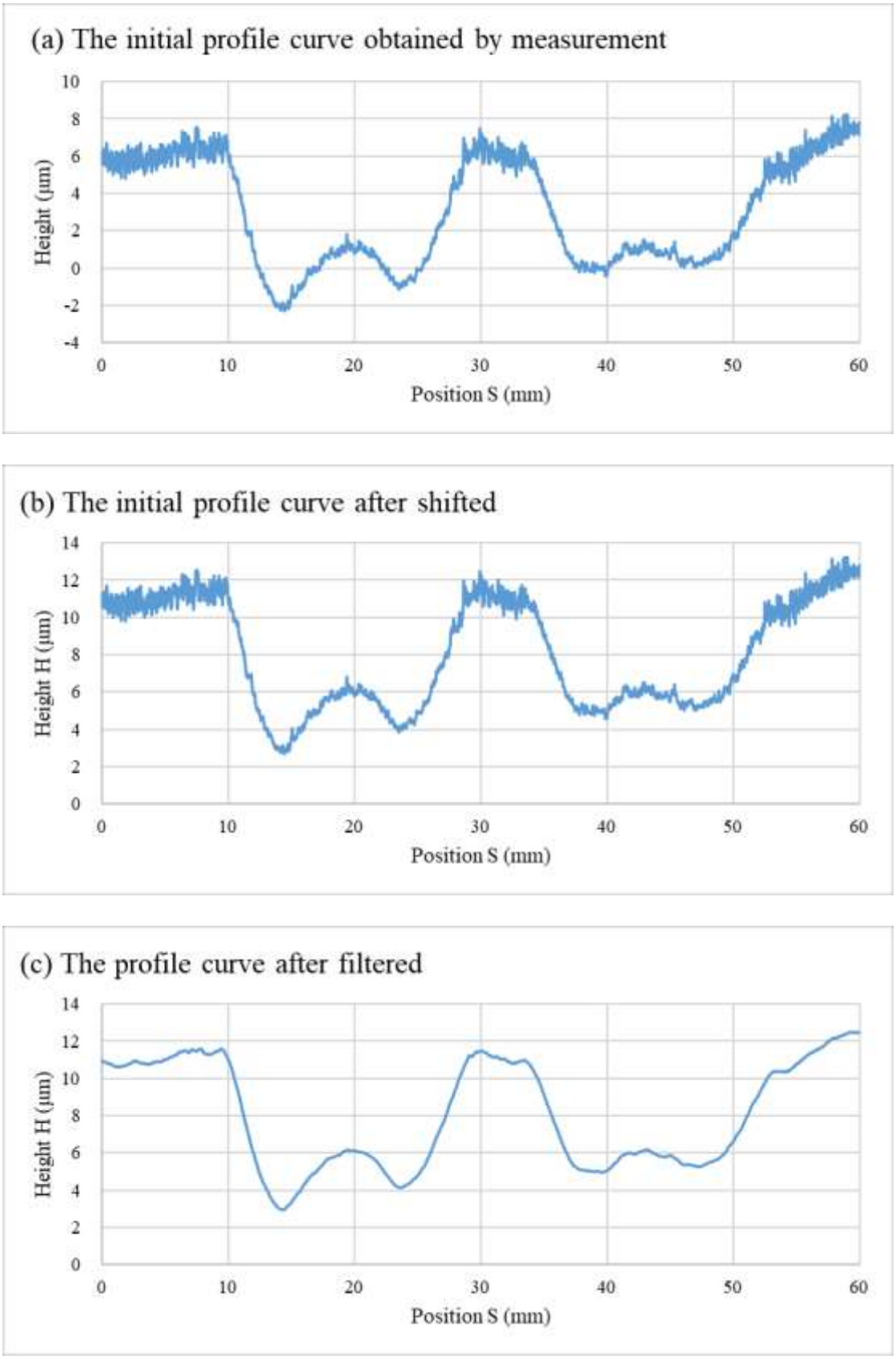

Fig.2. 7 Regional division method

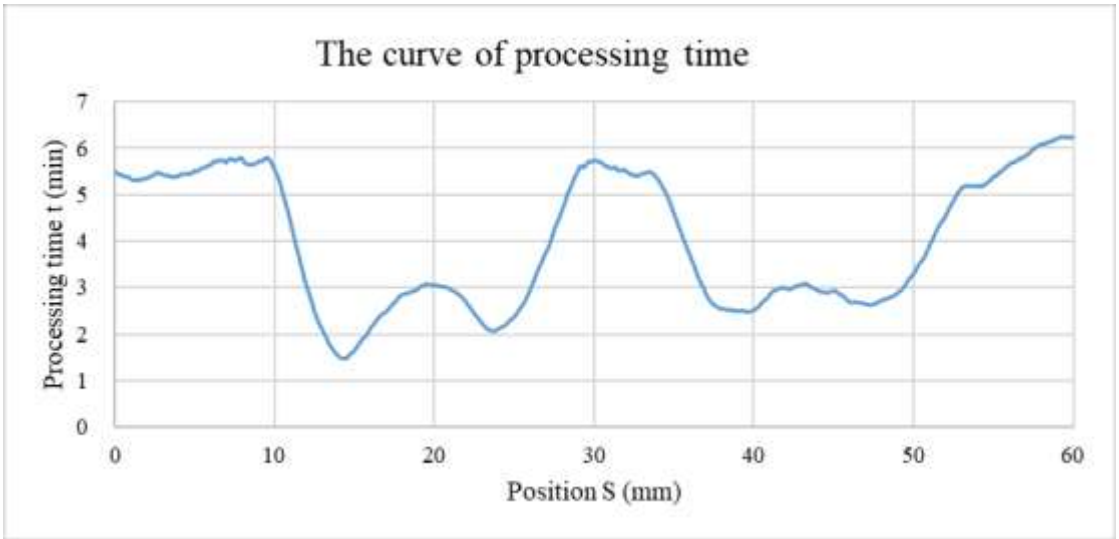

Fig.2. 8 The curve of processing time

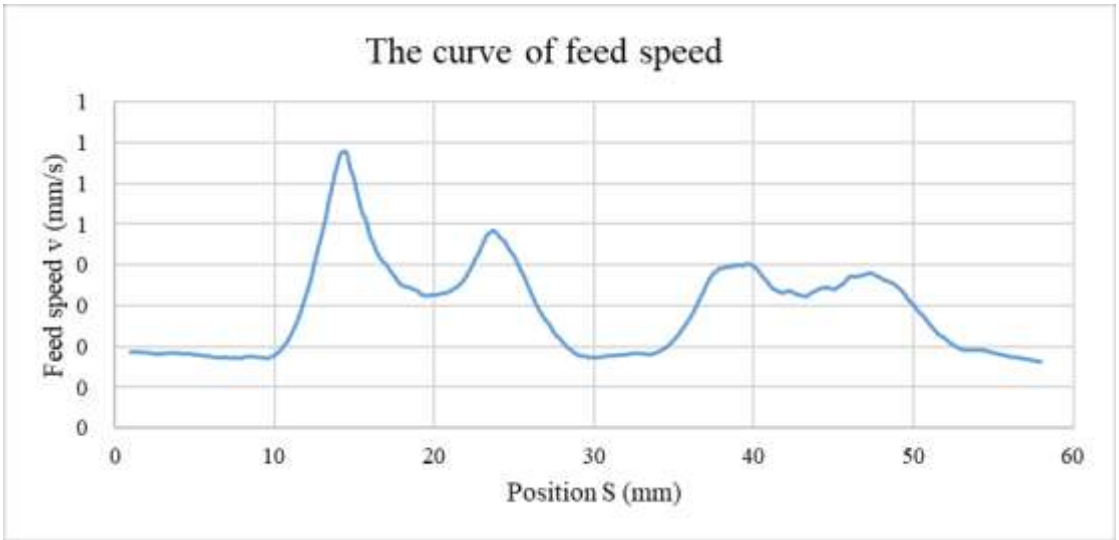

Fig.2. 9 The curve of feed speed

So now the key problem is how to make the control system can control the motor to move according to the feed speed curve. The specific realization method is determined by the actual mechanical structure and motor control mode. One way to achieve this is to directly control the speed of the motor by using analog quantities, which can make the motor run according to the speed curve shown in Fig.2.8. But we need to make a transformation of the velocity curve, and transform it into a velocity versus

time curve. In this way, due to the control error, it may not be able to accurately correspond the displacement and velocity.

Another way is to control the position of the motor, divide the speed curve into several segments, and calculate the average speed of each segment, as shown in Fig.2.9, which is the speed curve segmented according to 1mm 1 segment. It can be seen that the velocity curve is basically consistent with that shown in Fig.2.8. In fact, the original velocity curve is also equivalent to the curve obtained by 0.01mm each section. For this equally-spaced scheme, the smaller the standard of the sections, the closer we get to the velocity curve we need.

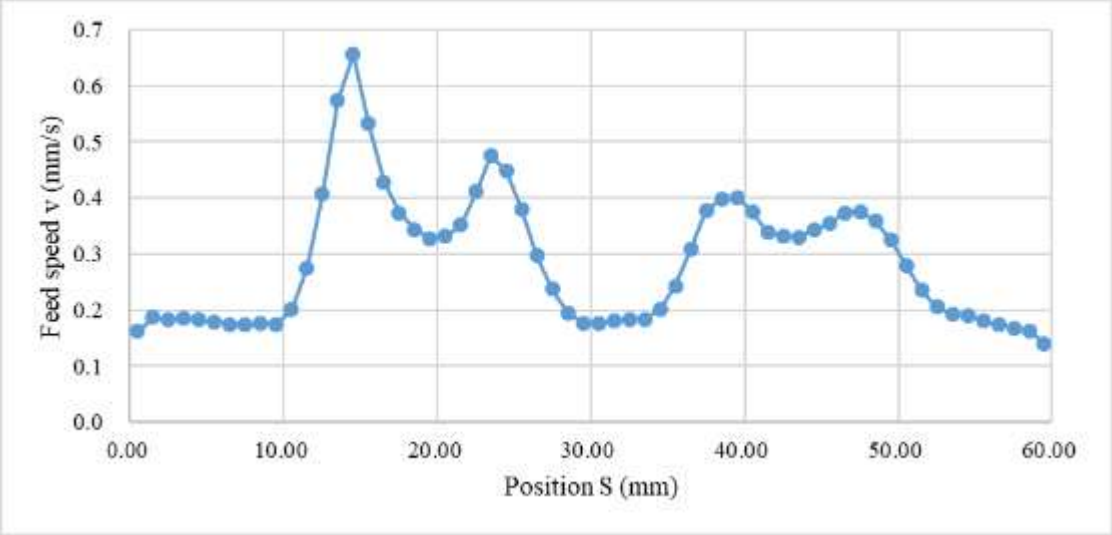

Fig.2. 10 The speed curve by every millimeter

If the division is too large, the speed curve will be distorted. But when the division is too small, the speed of the motor will change frequently, which requires high performance of the motor. In addition, for the area with sharp speed change, if the division is too small, the rapid change of speed cannot be realized due to the performance of the motor. From the point of the profile curve of the workpiece, we can change the partition curve of

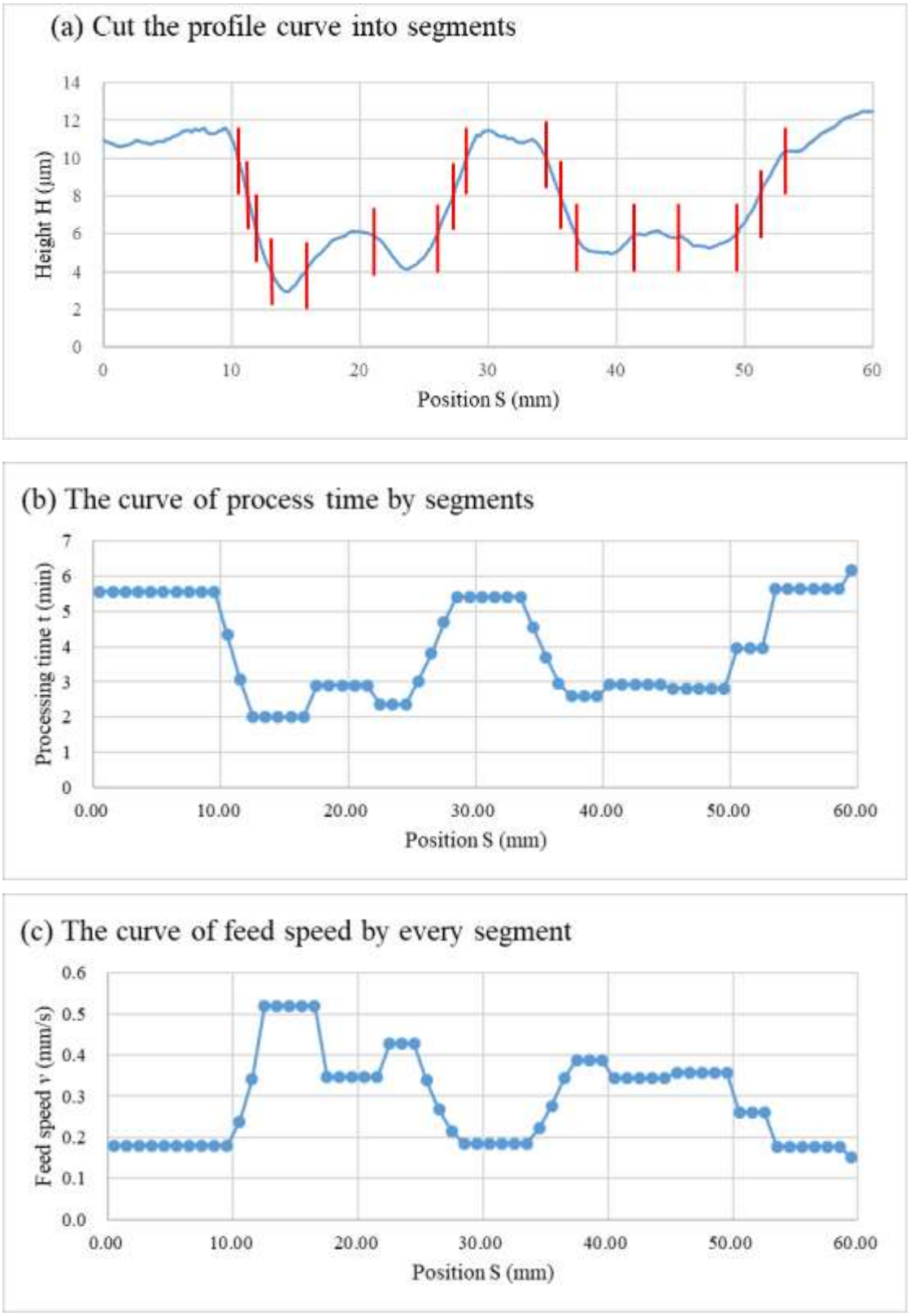

Fig.2. 11 The curves of dividing the height, time and speed into segments

standard, here in this study, on the basis of the change is according to the height of the curve, which is less than a fixed value when the height of the curve changes, considered an area, in this method, we can filter after the outline of the curve as shown in Fig.2.10 (a) the results of the division. Here we set Δh =2μm.

After segmentation, we calculate the average height of each segment to obtain the approximate curve of the workpiece surface. Then, according to this curve, the processing time curve shown in Fig.2.10 (b) is calculated. Thus, the finishing speed curve after segmentation is calculated as shown in the Fig.2.10(c).

The motor used in this research is the stepper motor of Oriental Motor, and its operation mode has two kinds of position control mode and speed control mode. Position control mode can accurately control the displacement of each section, which is conducive to improve the accuracy of finishing position. And its speed control way is through the way of communication, by the control of it at any time to send instructions to change the speed. This kind of control mode has communication time delay, about 20ms, which will cause the error of processing position. Therefore, in order to facilitate the implementation, this paper chooses the second partition method.

In summary, the data processing flow is shown in Fig.2.11. First, it is necessary to filter the collected data. Then setting the target finishing position, and calculate the profile curve of the height change of the workpiece surface. According to the inverse relationship between the removal height and the feed speed, the processing time corresponding to each segment on the profile curve is calculated. So as to calculate the feed speed of each curve.

2.4 Conclusions

In this chapter, the processing principle of the corrective abrasive finishing using MAF is introduced. The main content can be summarized as follows.

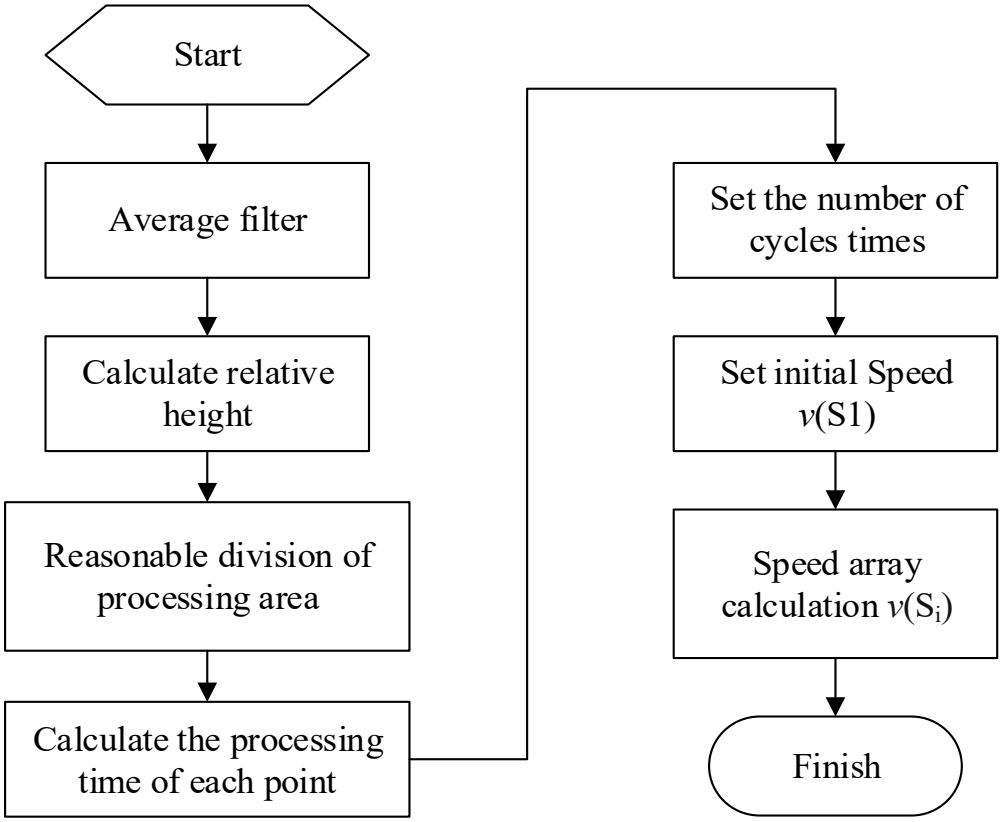

Fig.2. 12 Data processing Schematic

(1) The processing principle of conventional plane MAF technology is introduced.

(2) The processing principle of the corrective abrasive finishing using MAF is introduced. The inverse proportional relationship between the height change of the workpiece surface after the material removed and the feed speed is analyzed by mathematical model.

(3) An example is given to illustrate the process of obtaining the speed curve of the corrective abrasive finishing.

(4) The flow of data processing and the steps to obtain the feed speed curve are explained.

Chapter III Experimental device

3.1 Introduction

The task of this chapter is to introduce the experimental equipment and detection equipment used in this chapter, and the magnetic pole used in this chapter is simulated, and the size of the magnetic brush is described. At the same time, the measuring methods of magnetic field intensity of magnetic pole and pressure of magnetic abrasive brush are introduced.

3.2 Experimental setup

Figure 3.1 is the system structure diagram of experimental setup. It includes debugging computer, motion control circuit board, X-Y stage driver, linear slide driver, and DC motor driver. The computer can program the motion control circuit board through USB, and control the position and speed of X-Y Stage through RS-232. The motion control circuit board can control the speed of the DC motor through the DAC, and its speed is fixed at 400rpm in this study. At the same time, the motion control circuit board controls the linear motor through the RS-485 bus, and changes the feed speed of the workpiece as required. As shown in the system block diagram. The computer programs the STM32 circuit board by USB to control the processing position, feed speed and rotation speed. The STM32 control board communicates with the X-Y stage driver through the RS232 interface to control the processing position and trajectory. The STM32 control board communicates with the linear motor driver through the RS485 interface to realize the control of the feed speed. The STM32 control board uses DAC to directly output analog signals to control the

speed of the DC motor.

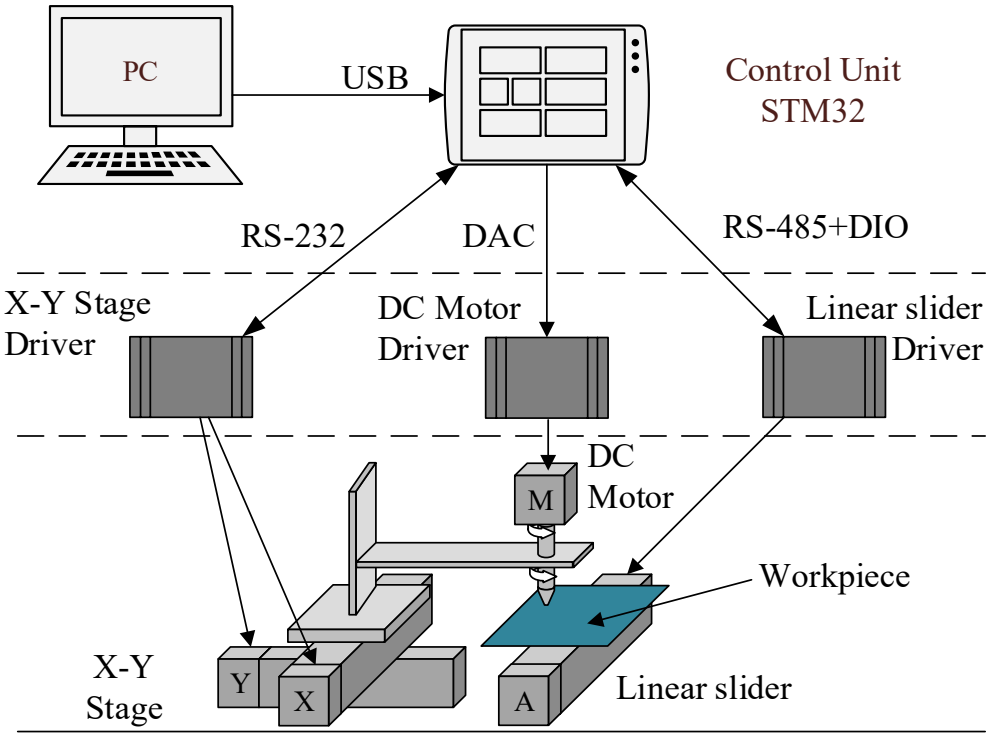

Fig.3. 1 The system structure diagram of experimental setup

Figure 3.2 is the photo of the electrical part, which includes the computer, control circuit board, X-Y stage driver, linear motor driver, DC motor driver, speed meter, and 24VDC power supply.

The photo of the experimental setup used in this paper is shown in Fig.3.3. X-Y stage is used to control the processing position of the workpiece. The DC motor drives the magnetic poles and the magnetic brush rotating to grind the workpiece. The linear feed motor realizes the control of the feed speed and by changing its speed to realize variable speed processing. The height adjustment device is used to adjust the processing gap, which can be accurate to 0.1mm.

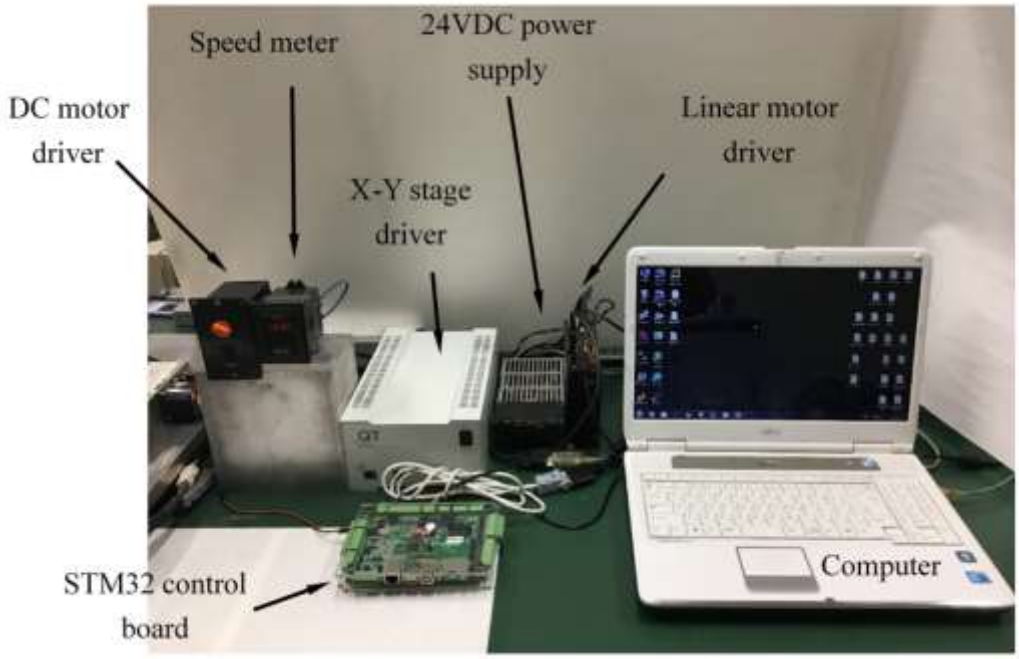

Fig.3. 2 The photo of the electrical part

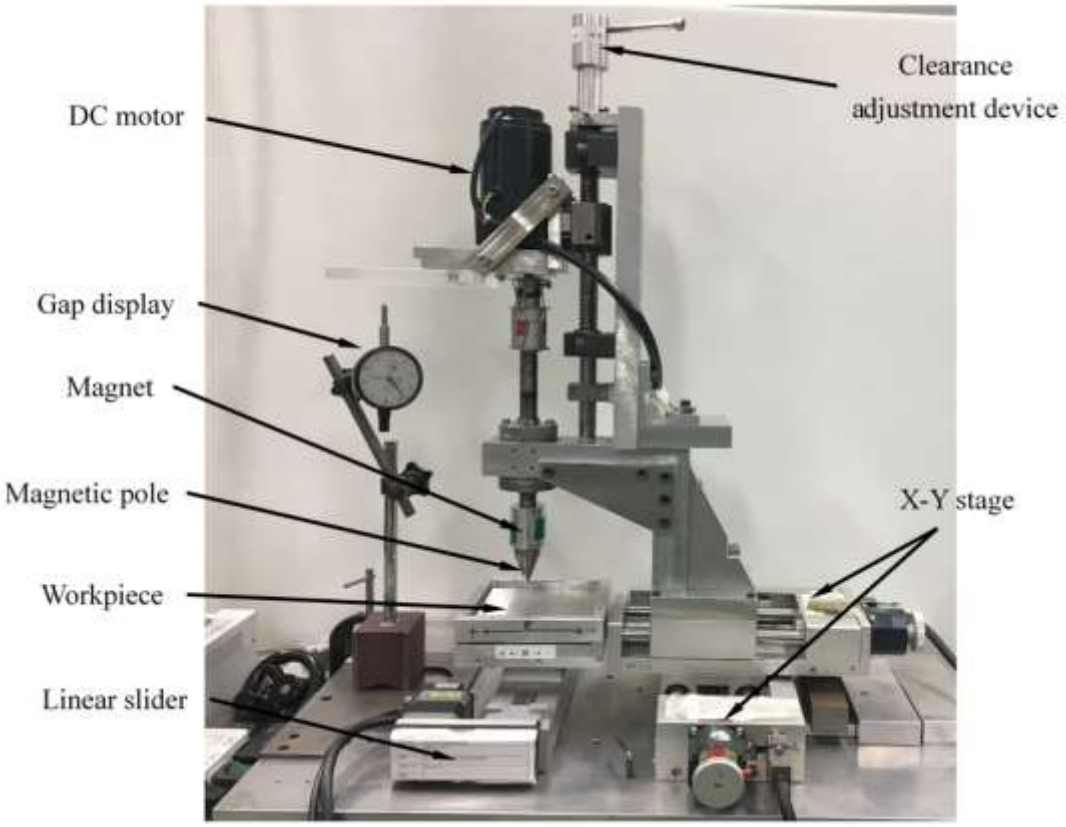

Fig.3. 3 The photo of external view of the experimental setup

Figure 3.4 shows an enlarged picture of the magnet and magnetic pole part. There are two cylindrical magnets with a height of 12.5mm and a diameter of 23mm under the rotating axis. Under the magnets is an iron magnetic pole. The outside of them is an aluminum shell. In this research, two shapes of magnetic poles are used. The one is a cylindrical pole with a height of 5 mm and a diameter of 23 mm, and the other one is a mesa-shaped magnetic pole with a diameter of 23 mm on the larger side and 1 mm, 2 mm, or 3 mm on the smaller side. Fig.3.5 is a photo of a magnetic pole that can be replaced.

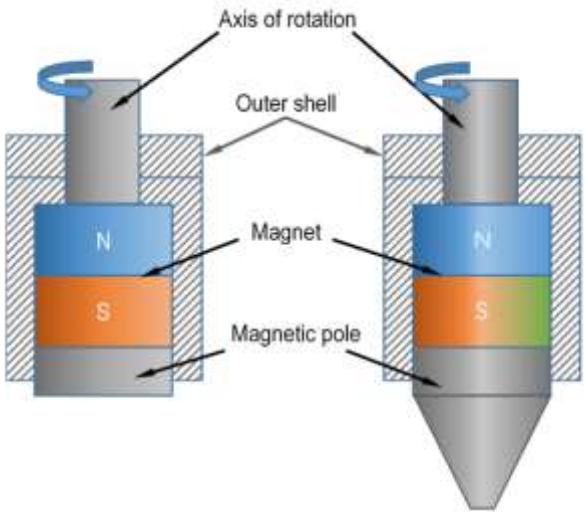

Fig.3. 4 The expanding photograph of the magnet and magnetic pole

Fig.3. 5 Magnetic pole shape

3.3 Magnetic pole and the analysis of magnet field

3.3.1 The simulation of Magnet field

In order to study the influence of the change of the magnetic pole shape on the magnetic field distribution, the "Magnet7" software is used to simulate the magnetic field distribution of the magnetic pole. Two types of magnetic poles are mainly used in this chapter, as shown in Fig.3.4. It will be used in subsequent research to obtain a lot of useful data.

3.3.2 Magnet field measurement

In this study, while simulating the magnetic field, the actual measurement was also performed with an instrument. The instrument used here is GM-4002, and the probe is T-402. The measurement method is shown in the Fig.3.6. The probe is placed under the magnetic pole, and the magnetic pole is moved by controlling the motor. At the same time, the data of the magnetic field change is transmitted to the computer using RS232.

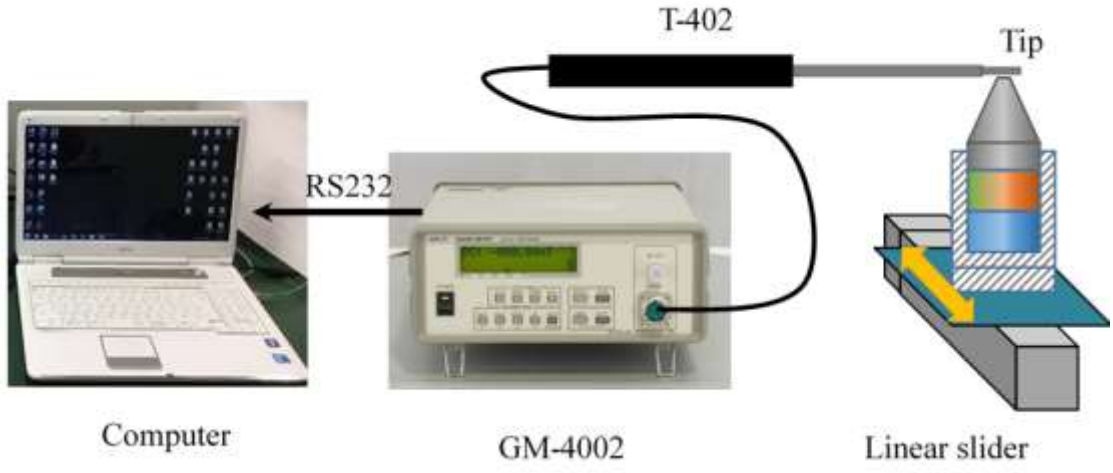

Fig.3. 6 The method of measuring magnetic field strength

Figure 3.7 shows the size of the probe T-402. It can be seen that the end of the probe is 1.9 mm wide and 1 mm thick.

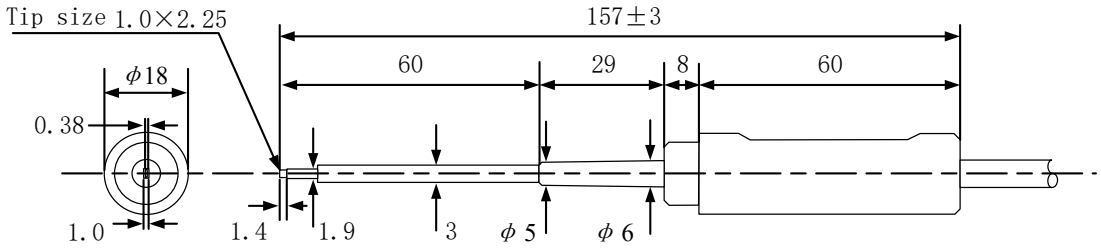

Fig.3. 7 Dimensions of probe T-402

3.3.3 Finishing force measurement

In order to better analyze the characteristics of the magnetic poles, a device was designed to measure the pressure distribution of the magnetic brush processing. The measurement method is shown in the Fig.3.8 and Fig.3.9. The pressure sensor used here is the LMA-A-5N small pressure sensor from KYOWA. The sensor can convert the pressure into an electrical signal, which is amplified by an amplifier and sent to the data recording instrument. In this research, the amplifier used is CDV-700A, and the data logging instrument is LOGGER GL240.

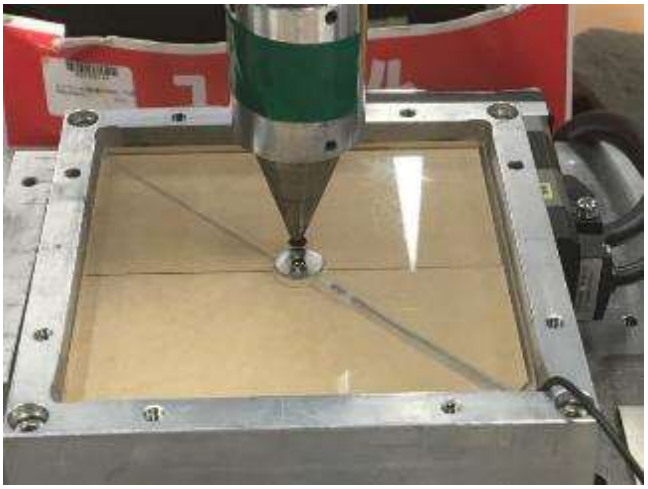

Fig.3. 8 Photo of pressure measuring device

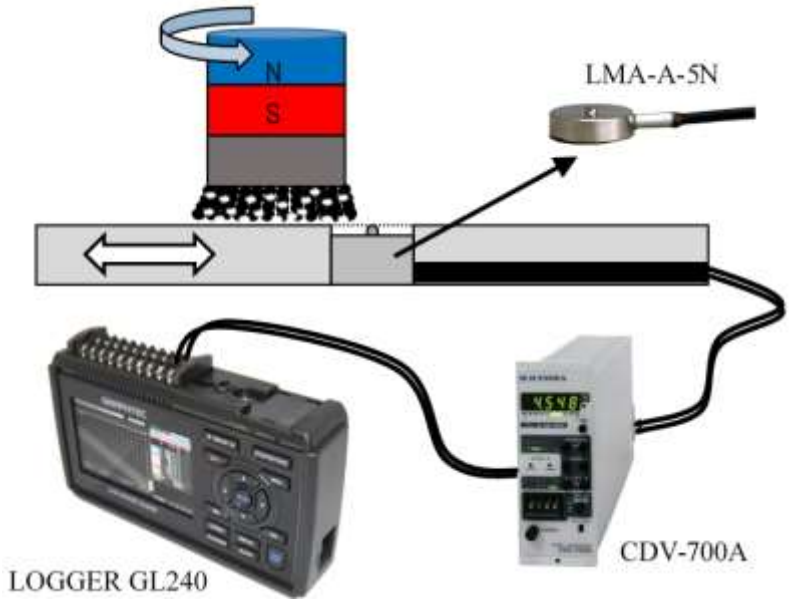

Fig.3. 9 Schematic diagram of pressure measuring device structure

3.4 Composition of MAF the abrasive particles

In this study, compound magnetic finishing fluid formed by mixing magnetic particles, abrasive particles and finishing fluid was used as a finishing tool. In previous studies, it has been proved that the use of oil-based slurry can better maintain the state of magnetic clusters, obtain better surface quality and improve finishing efficiency. Therefore, oily polishing fluid was used in this study.

According to the initial roughness of the workpiece surface and the hardness of the workpiece, the appropriate size of magnetic particles is selected, which helps to improve the finishing efficiency and reduce the finishing time. In this study, the magnetic particles used are shown in Fig.3.10. The average diameter of magnetic particles from Fig3.10 (a) to (c) is 330 μm, 149 μm, 75 μm, respectively. It can be seen that the magnetic particles with an average diameter of 75 μm, 149 μm, and 330 μm are electrolytic iron powder, and most of their shapes are similar to flakes. And

Fig3.10 (d) is KMX80 that consists of dispered aluminum oxide grains in iron matrix particles with the average diameter of 80 μm.

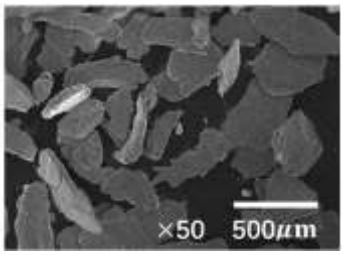

(a) Fe 330 μm

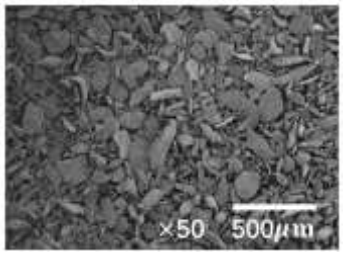

(b) Fe 149 μm

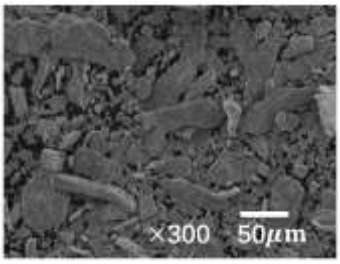

(c) Fe 75 μm

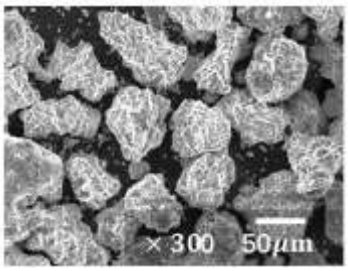

(d) KMX 80 μm

Fig.3. 10 SEM images of magnetic particles

The abrasive particles used in this study are WA particles as shown in Fig.3.11. WA is a white alumina abrasive material which is made of molten alumina crushed into particles, and composed of type a corundum crystal. The purity of Al2O3 is high purity of 98.0% or more, and it has hardness next to silicon carbide. As a widely used representative typical powder, it maintains sharp particle size distribution and stable particle shape. The WA fine powder is suited for making finishing whetstones and also as a fine-finishing on abrasive papers. Because of its superior finishing qualities, it is also suited for use as a fine-finishing on abrasive tapes. Table 3.1 shows the standard specifications of particle size. Among them, the abrasive particles used in this article were observed by SEM. Fig.3.11 is the SEM image of abrasive particles.

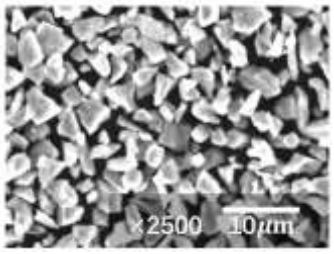

(a) WA#4000

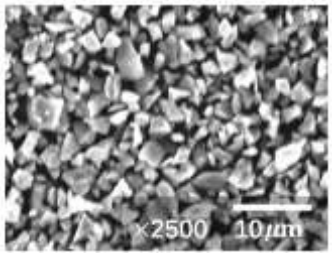

(b) WA#6000

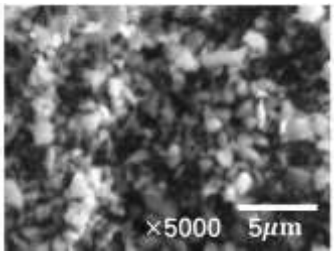

(c) WA#8000

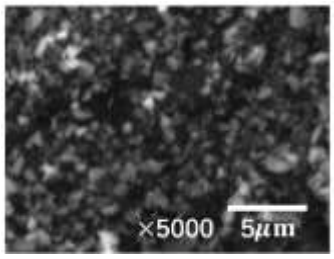

(d) WA#10000

Fig.3. 11 Images of abrasive particles by SEM

Table 3. 1 Standard specifications of particle size

Particle size	Particle distribution (μm)			
	Maximum particle size	Particle size at 3% point	Particle size at 50% point	Particle size at 94% point
# 1000	≦32.00	≦27.00	11.9 ± 1.00	≧7.00
# 1200	≦27.00	≦23.00	9.90 ± 0.80	≧5.50
# 1500	≦23.00	≦20.00	8.40 ± 0.60	≧4.50
# 2000	≦19.00	≦17.00	6.90 ± 0.60	≧4.00
# 2500	≦16.00	≦14.00	5.60 ± 0.50	≧3.00
# 3000	≦13.00	≦11.00	4.00 ± 0.40	≧2.00
# 4000	≦11.00	≦8.00	3.00 ± 0.40	≧1.30
# 8000	≦6.00	≦3.50	1.20 ± 0.30	≧0.60
# 10000	---	---	0.50 ~ 0.70	---
# 20000	---	---	0.40 ~ 0.50	---

3.5 Conclusions

In this chapter, the experimental setup of the corrective abrasive finishing using MAF is introduced in detail. The main content can be summarized as follows.

(1) The processing principle of modified planar MAF process in this study is introduced. The control circuit and mechanical structure of the experimental device are introduced. The main parameters of each part are given.

(2) The experimental setup for measuring the magnetic field strength is introduced, and the setup for measuring the pressure of the magnetic brush is designed.

(3) The magnetic particles and abrasive particles used in this study are introduced.

Chapter IV Investigation on correction MAF with 23 mm magnetic pole

Magnetic abrasive finishing (MAF) is a precision surface polishing method. At present, most studies on planar MAF are focused on improving the surface roughness accuracy and the uniformity of roughness. In practical application, the initial surface of the workpiece is not only a rough surface, but also a highly uneven plane. While the traditional processing method improves the surface roughness accuracy, the original surface is basically unchanged. In this paper, a processing method is studied. According to the uneven distribution of magnetic brushes, the reasonable distribution of processing speed and processing time can finally achieve the purpose of improving the surface flatness. At the same time, this paper analyzes the non-uniform characteristics of the magnetic pole and the magnetic brush itself, and verifies the effectiveness of the processing method through experiments.

The task of this chapter is to verify the validity and feasibility of the method proposed in this chapter through the experiment of variable speed finishing with 23mm magnetic poles. In order to achieve this goal, you need to complete the content.

4.1 Introduction

In a wide range of industrial applications, there are high requirements for fine surface finish. Therefore, a magnetic abrasive finishing (MAF) process has been proposed to produce highly finished surfaces for work pieces in critical applications such as aerospace components and semiconductor factories [52]. MAFF process is to fill the magnetic

abrasives between the magnetic pole and the work piece, and the magnetic abrasives form the magnetic brush in the magnetic field. The magnetic brush is pressed against the work piece due to the magnetic force. Because the magnetic force acting on a single magnetic particle is very small, this process can achieve a small amount of material removal and achieve ultra-precision finishing of the surface [53].

In the early works, Shinmura et al. [10] described the process principle and the finishing characteristics and analyzed the effect of the shape of the magnetic pole on the finishing properties. Gupta et al. [54] discussed the effects of process parameters such as finishing gap, current supply, input voltage, finishing time, speed, abrasive mesh size, abrasive weight, and finishing force on surface finish quality. Mulik et al. [55] study on the fabrication of ultrasonic assisted magnetic abrasive finishing (UAMAF) integrated the use of ultrasonic vibrations and magnetic abrasive finishing (MAF) process to finish surfaces to nanometer order in a relatively short time. Jiao et al. [50] developed a new experimental device to improve surface integrity and surface uniformity through various processing trajectories. Zou et al. [57, 58] proposed the MAF process using an alternating magnetic field and clarified its finishing principle. The effects of magnetic abrasives on finishing force, finishing efficiency and surface roughness were discussed, and it was proved that the MAF process using an alternating magnetic field can achieve ultra-precision finishing of ceramic work pieces.

However, there is a common problem in the uniformity of the surface for most planar MAF studies. Since the magnetic field at the edge of the magnet is strong, the magnetic flux density at the edge of the magnetic pole is high. In addition, the centrifugal effect in circular motion of the magnetic

pole makes the distribution of magnetic particles more uneven and concentrated on the edge of the magnetic pole. In the previous study, the uniform processing at a constant speed often only improved the roughness of the surface, but had little effect on the surface morphology. In order to solve this problem, this paper presents a method of variable speed processing in different regions, and proves its effectiveness through experiments.

4.2 Processing principle

The schematic of the principle of experimental setup is shown in Fig.4.1. The X-Y Stage is used to achieve precise control of the processing position. The linear slide realizes the motion control of the workpiece feed. It is filled with mixed magnetic abrasive particles (magnetic particles and abrasive particles) and abrasive fluid between the workpiece and the magnetic pole. The magnetic particles are arranged along the lines of magnetic force to form a flexible magnetic brush. The magnetic pole can rotate under the driving of the motor, and the material is removed due to the relative friction between the magnetic brush and the work piece. The distance between the magnetic pole and the work piece can be changed by changing the height of Z-adjustment, thereby changing the pressure and friction.

The rotation of the magnetic poles is driven by a DC motor, and the speed of the magnetic pole rotation is controlled by a power control device to adapt the needs of the experimental conditions. The control of the processing position is realized by inputting the control instructions in the computer to control the movement of the X-Y stage. The work piece is placed on a linear slider to linearly move the workpiece. Linear sliders can be used to move at different speeds in different region.

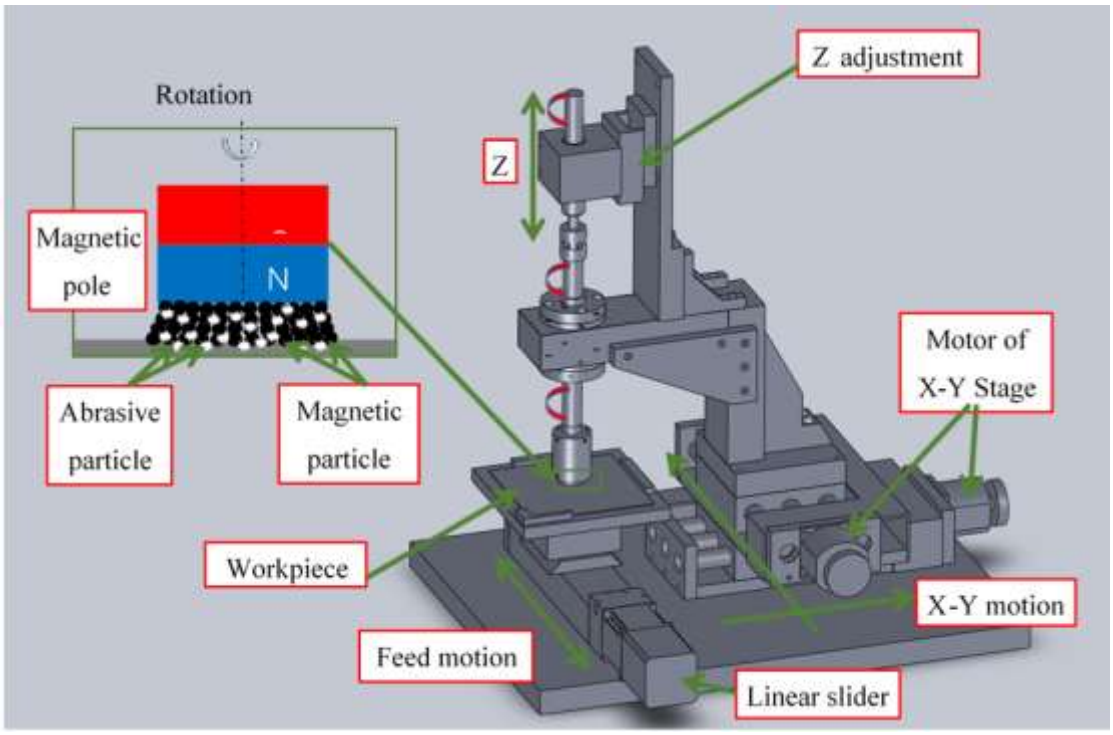

Fig.4. 1 The schematic of the principle of experimental setup

4.3 Magnetic pole simulation

The magnetic pole of this design is composed of two 12.5mm high cylindrical artificial magnets and a 5mm high cylindrical iron core, as shown in Fig.4.2 (a). Fig.4.2 (b) shows the distribution of magnetic particles on the magnetic pole. It can be seen from the figure that the magnetic particles are mainly concentrated on the edges. The width of the magnetic brush is about 6mm. There are almost no magnetic particles in a circle with an intermediate diameter of about 14mm. At the same time, due to the high-speed rotation of the magnetic pole during the finishing process, the centrifugal movement of the magnetic particles is caused, which further exacerbates its marginalization. It is precisely because of the marginalization of magnetic particles that it leads to uneven processing.

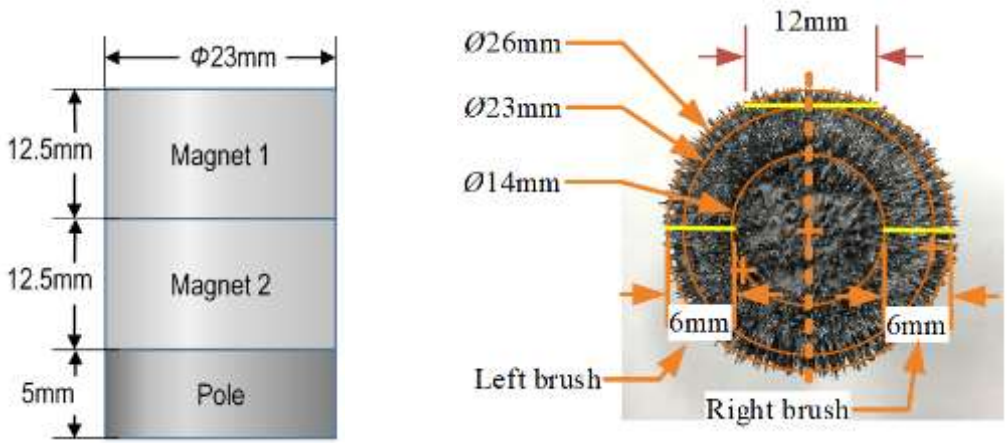

(a) Magnetic pole (b) Distribution of magnetic particles

Fig.4. 2 Distribution of magnetic particles

The magnetic field is simulated near the magnetic pole by using Magnet 7 software. Table 4.1 is the parameter setting of each component of the simulation experiment. Fig.4.3 are the simulation results. From Fig.4.3(a), we can see the distribution of magnetic lines of induction in the entire simulation area. Fig.4.3 (b) is a simulation analysis of the magnetic field distribution on the under surface of the magnetic pole. Fig.4.3 (c) is the magnetic field intensity curve at 0.5mm from the magnetic pole. According to the simulation results of Magnet 7 software, it can be seen that for a magnetic pole composed of a cylindrical magnet and a cylindrical iron, the magnetic field strength is the strongest at the edge, but the magnetic field strength at the center of the pole is almost zero.

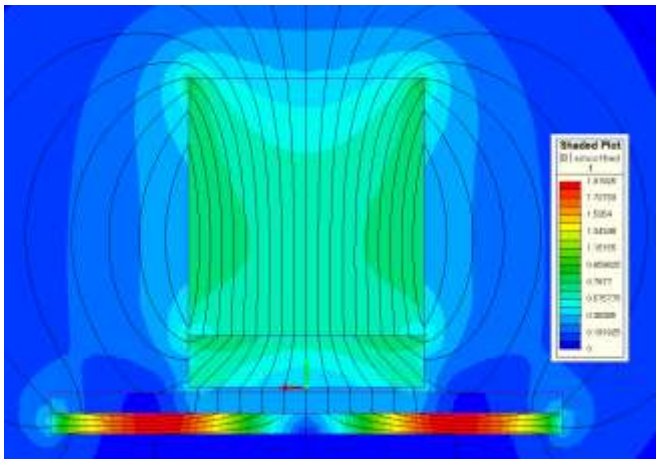

(a) Magnetic flux lines

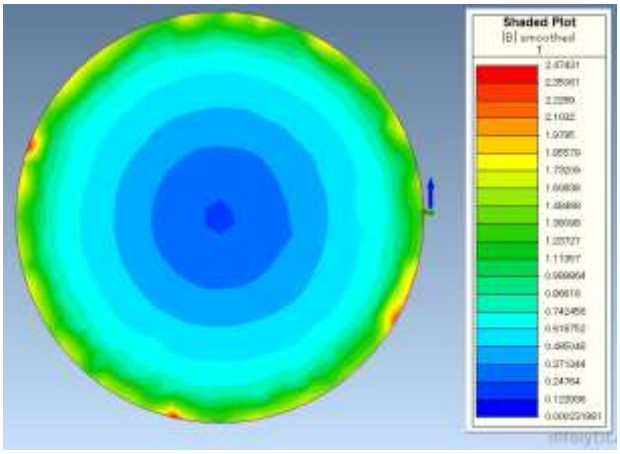

(b) Magnetic field simulation at bottom of magnetic pole

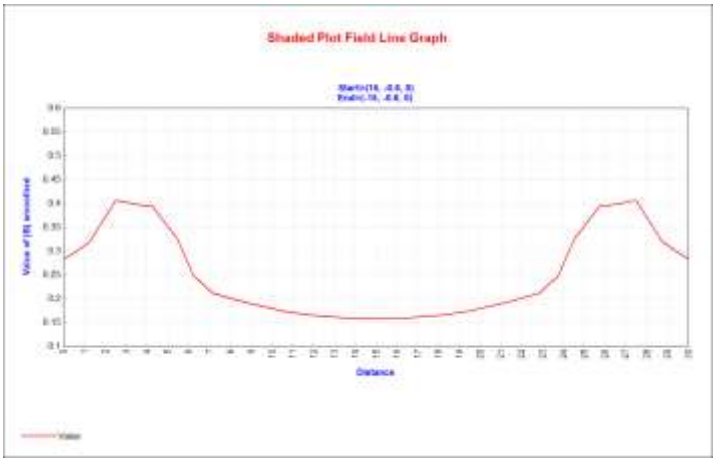

(c) Magnetic field intensity curve at 0.5mm from the magnetic pole

Fig.4. 3 Simulation models of 23 mm magnetic pole

Table 4. 1 Simulation conditions

Components	Mesh (mm)	Materials	Size (mm)
Magnet	1	NdFeB: Neodymium Iron Boron	$\emptyset 23 \times 25$
Magnetic Pole	0.1	MU3: Relative permeability 1000	$\emptyset 23 \times 5$
Gap	0.5	AIR	
Workpiece	1	Aluminum	$100 \times 100 \times 2$
Iron plate	1	MU3: Relative permeability 1000	$100 \times 100 \times 2$
Air	1	AIR	$200 \times 200 \times 200$

4.4 Fixed-point processing experiment

Experimental conditions are show in Table 4.2. Here, a finishing gap of 1 mm and a rotation speed of 500 revolutions per minute are used to process the fixed position of the SUS304 steel plate for 5 minutes. Mixed type of magnetic abrasive is 3 g of 149μm iron powder & 1 g of #8000 WA particles and 1.0 ml of Oil-type.

Figure 4.4 shows the results after continuous processing at the fixed position for 5 minutes. It will generate a circular finishing area. The surface morphology before and after processing is measured along the axis of the processing area. Fig.4.4 (a) is the surface curve before processing, and Fig.4.4 (b) is the surface curve after processing. The results show that at the edge of the magnetic pole, the amount of material removed is obvious, while the central part of the magnetic pole hardly changes. The effective processing area is equal to the width of the magnetic brush, 6 mm on each side.

Table 4. 2 Experimental conditions

Workpiece	SUS304 stainless steel plate (100× 100×1 mm)
Magnetic pole	Nd-Fe-B rare earth permanent magnet (Ø23× 24 mm)
Mixed type of magnetic abrasive	3 g of 149μm iron powder & 1 g of #8000 WA particles
Abrasion liquid	Oil-type : 1.0 ml
gap	1.0 mm
Finishing time	5 min
Rotation speed	500 rpm

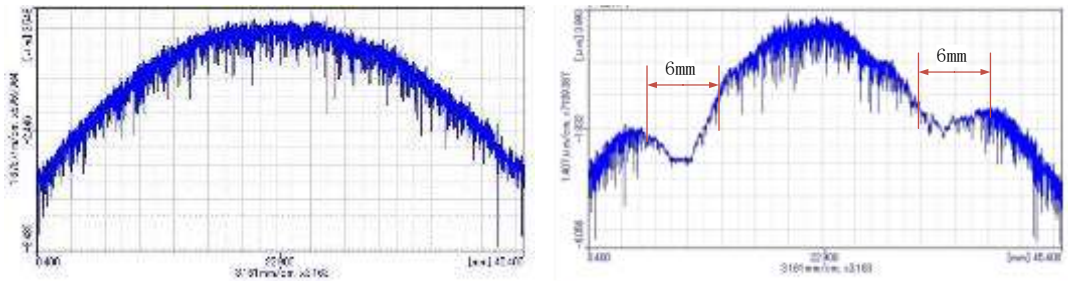

（a） Before processing （b）After processing

Fig.4. 4 Analysis of fixed-point processing data

Using the same method, process different positions of the same steel plate for 5, 10, 15, and 20 minutes, and measure the experimental results. After processed, we measure the profile along the yellow center line. The measurement result is shown in Fig.4.5.

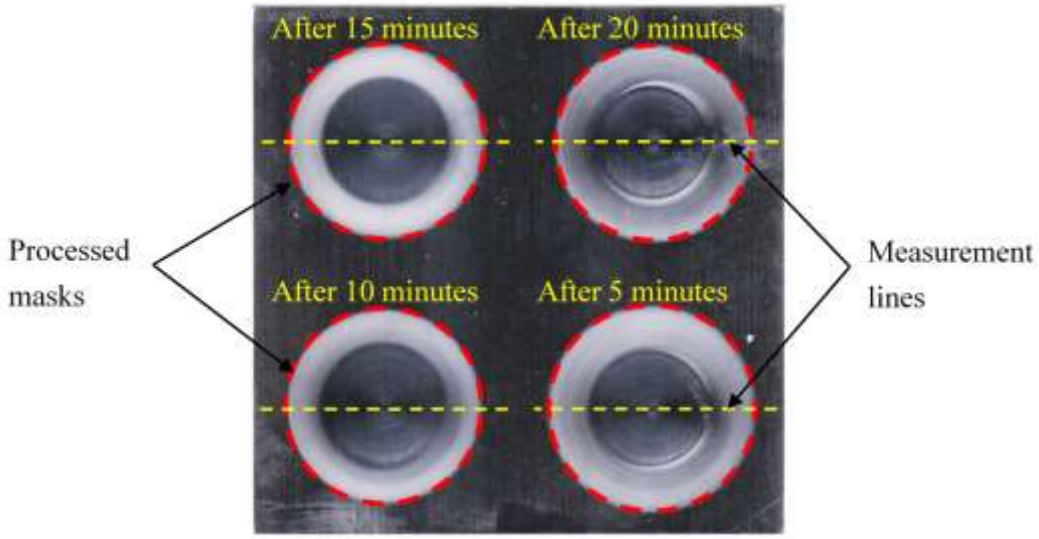

Fig.4. 5 Experiments of fixed-point processing

4.5 Uniform speed and variable speed finishing experiment

As shown in Fig. 4.5, a circular finishing area with a width of 6 mm is produced. If the direction of horizontal to right is used as the processing direction, the magnetic brush can be regarded as two parts of left and right, as shown in Fig.4.2 (b). The magnetic brush width of the two parts is about 6mm. The magnetic brush on the right part is finishing at the front, and then the magnetic brush on the left part is finishing at the behind. The time interval between the two parts of the magnetic brush processing is equal to the distance between them divided by the feed speed. The farther from the axis in the finishing direction, the smaller the distance between the two parts of the magnetic brush until they are joined together, and the distance is about 0 mm. If the processing length is 6mm (magnetic brush width) as a unit, the equivalent processing time of two magnetic brushes with a distance of 0mm for each area is shown in Table 4.3 when the workpiece is moved at a constant speed.

Table 4. 3 Equivalent area finishing time for uniform speed processing

Area No.	1	2	3	4	5	6	7	8	9	10
Left Brush	T	T	T	T	T	T	T	T	T	
Right Brush		T	T	T	T	T	T	T	T	T
SUM	T	2T	2T	2T	2T	2T	2T	2T	2T	T

It can be seen from Table 4.3 that, in terms of processing time, the area No.2-9 corresponds to the processing time of 2T. The time distribution is relatively uniform. In this way, the removal amount should be consistent, so the surface shape of the work piece should not change except for the roughness. Then if we allocate the processing time in different areas according to the original height of the work piece, we should get different results. Suppose we change the processing time by changing the feed speed, as shown in Table 4.4, assign the processing time of each area. The results show that the intermediate processing time is the longest, so the removal amount should be the largest. In this way, we expect to achieve the purpose of improving the surface flatness through this method.

Table 4. 4 Equivalent finishing time of variable speed processing

Area No.	1	2	3	4	5	6	7	8	9	10
Left Brush	1T	3T	5T	5T	5T	5T	5T	3T	1T	
Right Brush		1T	3T	5T	5T	5T	5T	5T	3T	1T
SUM	1T	4T	8T	10T	10T	10T	10T	8T	4T	1T

In order to improve the contrast of the experiment, three methods of processing were performed on the same work piece. As shown in Fig.4.6 (a), processing is performed at a uniform feed speed. As shown in Fig. 4.6(b), in the position of the vertical line, the processing time is different. Then quickly move to the next vertical line position. As shown in Fig.4.6(c), processing is performed at different feed speeds in different segments. The length of time for zone variable speed processing is allocated according to the ratio in Table 4.4. And T = 1min, then the processing time and speed of each area are shown in Table 4.5. The total processing time is 33 minutes. The upper area is selected for uniform speed processing, but in order to be comparable, the processing time is also set to 33min, and the processing distance is set to 6 ×(9+1) = 60mm. Therefore, the speed is set to 0.027 mm/s. Experimental conditions are show in Table 4.2.

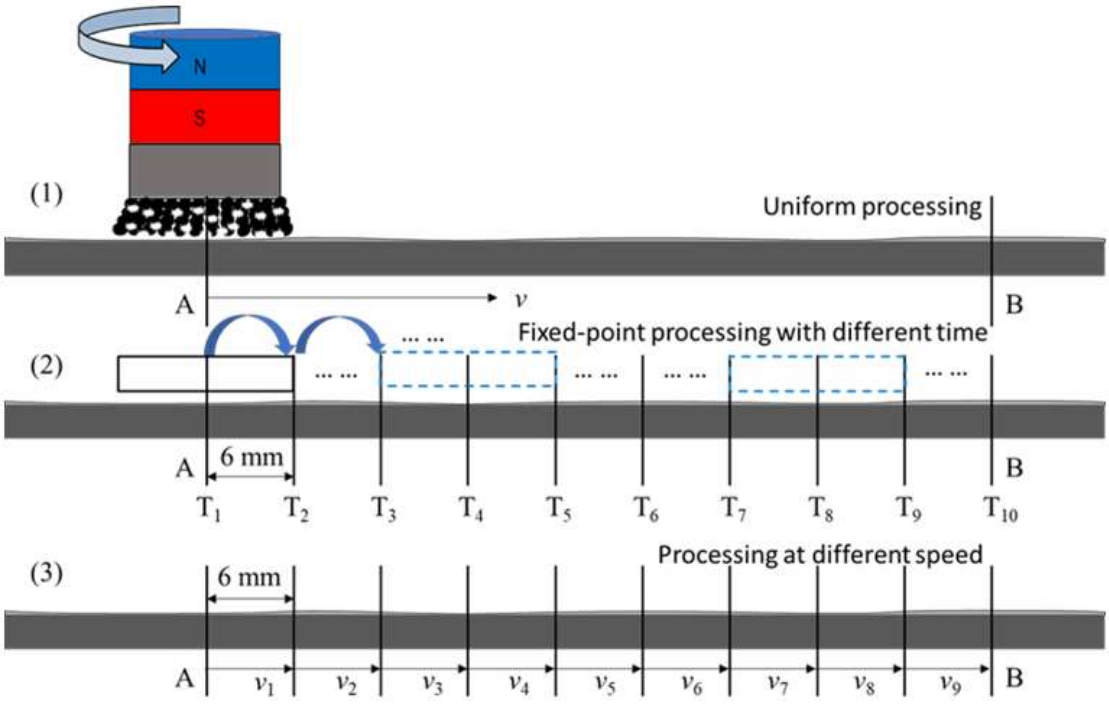

Fig.4. 6 3 kinds of processing methods: (a)Uniform processing(b)Fixed-point processing with different time (c)Processing at different speed

Table 4. 5 Time and speed distribution of variable speed processing

Area No.	1	2	3	4	5	6	7	8	9
Time(min)	1	3	5	5	5	5	5	3	1
Speed(mm/s)	0.1	0.033	0.02	0.02	0.02	0.02	0.02	0.033	0.1

Before and after processing, use a surface roughness tester (Surface SV-624-3D) to test the surface topography along the processing direction to measure the surface curve.

4.6 Experimental Results and Analysis

Figure 4.7 is photos of the processed workpiece with three different processing methods, and the positions of the measurement curves are marked on it. Fig.4.7 (a) is the photo of the processed workpiece at the uniform speed processing. Fig.4.7 (b) is the photo of the processed workpiece at a fixed point with variable time. Fig.4.7 (c) is the photo of the processed workpiece at variable feed speed processing. From the appearance, the workpiece processed by the second method has obvious boundaries because the processing of the magnetic brush is discontinuous. The surface processed by the first method and the third method is not very different in appearance. Because processing is continuous, there are no sharp boundaries. Therefore, it is necessary to further measure the contour curve for judgment. Some profile curves were measured through the SV-624-3D, along the dotted line in the figure. The measurement results are shown in the Fig.4.8, Fig.4.9 and Fig.4.10.

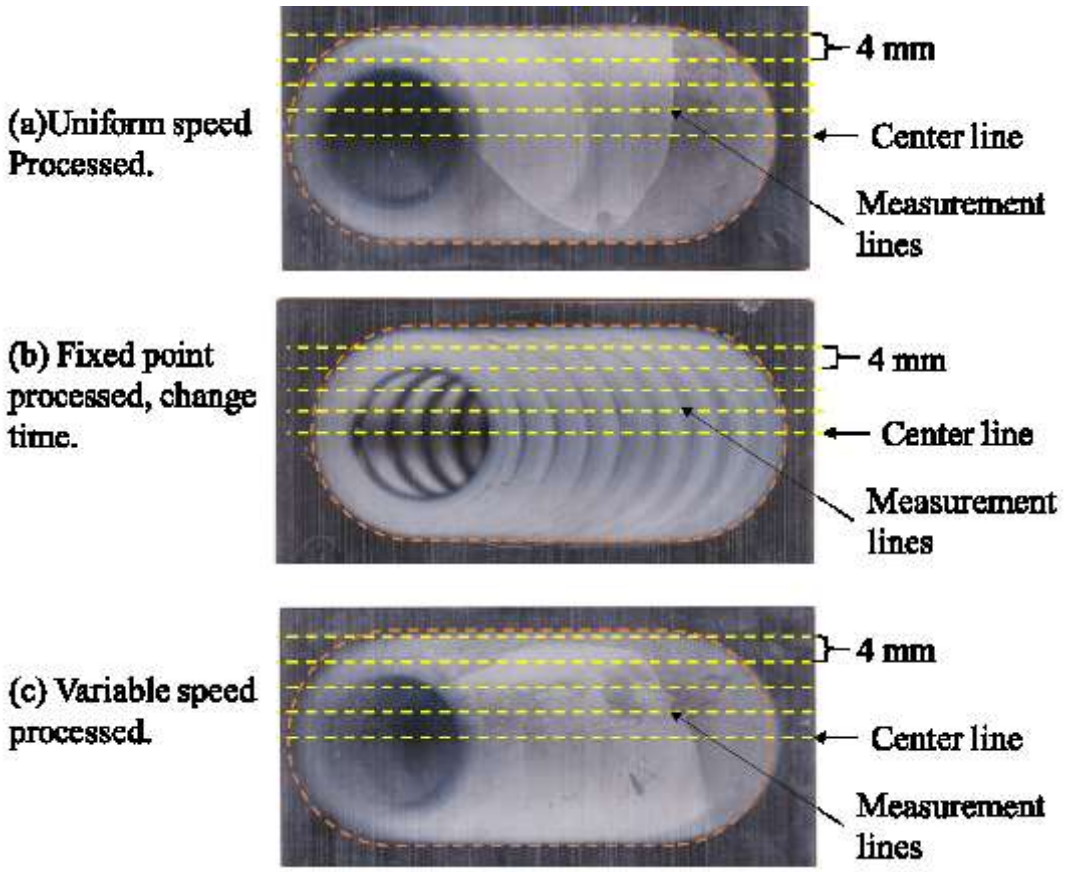

（b） Uniform speed processing and variable speed processing

Fig.4. 7 The position of processing and measurement

As shown in Fig.4.8, it is a comparison of the surface curves before and after finishing by the uniform speed processing. It can be seen that after processing, the surface smoothness is improved, but the surface morphology is still almost no change at all.

As shown in Fig.4.9, it is a comparison of the curves before and after processing at a fixed point change time. It can be seen from the figure that the processing is relatively uniform in the edge part and the center line part of the processing track when using the fixed-point processing. But it is not very obvious, and the other positions will produce concave and convex changes as shown in Fig.4.9 (b). The reason for the uneven change is that fixed-point processing leads to the processing discontinuous.

As shown in Fig.4.10, the variable feed speed processing is performed according to the different processing time of different areas. It can be seen from the figure that due to the continuity of motion, the processed surface changes relatively uniformly, and it has a corrective effect.

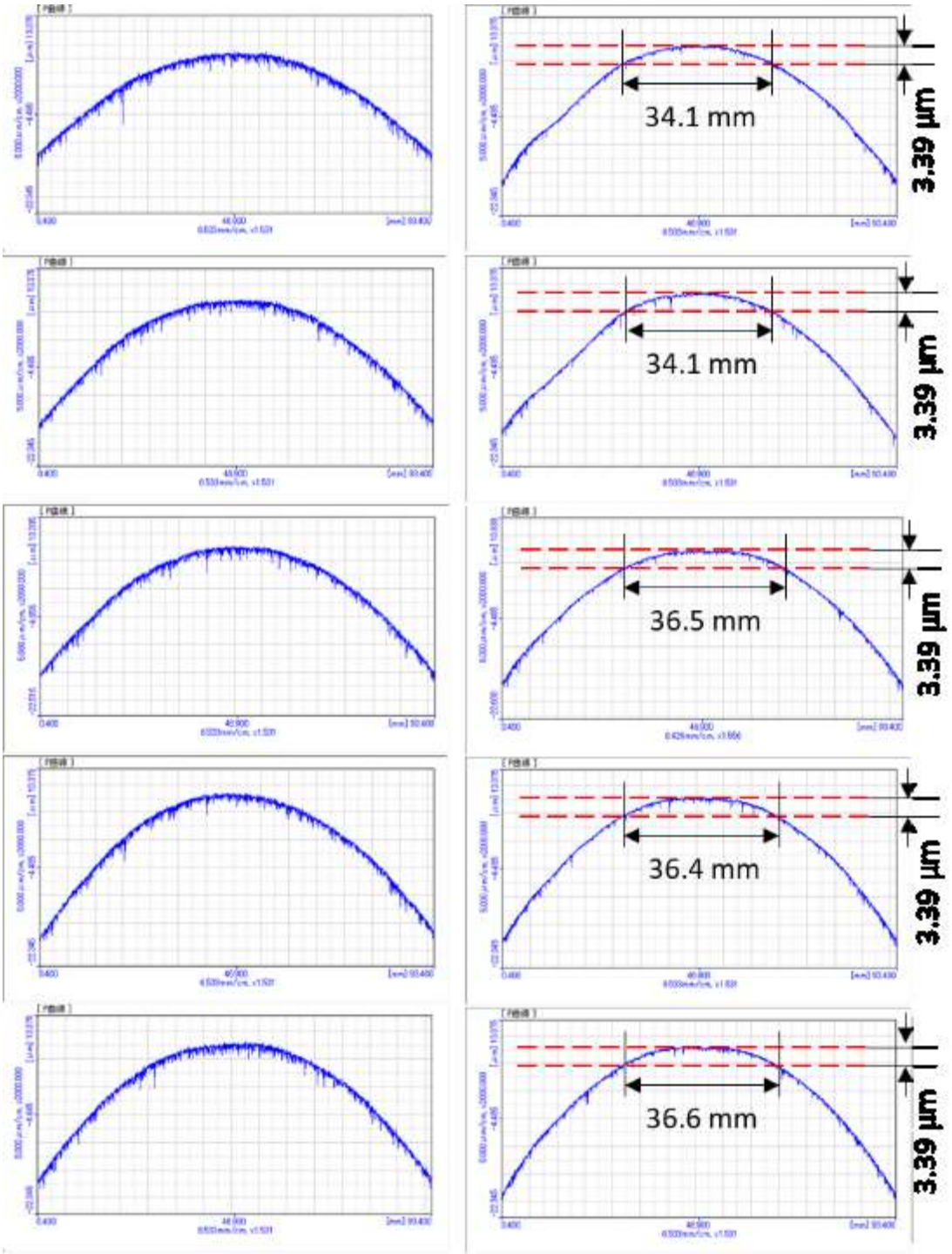

Fig.4. 8 Surface comparison before and after uniform speed processing

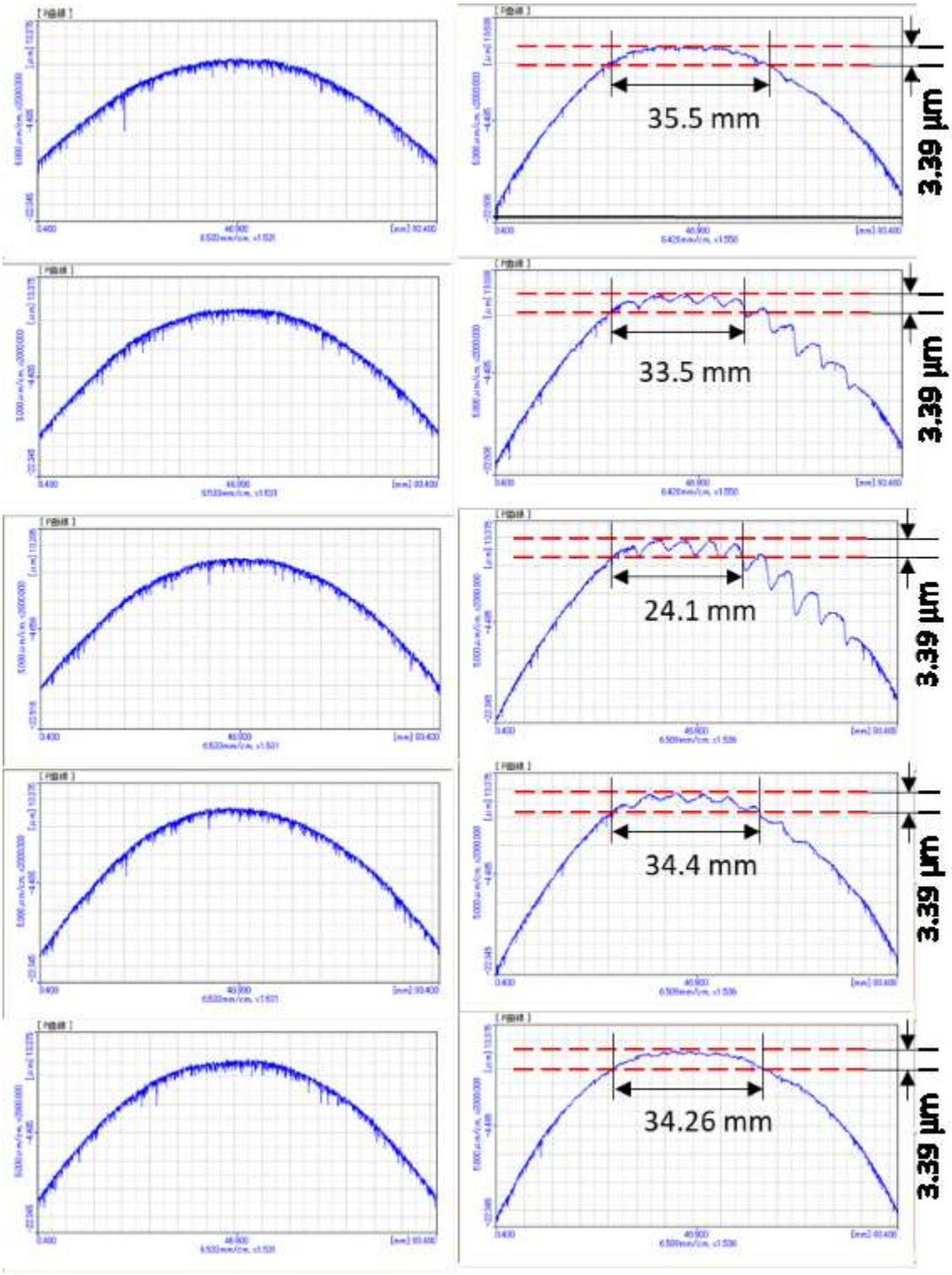

Fig.4. 9 Surface comparison before and after fixed-point and change-time processing

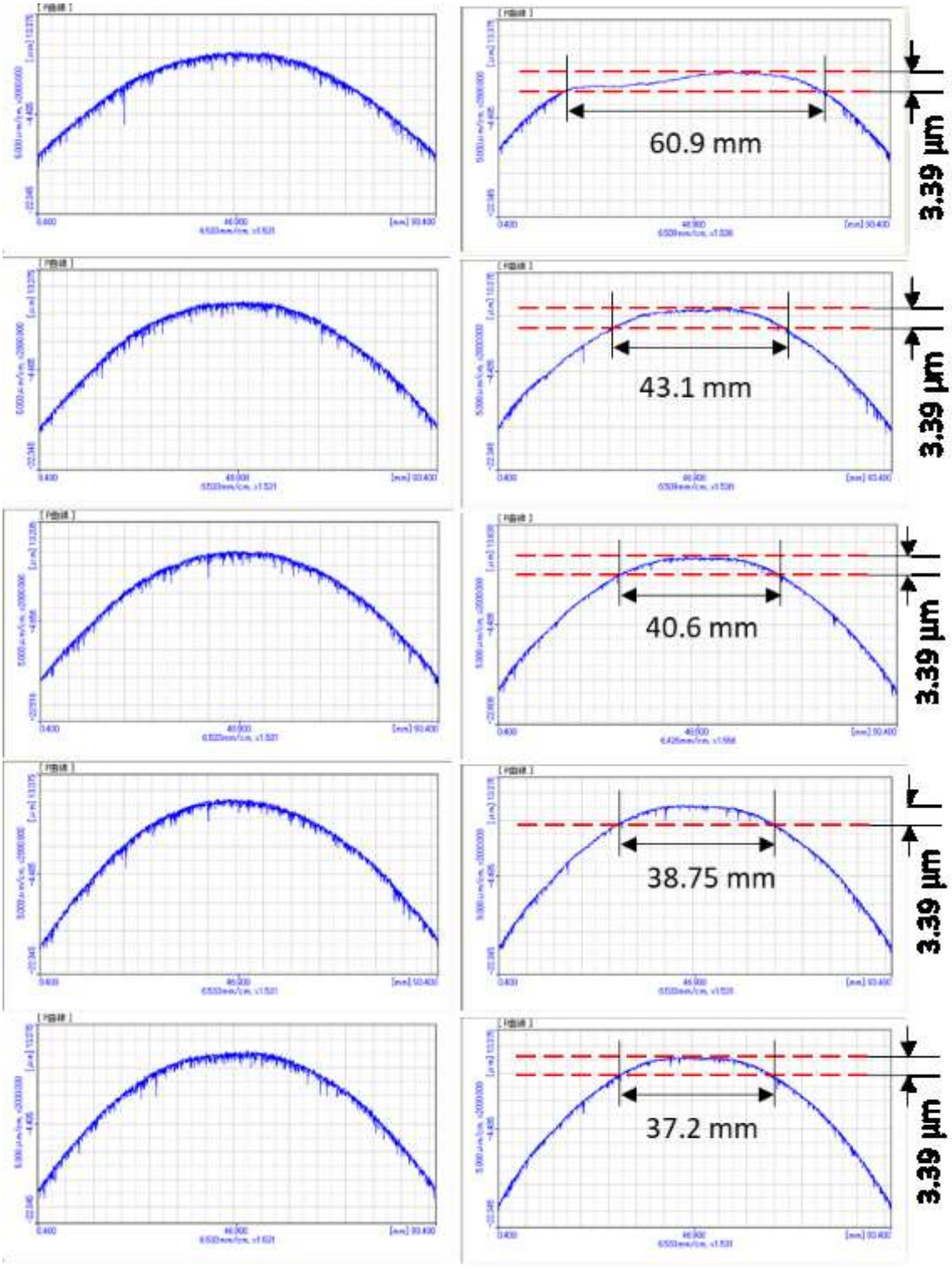

Fig.4. 10 Surface comparison before and after variable feed speed processing

In the edge part of the processing track, the effect is the best, and the closer to the center line, the worse the effect. This is because at this position, the left and right parts of the magnetic brush are continuous, which can well satisfy the time allocation in Table 4.4. However, as the distance between the left and right parts of the magnetic brush is getting farther and farther, it cannot realize the time allocation in Table 4.4. When we take a height difference of 3.39 μm to measure Fig.4.10, it is reduced from 60.9mm on the upper edge of the processing track to 45.5 mm on the center line. Therefore, it can be concluded that the closer the left and right parts of the magnetic brush, the better the correction effect.

Figure 4.11 is the movement trajectory of the magnetic brush simulated by Graph software at different movement conditions. Fig.4.11 (a) is a motion trajectory of the outer edge of the magnetic brush at moving at a constant speed. Fig.4.11(b) is a motion trajectory of the outer edge of the magnetic brush when the speed is changed in every 6 mm. The speed is set according to Table 4.3 (uniform speed processing) and Table 4.4 (variable speed processing). It can be clearly seen that the grid density of each point on the same horizontal line in Fig.4.11 (a) is very uniform, and the processed amount of each point of the work piece is the same. In Fig.4.11 (b), the grid density of each point is different, and the amount processed is greater for areas with dense grid. In contrast, areas with sparse grids have smaller processing amount. The results of the above simulations and experiments are consistent with the design ideas of this article.

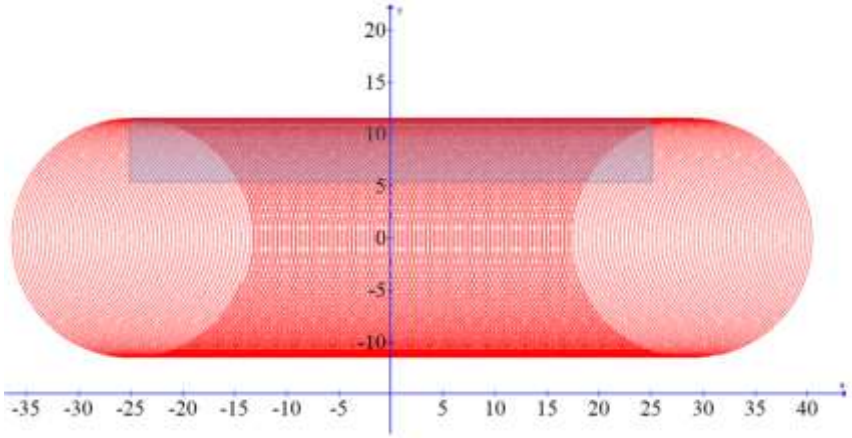

(a) Uniform speed processing

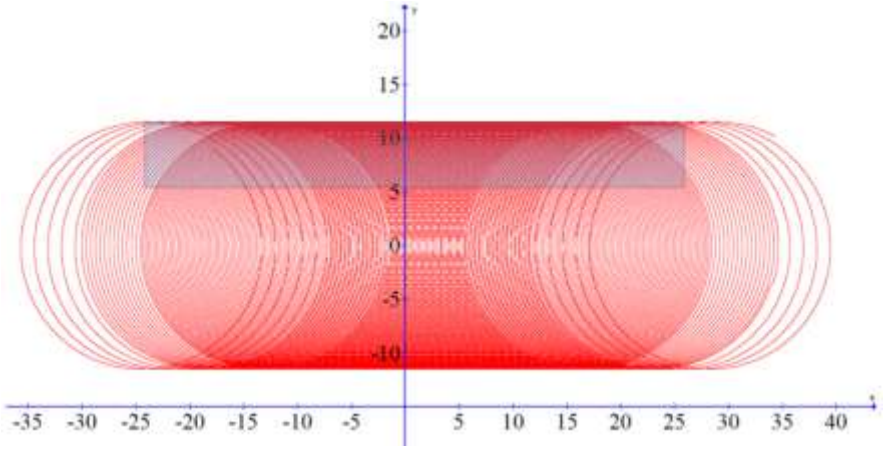

(b) Variable speed processing

Fig.4. 11 The trajectory of magnetic brush in different motion

4.7 Conclusions

This chapter proposed a method to modify the surface profile by changing the feed speed of the work piece in different areas. It is proved that the method is effective and feasibility through the consistency of experimental and theoretical analyses. Conclusions are summarized as follows:

(1) In this chapter, the feasibility of improving the flatness of the workpiece surface by this method is proved by experiments and theoretical

analysis.

(2) Since the distribution of the magnetic field on the magnetic poles is not uniform, it leads to non-uniform distribution of magnetic particles, and mainly concentrated on the edge of the magnetic pole. This is the main factor affecting flatness.

(3) The surface roughness can be improved after uniform speed processing, but because the effective processing time of each part is equal. There for, the surface morphology is basically consistent with the original surface morphology.

(4) The surface roughness accuracy and the surface smoothness are improved by this method. By performing variable speed treatment in different areas, the position with high initial surface is processed for a long time, and the processing time with low initial surface is short, thereby achieving the purpose of improving the overall surface flatness.

Chapter V Investigation on correction MAF with 1 mm magnetic pole

On the basis of ordinary plane magnetic abrasive finishing, a processing method is proposed that can corrective the profile of plane. This method is to plan the feed speed during processing according to the height change curve of the initial surface and the processing effectiveness of magnetic abrasive finishing, so as to control the effective finishing time of different areas, and finally obtain the consistent height on the surface of the workpiece. In order to accurately trim the surface of the workpiece, a small magnetic pole with diameter of 1mm is designed, and a ferromagnetic plate is placed under the workpiece to make the magnetic field distribution relatively uniform near the magnetic pole. The experiment on the aluminum plate (A5052) proves that after 60 minutes of processing using this method, the extreme difference of the workpiece surface height can be reduced to 2.18μm, and the standard deviation can reach 0.4μm. At the same time, the measurement results performed at different positions in the finishing area can achieve similar flatness. The variable speed finishing method compared with the uniform speed processing obvious improvement in flatness.

5.1 Introduction

With the rapid development of electronic technology, optical technology, aerospace technology, etc., in many fields, the requirements for the surface accuracy of the workpiece are getting higher and higher. This includes both the smoothness of the surface and the shape accuracy of the surface [59,52].

The Magnetic abrasive finishing(MAF) process uses magnetic particles to form a flexible brush-like structure under the action of a magnetic field, and mixes the abrasive particles between the magnetic particles, and uses a motor to drive the magnetic brush to move, thereby driving the abrasive particles to move relative to the workpiece to achieve the finishing of the workpiece The effect is to realize the finishing of the surface [10].

In the previous research, Shinmura et al. conducted a detailed study on the basic principles and basic characteristics of MAF, and developed a plane magnetic polishing device using electromagnets [504, 15]. Shinmura, Yamaguchi et al. [60, 20] applied MAF technology to the processing of cylindrical outer surface and tube surface processing, and analyzed the influence of magnetic pole shape on finishing performance. Yamaguchi [21] applies magnetic abrasive finishing technology to the processing of curved tubes. The research reveals a mechanism that smooth the inner surface of alumina ceramic tubes and improves roundness accuracy. Jeong-Du Kim et al. [30] developed a new concept of finishing technology or electromagnetic abrasive jet processing system, which can complete the processing of curved pipes, and predicts the processing conditions through simulation, and analyzes some characteristics of the finishing. Yin SH, Shinmura [61, 62] proposed the vibration-assisted MAF process to polish 3D micro-curved surfaces, and discussed the vibration of the workpiece under three vibration modes (horizontal vibration, vertical vibration and compound vibration) on the magnetic field, and studied the influence of polishing pressure, abrasive performance and abrasive performance on polishing performance during processing. Mulik RS et al. [63] conducted research on ultrasonic-assisted magnetic abrasive finishing and designed an experimental device. This technology can finish the surface to

nanometer level in a short time. Experiments show that within 80 s, UAMAF can obtain surface roughness values as low as 22 nm on AISI 52100 hardened steel workpieces. Misra A et al. [64] established a mathematical model for the material removal of ultrasonic-assisted magnetic abrasive finishing, and the total material removal is attributed to two simultaneous independent phenomena-steady-state material removal and transient material removal. The model indicates that there is an exponential relationship between MR and completion time. Sun et al. [41] have proposed an effective method of combining surface magnetic abrasive finishing (MAF) and electrolysis. Through the EMAF process, the surface roughness can be reduced from the original roughness of 393.08 nm Ra to 30.94 nm Ra within 40 minutes. Zou and Xing [40, 58, 65] further studied the relationship between electrolysis current and processing efficiency, and refined the surface of aluminum alloy A5052. Wu [36] proposed an ultra-precision magnetic abrasive finishing process using a low frequency alternating magnetic field to increase the surface roughness of SUS304 stainless steel plate from 240.24 nm to 4.38 nm. Based on this, Zou [53] proposed a method for surface polishing of alumina ceramics through the use of a low frequency AC magnetic field magnetic abrasive polishing (MAF) process, and studied the influence of important process parameters on the finishing performance. They analyzed the feasibility of super finishing 5052 aluminum alloy sheet, and analyzed the influence of relevant process parameters on finishing performance. The experimental results show that the surface roughness of 5052 aluminum alloy plate increases from 318 nm to 3 nm within 15 minutes [38].

However, planar MAF also has some technical difficulties. For example, due to the edge effect of the magnetic field distribution of the circular

magnetic pole, the magnetic field strength at the edge of the magnetic pole is high, while the magnetic field strength at the center position is weak, which leads to uneven distribution of magnetic particles, so that the pressure on the workpiece is different at each point of the magnetic brush. Lead to surface of the workpiece is uneven surface. Zou Y H, Jiao [49, 50] proposed a processing method to change the trajectory of the magnetic brush. On the basis of the rotation of the magnetic brush, the movement of revolution is added to improve the uniformity of the polishing surface. Zou conducted further studies on this method and proved that the revolution radius is an important factor affecting the surface flatness, and proposed an effective method for evaluating the surface profile [51].

5.2 Processing principle

Magnetic abrasive finishing technology is that magnetic particles form a brush-like structure under the action of a magnetic field, driven by a rotating motor, the abrasive particles move to achieve the effect of removing material. Fig.5.1 is a schematic diagram of the principle of processing. The magnetic poles and magnetic particles are magnetized under the function of the magnet, and the magnetic particles are arranged in order to form a brush-like structure. The abrasive grains are mixed in the brush-like structure. Driven by the motor, the magnet, magnetic pole, and magnetic brush rotate together to push the abrasive particles to move relative to the workpiece, so the workpiece can be finished in the feed direction. The iron plate under the workpiece helps to strengthen the magnetic field strength near the pole end face.

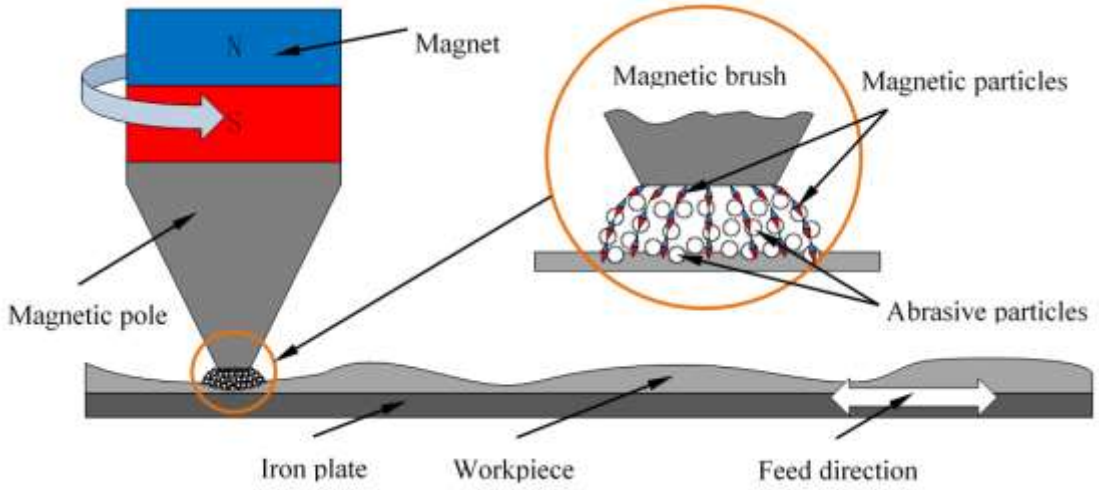

Fig.5. 1 Schematic of finishing principle

When the surface morphology of the workpiece has ups and downs, according to the changes of the surface morphology, the processing time of each area can be reasonably allocated to reduce the surface height difference.

5.3 Magnetic field analysis

5.3.1 Simulation of magnetic field

In this study, the magnetic pole is composed of a cylinder and a frustum cone and the material is SS400 (JIS). The shape of the magnetic pole is shown in Fig.5.2. The height of the cylindrical part is 5mm, and the diameter of the bottom surface is 23mm. The height of the frustum cone is 30mm, the diameter of the large base is 23mm, there are 3 types of diameters of the small base, namely 1mm, 2mm and 3mm. In order to study the influence of the change of the magnetic pole shape on the magnetic field distribution, the "Magnet7" software is used to simulate the magnetic field distribution of the magnetic pole. Based on the above dimensions,

simulation models were established, as shown in Fig.5.3. The simulations were carried out with and without the magnetic plate under the workpiece. Table5.1 shows the parameters of each component in the simulation experiment.

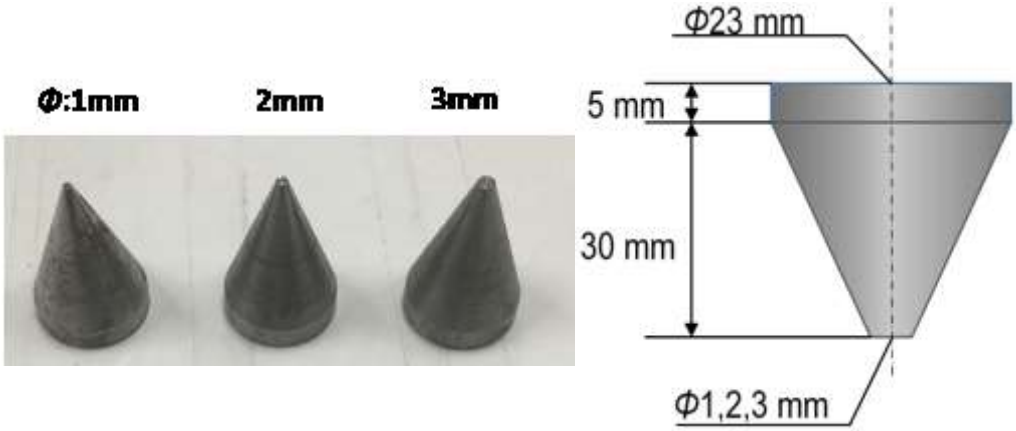

Fig.5. 2 Magnetic pole shape

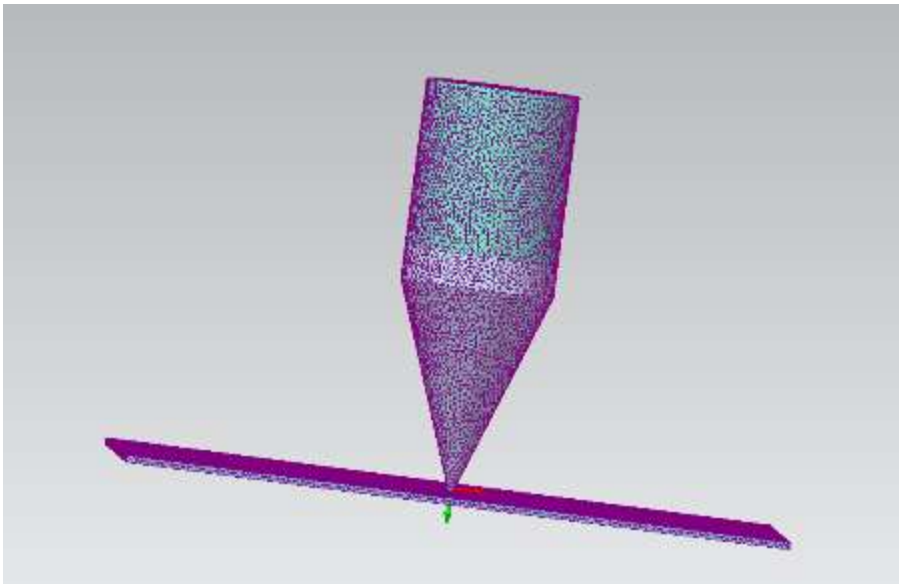

Fig.5. 3 Simulation model of magnetic pole

Table 5. 1 Simulation conditions

Components	Mesh (mm)	Materials	Size
Magnet	1	NdFeB: Neodymium Iron Boron	Ø23 mm × 25 mm
Magnetic Pole	0.1	MU3: Relative permeability 1000	Cylinder: Ø23 mm × 5 mm, Frustum cone: Large base diameter is 23 mm, Small base diameter is 1 mm, Height 35 mm.
Gap	0.5	AIR	
Workpiece	1	Aluminum	100 mm × 100 mm × 2 mm
Iron plate	1	MU3: Relative permeability 1000	100 mm × 100 mm × 2 mm
Air	1	AIR	200 mm × 200 mm × 200 mm
Iron power	0.1	MU3: Relative permeability 1000	149 μm

The simulation results are shown in Fig.5.4 and Fig.5.5. It can be seen that the magnetic pole has the strongest of the magnetic field at the edge of the bottom surface, which is due to the edge effect. However, the magnetic field strength at 0.2mm below the magnetic pole is relatively uniform. This has nothing to do with whether a magnetic plate is placed under the workpiece, and the same conclusions can be obtained. But, after adding the magnetic plate, the magnetic field strength became significantly stronger, from 0.73T to 1.25T at 0.2mm.

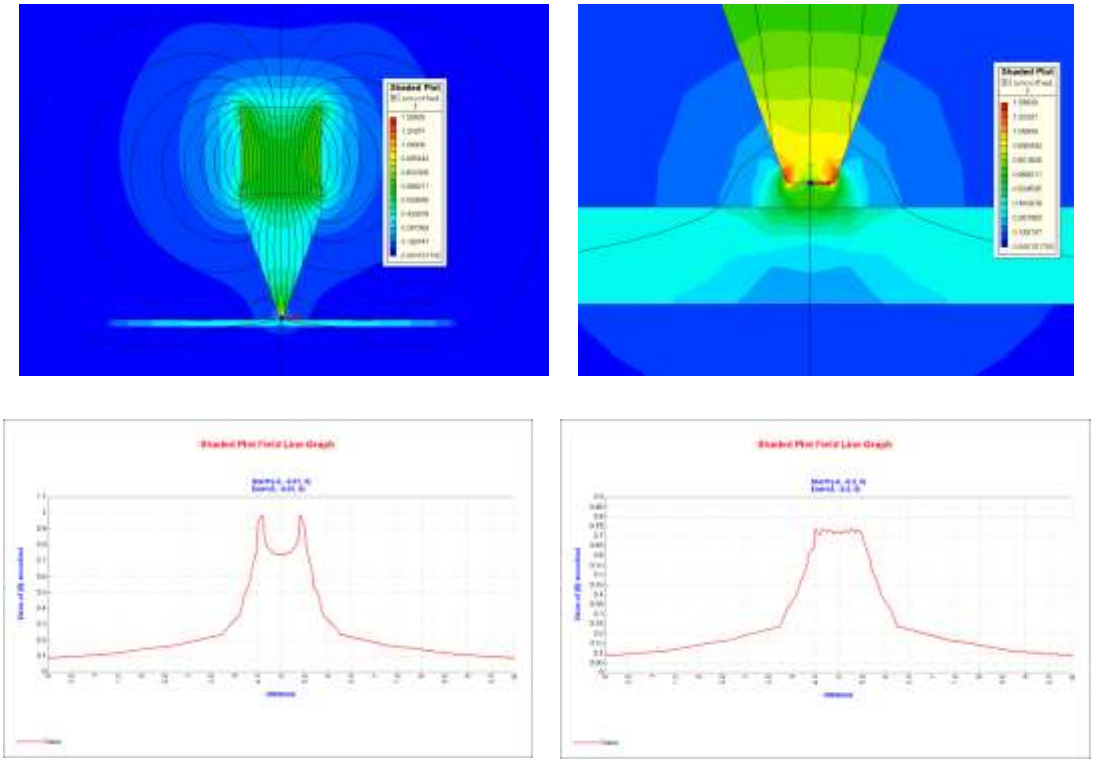

Fig.5. 4 The simulations without the magnetic plate under the workpiece

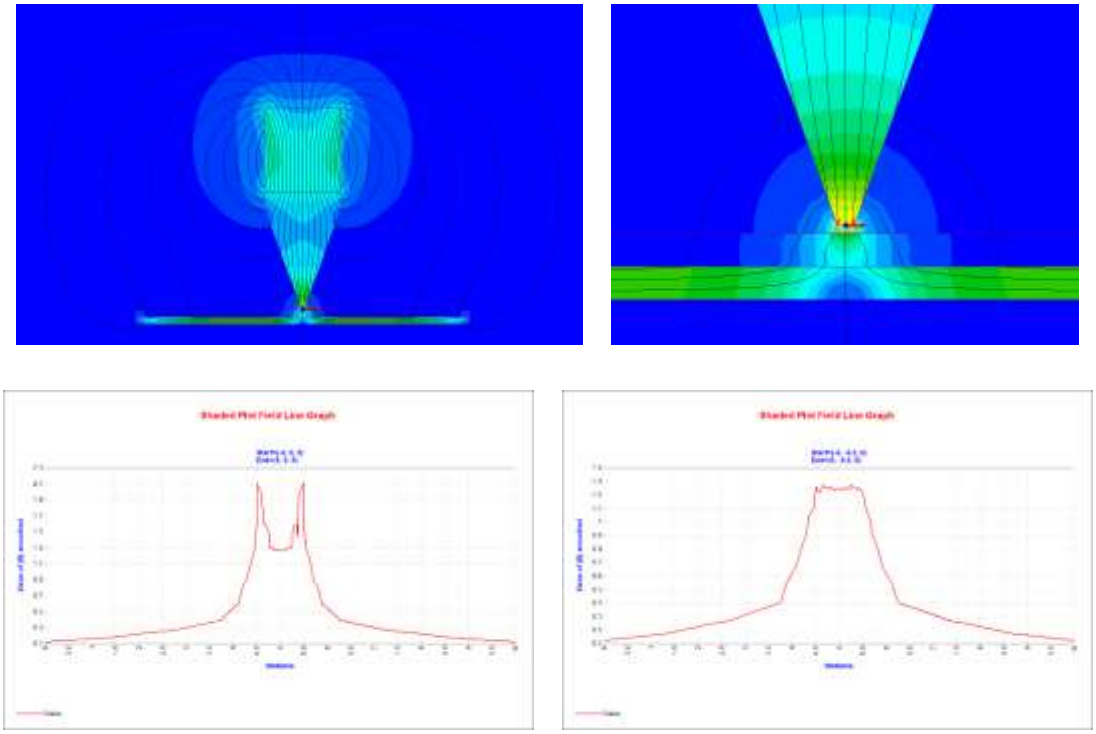

Fig.5. 5 The simulations with the magnetic plate under the workpiece

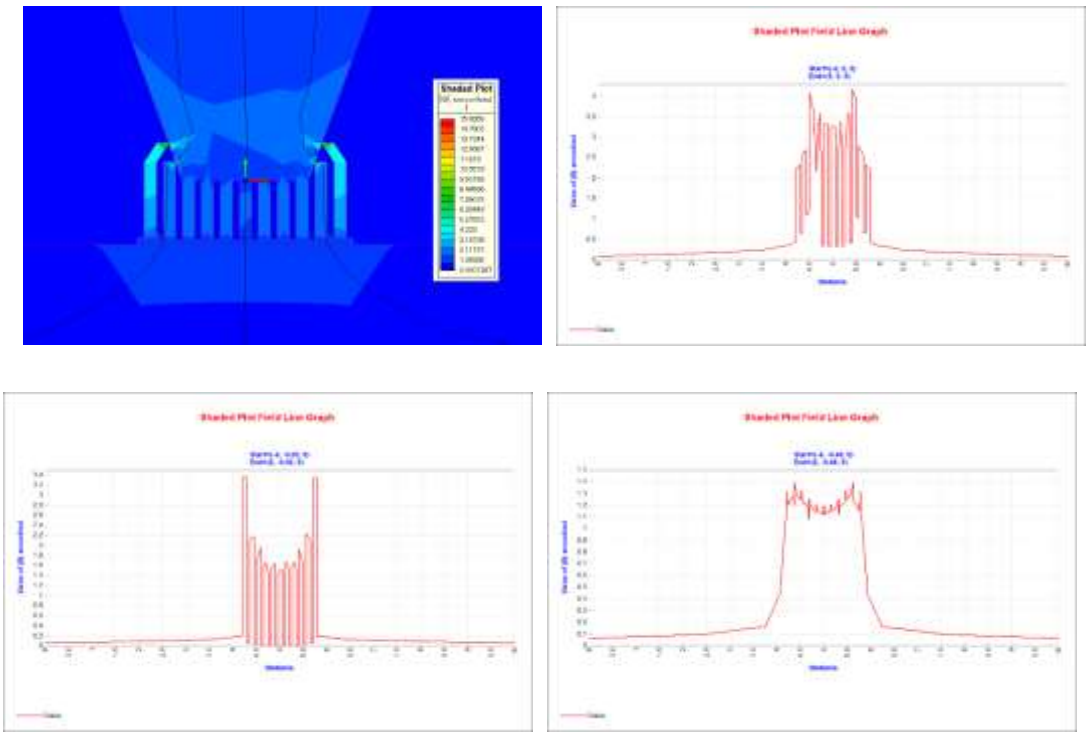

Fig.5. 6 The simulations with magnetic particles and without the magnetic plate

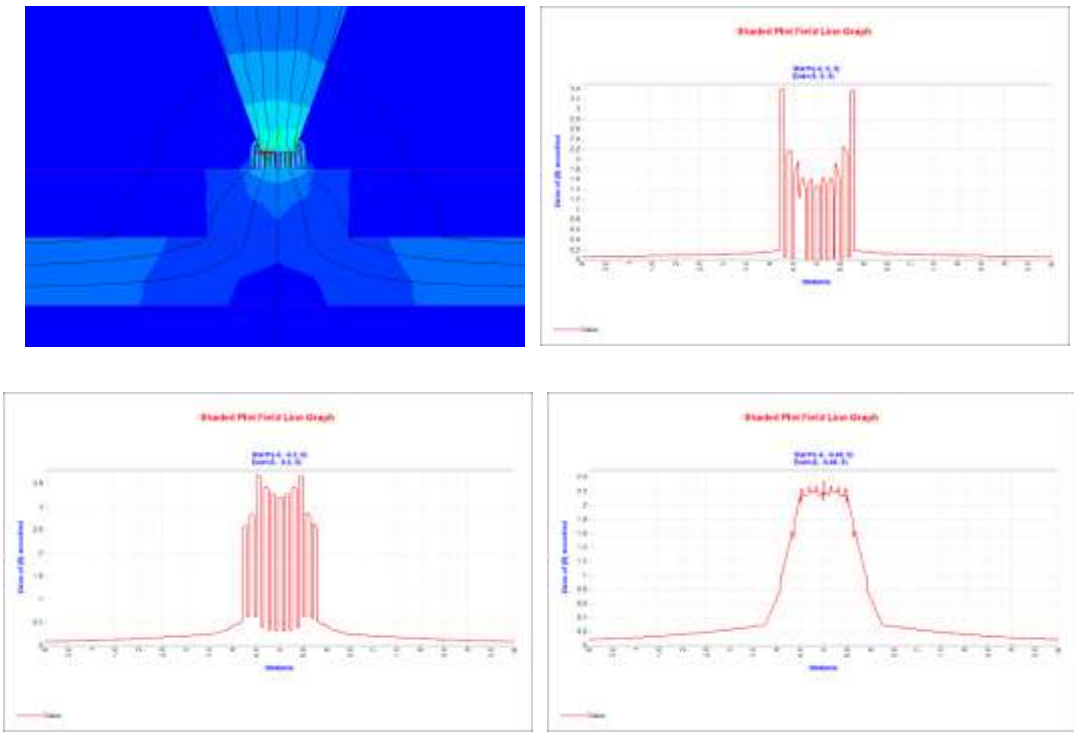

Fig.5. 7 The simulations with magnetic particles and with the magnetic plate

Figure 5.6 and Figure 5.7 is the simulation result after adding magnetic particles under the magnetic pole. It can be seen that when the iron powder is filled between the magnetic pole and the workpiece, the magnetic field changes, and the magnetic field distribution on the surface of the workpiece is close to the situation on the surface of the magnetic pole before the magnetic particles is added. Due to the limited amount of iron powder during simulation, the curve does not appear to be continuous. If there are enough magnetic particles, the curve will become continuous. After adding iron powder, the gap needs to be 0.5mm, then the magnetic field will become uniform.

5.3.2 Measurement of magnetic field

Figure 5.9 is the result of measuring the magnetic field near the magnetic pole using the Tesla meter shown in Fig.3.6. We have measured the poles with the poles of 1 mm, 2 mm, and 3 mm respectively. Within 10 mm on both sides of the magnetic pole, the distance between the sensor and the surface of the magnetic pole ranges is from 0 mm to 2.5 mm as shown in Fig.5.8. It can be seen from the experimental results that as the distance increases, the magnetic field strength becomes weaker and weaker, but due to the small magnetic pole diameter. The edge effect of magnetic field strength is weakened.

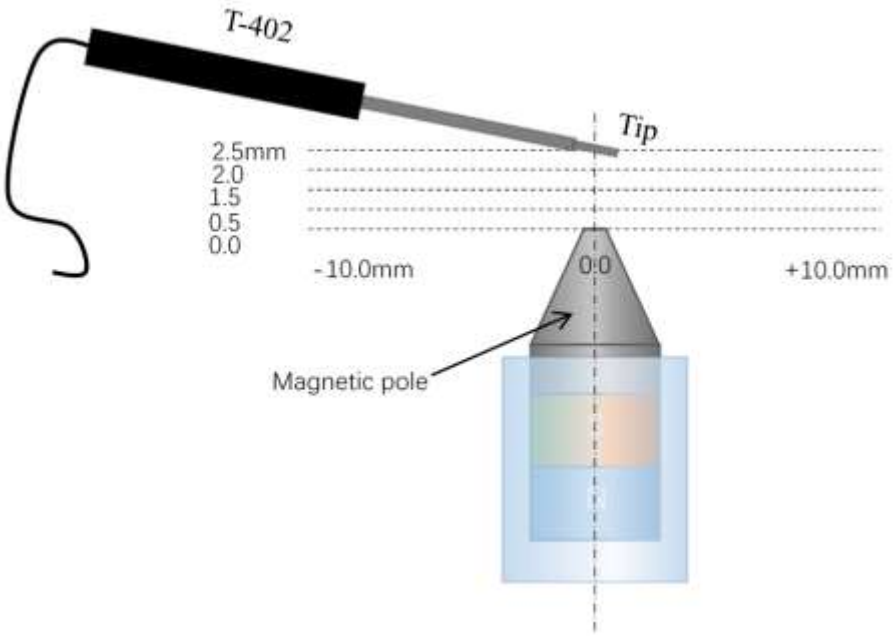

Fig.5. 8 The positions of measurement of magnetic field

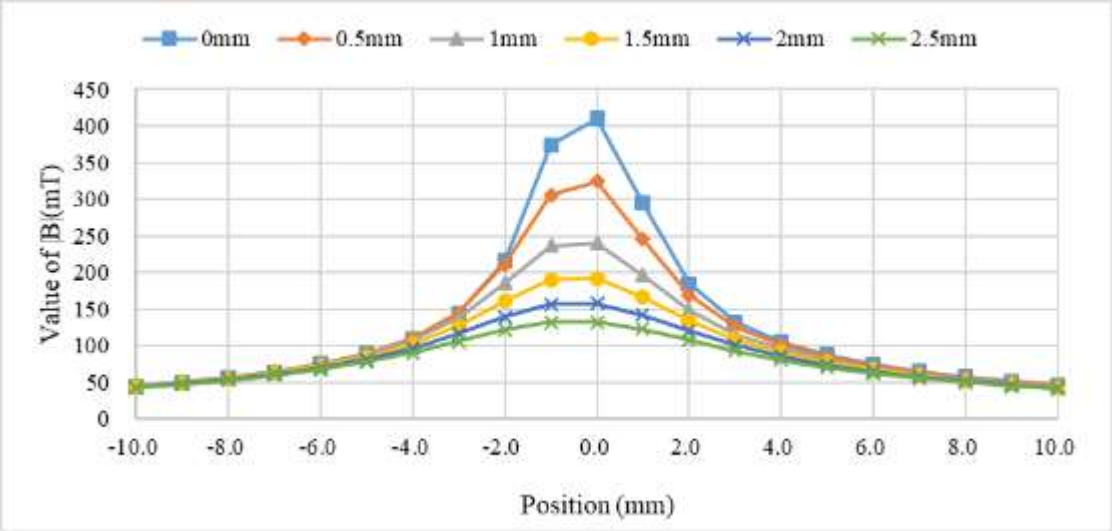

Fig.5. 9 The measured results of magnetic field

5.4 Measurement of magnetic brush pressure

The measuring system of the finishing force is shown in Fig.3.8. Place the sensor over the pole and connect with the signal conditioner. The output signal of the signal conditioner and the power supply are simultaneously connected to the logger. The measurement conditions of the finishing force

are shown in Table 5.2. Fig.5.10 shows the measurement results of the positive pressure of the workpiece of magnetic brush. When the gap is 0.2 mm, the pressure near the magnetic brush is between 0.463 N and 0.716 N, while when the gap is 0.3 mm, the pressure near the magnetic brush is between 0.193 N and 0.371 N.

Table 5. 2 Measurement conditions

Magnetic particles	Electrolytic iron powder, 149 μm in mean dia:0.2 g
Rotational speed	100 rpm
Feed speed	0.2 mm/s
Gap	0.2 mm, 0.3 mm

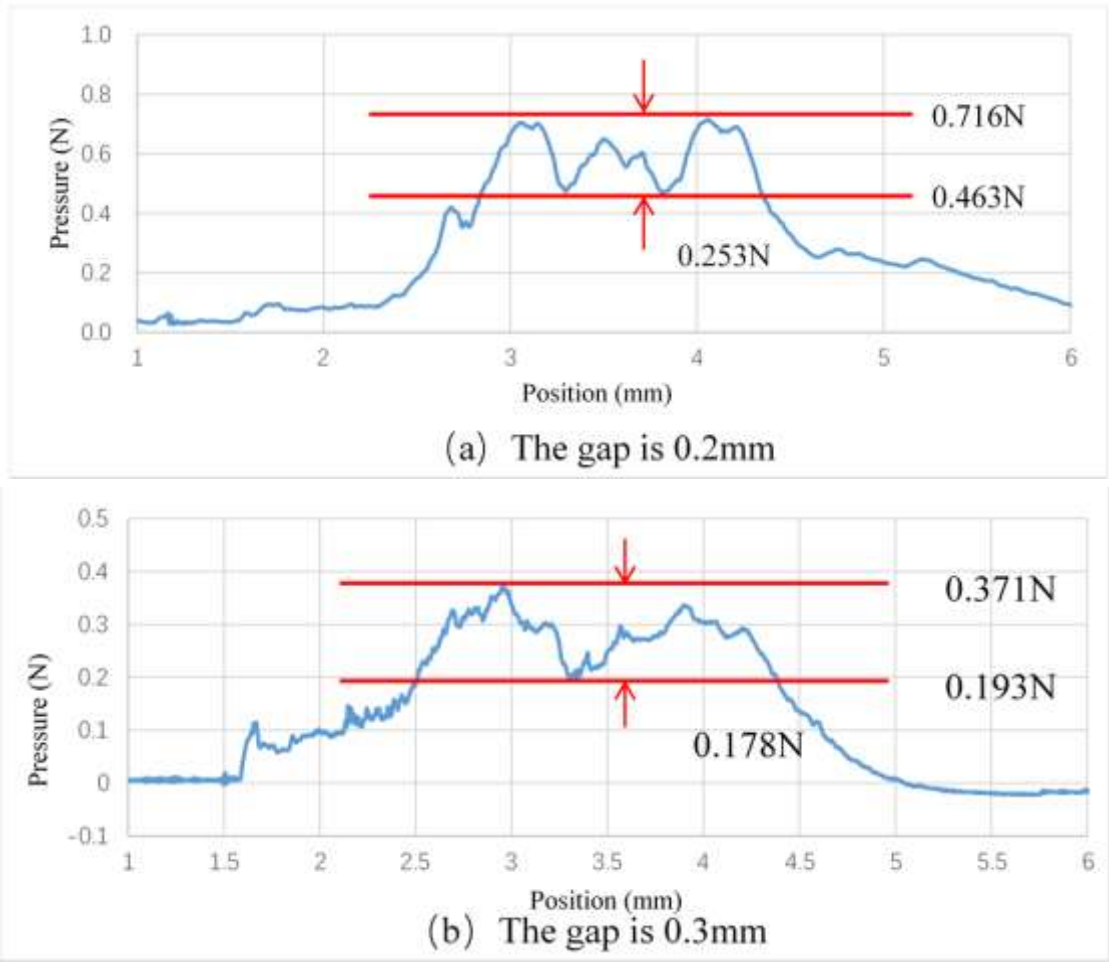

Fig.5. 10 The measured results of pressure

5.5 Processing characteristic measurement

In order to obtain better finishing parameters, we carried out experiments in three stages. Firstly, a better combination of magnetic particles and abrasive particles was obtained, then a better magnetic particles quantity and finishing gap were obtained under the combination. Finally, the processing efficiency of magnetic brush was evaluated by using the obtained finishing conditions.

5.5.1 Choosing the suitable abrasive combination experiment

Firstly, we need to experimentally select a relatively better combination of magnetic particles and abrasive particles. Three magnetic particles and three abrasive grains were used in this study. Magnetic particles include 75 μm and 149 μm electrolytic iron powder, and KMX80 μm. Abrasive particles include WA#4000, WA#8000, WA#10000. So there are 9 ways to combine them. The experimental method is shown in Fig.5.11, and a segment of trace is processed on a same aluminum plate in the same time with using different abrasive combinations.

The detailed experimental conditions are shown in Table 5.3. In this experiment, the processing length is 6mm. In order to ensure the integrity of each processing, the processing time is not used as the standard, but the number of round-trip processing is used as the standard for the same time. It is set that the cycle is processed 5 times. After processed, in the middle of the processing trace, along the direction perpendicular to the processing direction, we measured the cross-sectional curve of the surface of the workpiece, to compare the results and to select the better combination. The combination will be used for the following experiments.

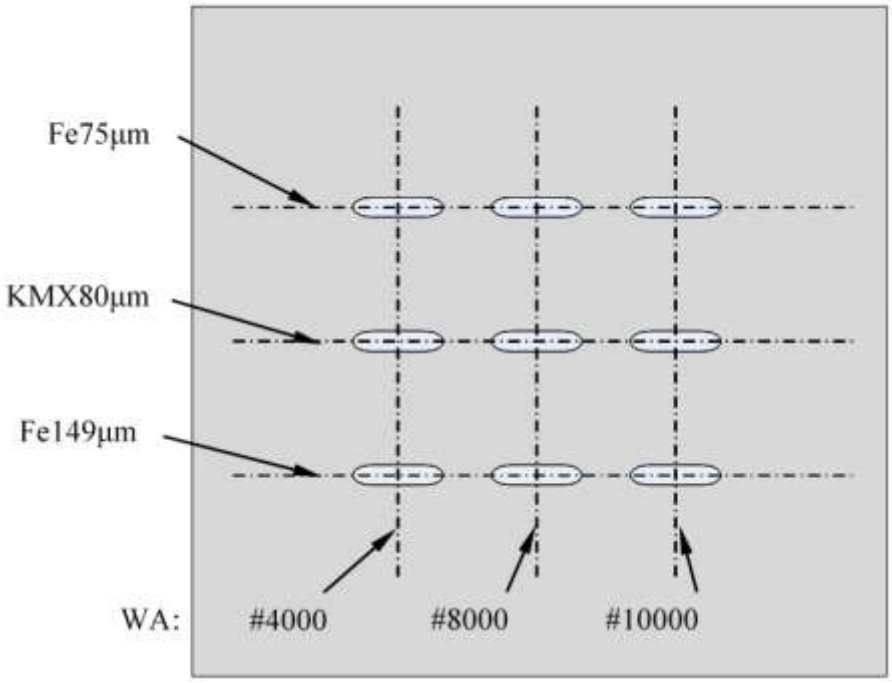

Fig.5. 11 Schematic diagram of processing position

Table 5. 3 Experimental conditions of evaluating finishing efficiency

Workpiece	A5052 plate (100 mm × 100 mm × 2 mm)
Magnetic pole	Nd-Fe-B rare earth permanent magnet (Φ1×35 mm)
Magnetic abrasive	0.02 g iron powder of 75 μm, 149 μm, or 0.02 g KMX80μm
Abrasion liquid	0.5 mL of oil (Honilo 988) & 1 g WA particles of #4000, #8000, #10000
Gap	0.2 mm
Finishing distance	6 mm
Finishing loops	5 loops
Feed speed	0.2 mm/s
Rotation speed	400 r/min

Figure 5.12 shows the results of the experiment. It can be seen from the figure that when Fe75 μm is used, the processing efficiency is the lowest and the processing depth of the workpiece surface is relatively shallow. Compared with KMX80 μm, the processing depth of Fe149 μm is close, but the surface processed with KMX80 μm is obviously rough. Therefore, Fe149 μm is selected as magnetic particle in this study. For different abrasive particles, the processing efficiency is improved with the decrease of particles, because smaller particles can more easily fill the gap of magnetic particles. However, in this experiment, there is little difference for Fe149 μm when it is combined with different abrasive particles. So Fe149 μm and wa#4000 is finally selected as the abrasive combination for subsequent experiments.

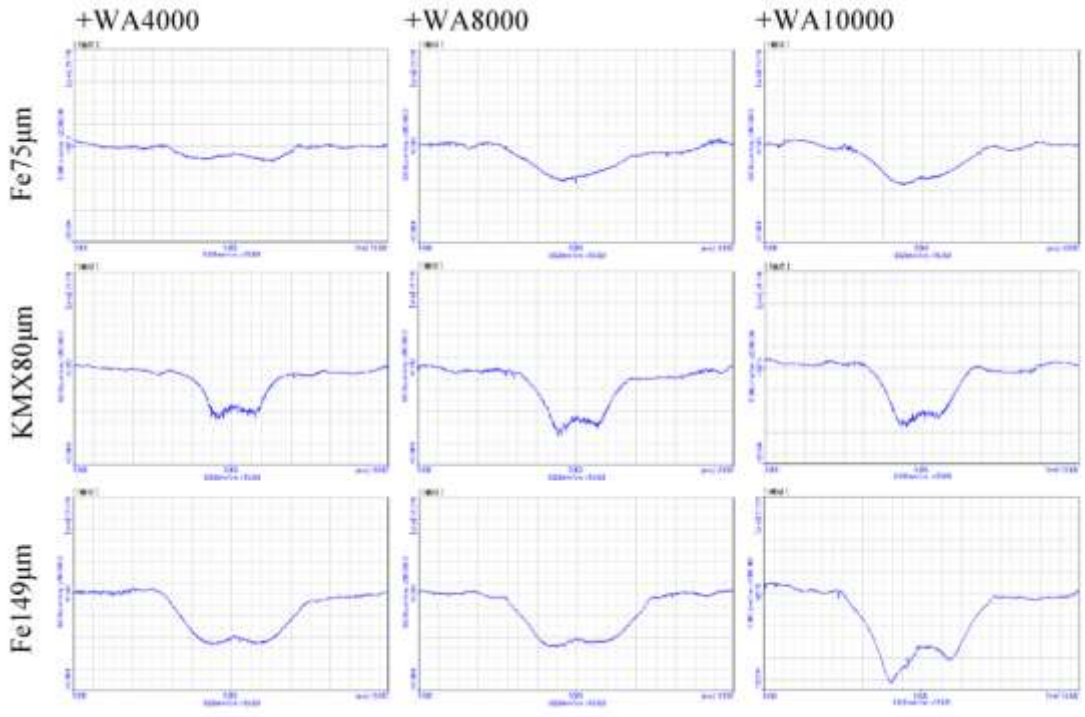

Fig.5. 12 The results after processing with different abrasive ratios

5.5.2 Experiments on iron powder quality and processing gap

This experiment mainly considers to choose an optimal finishing gap and iron powder quantity, so that the finishing section is the most uniform. Here, the processing gap is selected from 0.2mm to 0.5mm, and the iron powder quality is selected from 0.01g to 0.04g. Other processing conditions are still shown in Table 5.3. The method of evaluating the experimental results is also the same as the previous method. The experimental method is shown in Fig.5.13.

The experimental results are shown in the Fig.5.14. As the processing gap increases, the finishing efficiency becomes lower and lower. Therefore, the smaller the gap, the higher the efficiency. The increase of iron powder will also improve the processing efficiency, but at the same time, it will increase the processing radius. Therefore, after comprehensive consideration, the processing gap of 0.2mm and the mass of iron powder of 0.02g were selected as the processing conditions for subsequent experiments.

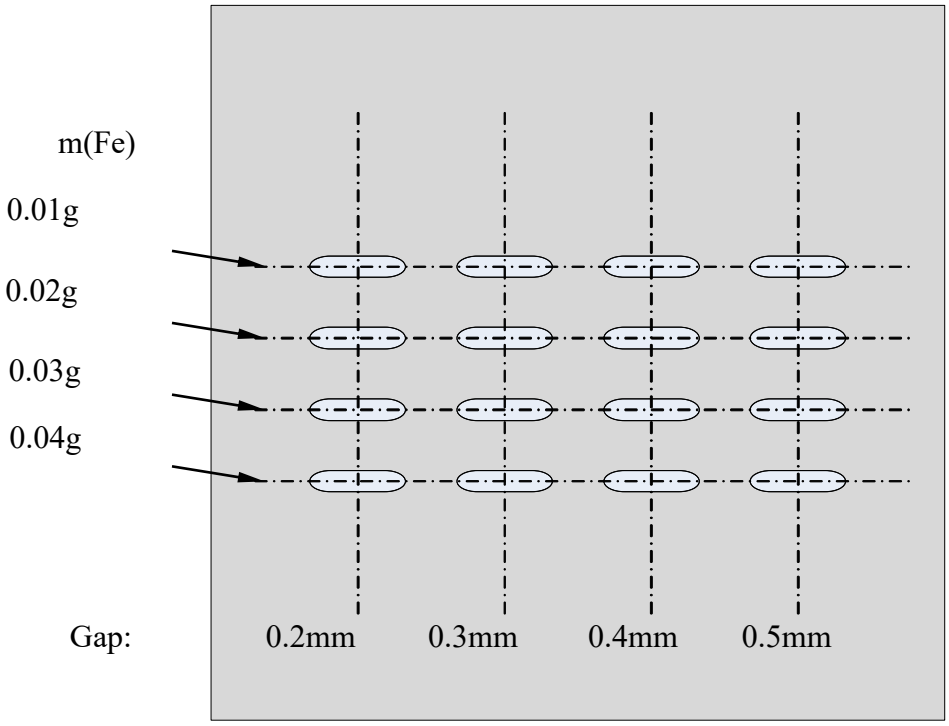

Fig.5. 13 Schematic diagram of processing position

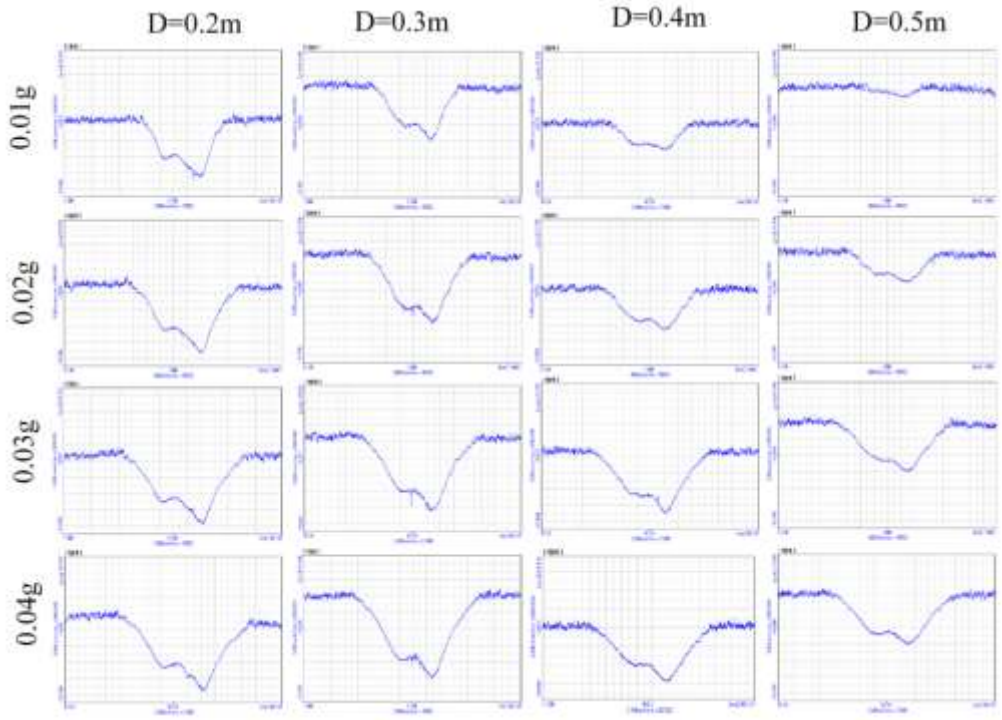

Fig.5. 14 The results of different gaps and iron powder amount

5.5.3 Magnetic brush processing efficiency experiment

To reasonably control the feed speed during finishing, it is necessary to measure the finishing efficiency of the magnetic pole. The finishing object is A5052 plate (100 mm × 100 mm × 2 mm). The calculation method of finishing efficiency is to process 5 tracks with a length of 6 mm on a same workpiece, as shown in Fig.5.15. Reciprocate finishing 2-4-6-8-10 loops respectively, and repeat four sets, then measure the surface curves, calculate the height change, and take the average to obtain an average finishing efficiency. The specific finishing conditions are shown in Table 5.4.

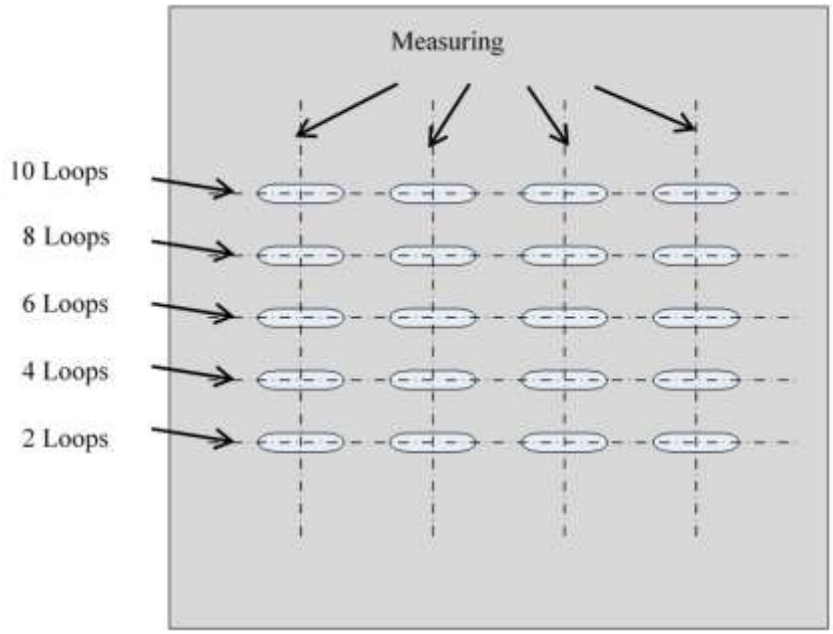

Fig.5. 15 Evaluation of finishing efficiency

Table 5. 4 Experimental conditions of evaluating finishing efficiency

Workpiece	A5052 plate (100 mm × 100 mm × 2 mm)
Magnetic pole	Nd-Fe-B rare earth permanent magnet (Φ1×35 mm)
Magnetic abrasive	0.02 g of 149 μm iron powder
Abrasion liquid	0.5 mL of oil (Honilo 988) & 1 g of #4000 WA particles
Gap	0.2 mm
Finishing distance	6 mm
Finishing loops	2-4-6-8-10 loops
Feed speed	0.2 mm/s
Rotation speed	400 r/min

Figure 5.16 is the average value of the finishing depth of each group according to the finishing method described as above. As the times of reciprocating finishing increases, the depth becomes deeper. Moreover, the finishing depth has a linear relationship with the number of reciprocations.

After calculation, the average height reduction of one reciprocating process is about 1.88 μm. The change in the feed speed will affect the speed of the abrasive particles and the finishing time at the same time. However, as mentioned above, the feed speed v in this paper is a small ratio to the composite speed V. Therefore, to simplify the model, the effect of feed speed on finishing time is only considered in this research.

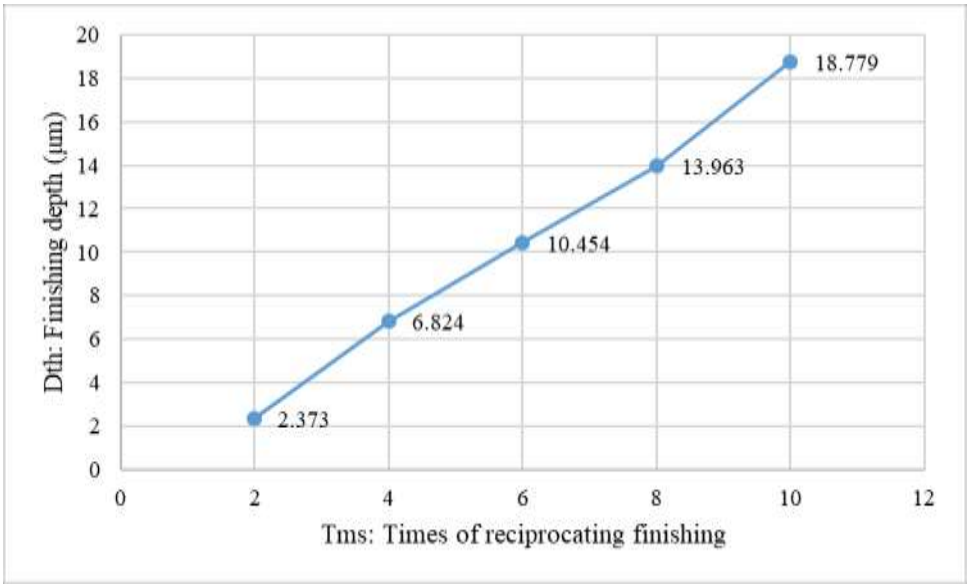

Fig.5. 16 The relationship between processing times and processing depth

5.6 Experimental conditions and method of plane corrective MAF

In order to realize the method described in this article, it is mainly divided into the following experimental steps:

(1) The first step is to pre-process the workpiece to produce an unevenly changing surface.

(2) The second step is to measure the surface after pretreatment, and to calculate the feed speed according to the surface curve after pretreatment,

and implement variable speed processing to achieve the effect of corrective finishing.

(3) The third step is to measure and analyze the experimental results.

The following is a detailed description of each step.

5.6.1 Workpiece Preprocessing

In order to produce the undulating surface of the workpiece, the workpiece needs to be pre-processed. The method is to use a 14mm diameter magnetic pole to process two tracks, and process them at a 0.6mm distance and 0.8mm distance for 20 minutes. The processing position and direction are shown in Fig.5.17. The detailed processing conditions are shown in Table 5.5.

Table 5. 5 Experimental conditions of preparation finishing

Workpiece	A5052 Aluminum Alloy plate (100×100×2mm)
Magnetic pole	Nd-Fe-B rare earth permanent magnet (Ø14×24 mm)
Magnetic abrasive	0.5 g of 149μm iron powder & 0.5g of #4000 WA particles
Abrasion liquid	0.5 ml of Oil(Honilo 988) & 1 g of #4000 WA particles
gap	0.6 mm and 08mm
Finishing distance	60mm
Finishing times	20 min
Feed speed	0.5mm/s
Rotation speed	400 rpm

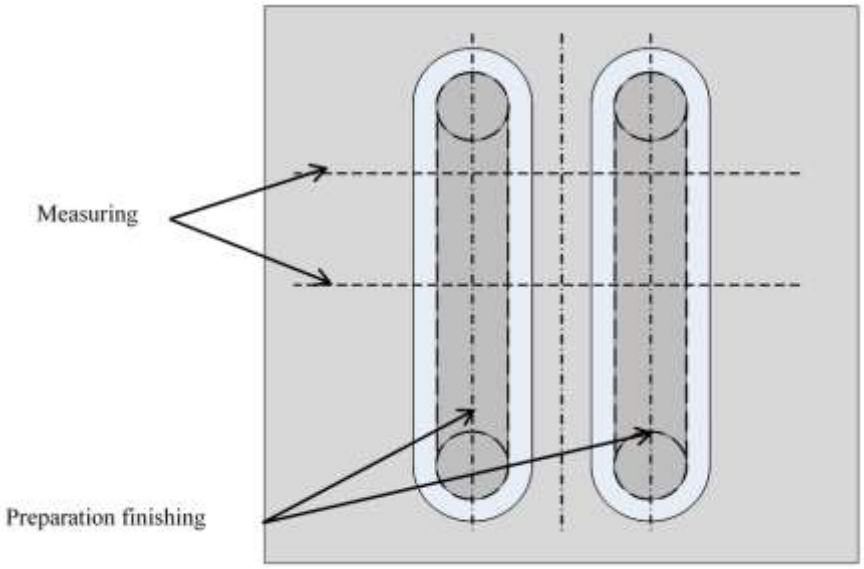

Fig.5. 17 Finishing position and measurement position description

5.6.2 Comparative experiment of variable speed and constant speed finishing

The pre-processed workpiece is processed to smooth the surface. The processing trajectory is perpendicular to the preprocessing processing trajectory, and the processing position and direction are shown in Fig5.17. The processing parameters are carried out according to Table 5.4, but the processing distance is 60mm, and the feed speed is carried out according to the calculated results. According to the processing principle, the feed speed array of the linear motor is calculated. The linear motor is controlled according to the speed array for variable-speed processing. In addition, as a comparative experiment, the workpiece was also processed at a uniform speed. The speed of uniform processing is equal to the average speed of variable processing. This can ensure that the total processing time of the two sets of experiments is equal. In order to ensure the effect of the magnetic brush, the finishing fluid is updated every 4 loops, and the

processing results of that stage are measured to observe the flatness of the workpiece.

5.7 Results and discussion

5.7.1 Surface curve after pretreatment

After preprocessing the workpiece according to the method described in 5.5.1, Fig.5.18 is a photograph of the workpiece after pretreatment. The surface morphology was measured, and the curves of two positions were obtained as shown in Fig.5.19. It can be seen that the edge of the magnetic pole is processed deeper and the middle processed shallower, forming a convex shape in the middle. This conforms to the general processing regulation. The surface of the processed area becomes smoother and lower, and the unprocessed area is rougher and higher. The two curves are used as the initial surface for variable-speed finishing and constant-speed finishing.

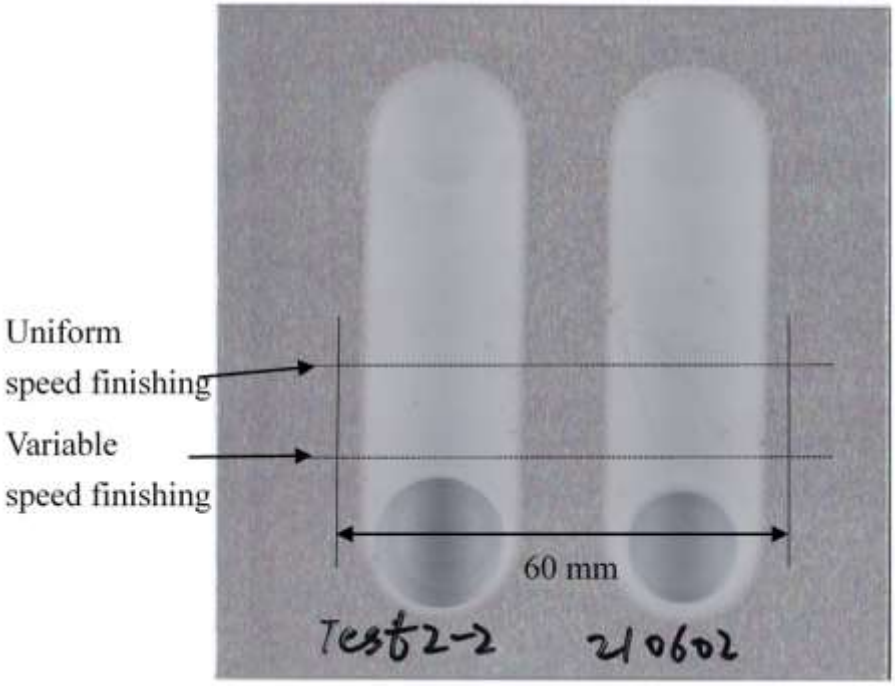

Fig.5. 18 Surface profile curves after pretreatment finishing

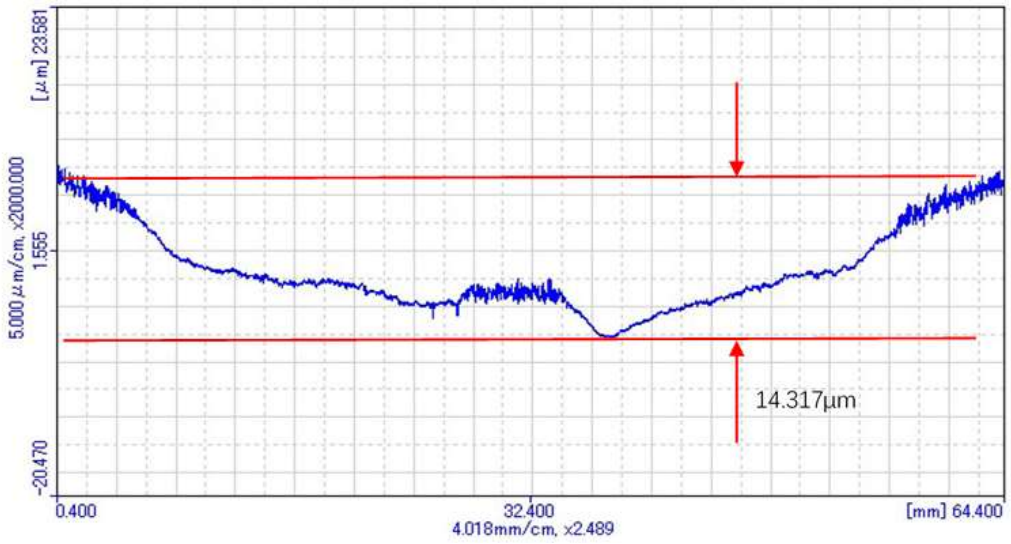

(a) Initial surface for variable speed finishing

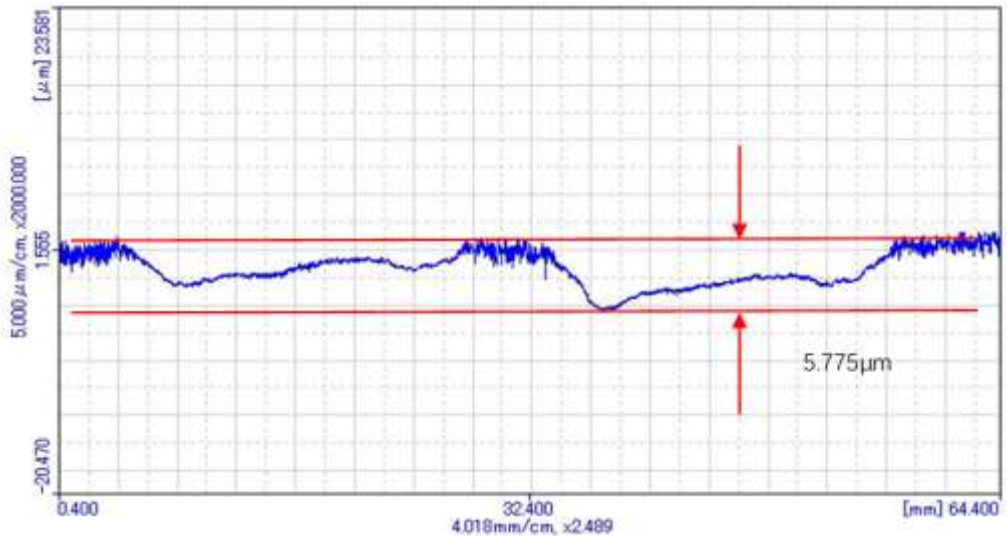

(b) Initial surface for uniform speed finishing

Fig.5. 19 Surface profile curves after pretreatment finishing

5.7.2 Comparison of surface curves of each stage

For the uneven surface formed after pretreatment, secondary processing is performed, using variable speed processing and uniform speed processing respectively. According to the measured data, the curve extreme difference of Fig.5.19 (a) is 14.3μm, and the target processing position is set to 2μm below the lowest point, so the maximum processing depth is

expected to be 16μm. According to the method described in chapter 2.2. It is necessary to calculate the speed sequence of variable-speed processing and calculate the equivalent speed of constant-speed processing. The uniform processing speed is the average speed during variable processing to ensure that the total processing time is consistent. The average speed during variable-speed finishing in this experiment was 0.39mm/s. In addition, variable-speed processing and uniform-speed processing are both in accordance with every 4 reciprocating (time: 20min) as a processing stage.

Figure 5.20 is the graphs of the surface curves measured after each stage of processing. It can be seen from the Fig.5.20 (b) that the surface morphology of the workpiece processed at a uniform speed remains basically unchanged. In the case of using uniform speed finishing, the result of 40 minutes of processing, compared with the result of 20 minutes, the extreme difference did not decrease. Similarly, the result of 60 minutes of processing is not much improved compared with the result of 40 minutes. Because the feed speed is constant, the removal amount of each area is almost the same, so the height change of each point is also the same. The surface after uniform processing only becomes smooth and less burrs than at the beginning.

As shown in Fig.5.20(a), the surface becomes smooth after variable speed processing. At the same time, the height difference of the surface is gradually reduced, and the surface tends to be smooth. After the third stage, the surface is the smoothest, achieving the effect of smoothing the surface. But it can be seen that there is still a small hollow that has not been well processed. This is mainly because the width of the hollow area is smaller than the effective width of the magnetic brush. It is needed to use a smaller

magnetic brush to process it.

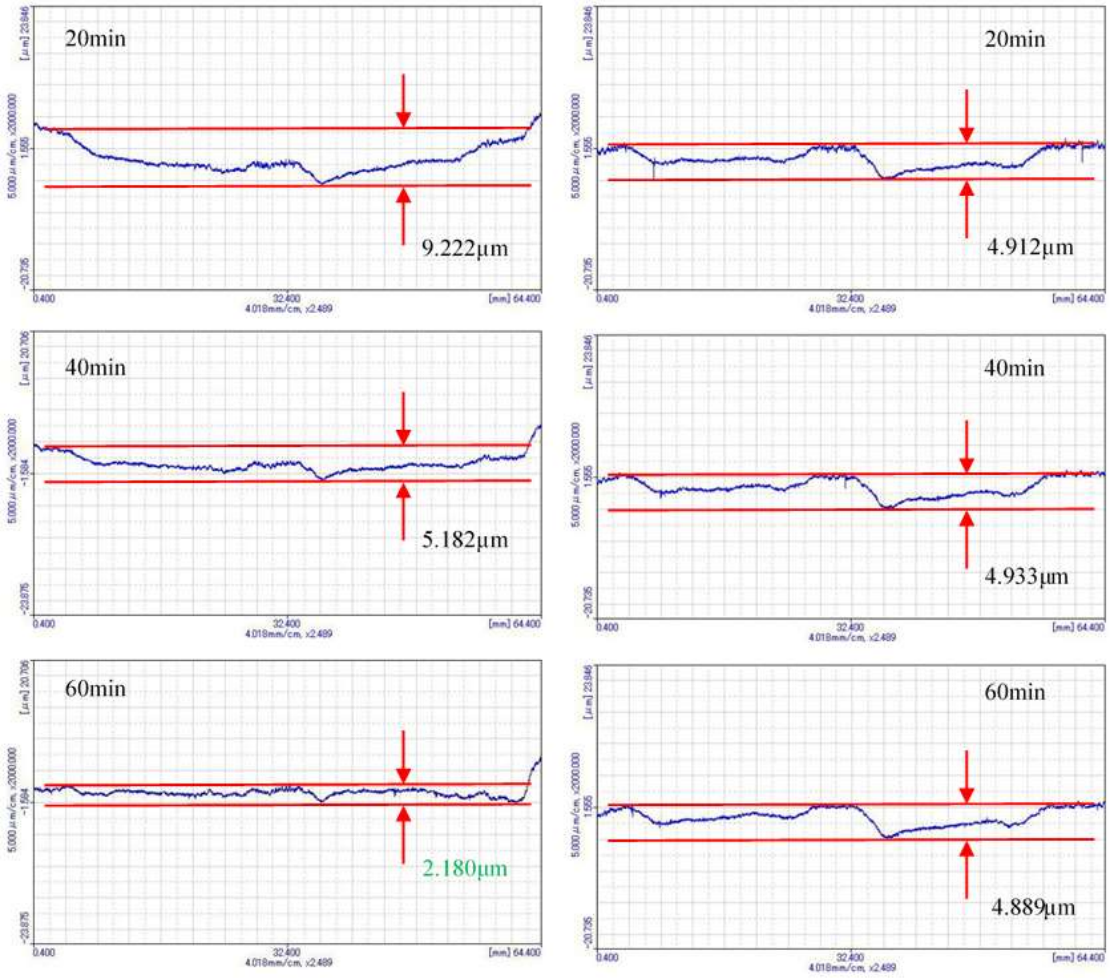

(a) After variable speed finishing (b) After uniform speed finishing

Fig.5. 20 Comparison of the surface curves of various stages

Figure 5.21 is the statistics of the extreme difference and standard deviation of each stage of the two processing. It can be seen from the figure that the extreme difference and standard deviation of the surface processed by the variable speed gradually become smaller, which shows that the flatness of the surface has been improved. The extreme difference and standard deviation of the surface at a constant speed are almost non-existent, indicating that the flatness of the surface has not been improved. In the initial state, the extreme difference and standard deviation of the

variable-speed processing area are much larger than the value of the uniform-speed processing area, but after 60 minutes of processing, the range and standard deviation are lower than the value of the uniform-speed processing.

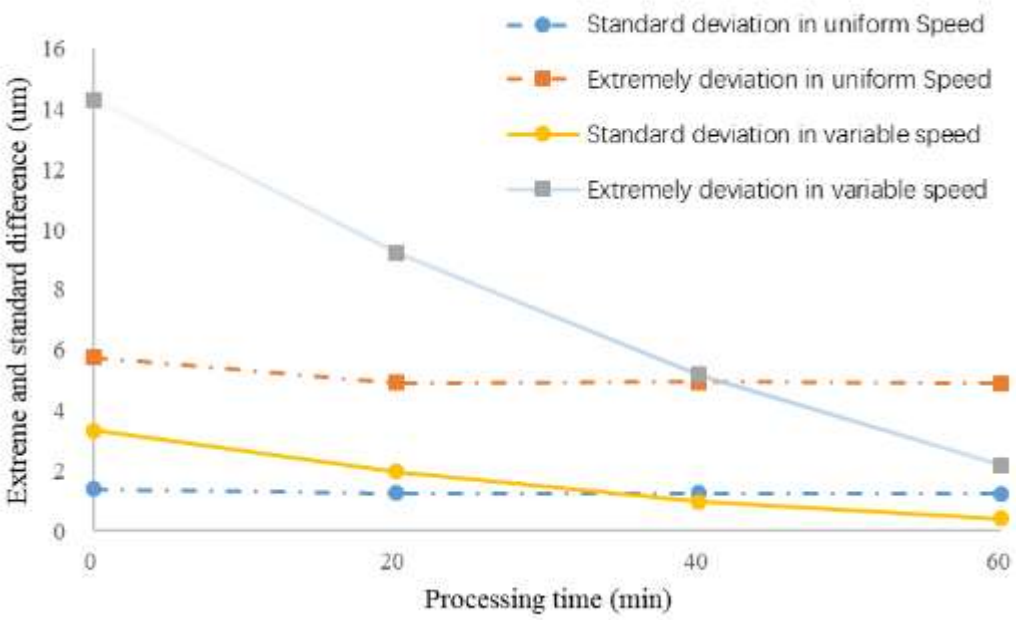

Fig.5. 21 Comparison of extreme and standard deviation of two kinds of finishing

5.7.3. Comparison of final effect horizontal position

It can be seen from Fig.5.20 and Fig.5.21 that correction finishing can effectively correct the curve of the workpiece into a straight line at the center line of the processing trace. Then, what is the situation in the complete area of magnetic brush processing. So we also detected four lines on both sides of the processing center line, and the interval between each line was 0.5 mm, as shown in Fig.5.22.

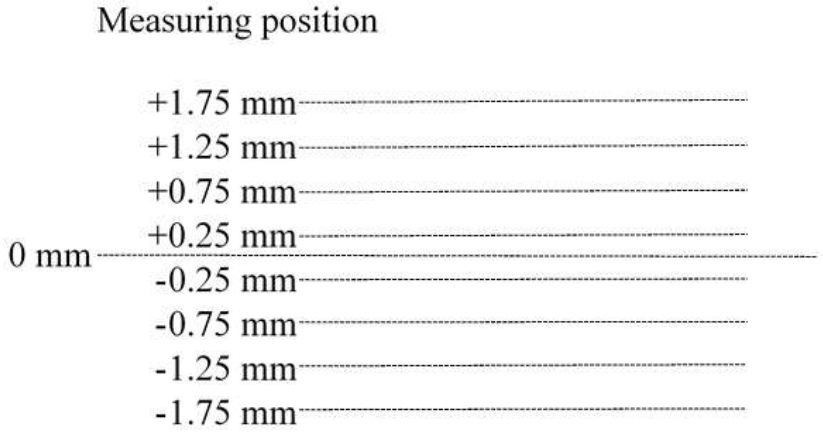

Fig.5. 22 Lateral comparison of workpiece surface after processing

Figure 5.23 is a measurement of different positions on the surface after 60 minutes of variable speed processing. The measurement interval is 0.5 mm. It can be seen from the figure that, except for the two farther from the center line, the flatness is better. And the distance from the center is closer, the flatness is better. From -1.25 to +1.25, there is a good correction effect, which also shows that the processing effect of small magnetic poles is better. The effective correction range can reach 2.5mm wide. This is conducive to the correction processing of a larger plane range.

In order to be able to describe the flatness of the surface more accurately, the range and standard deviation of each curve are counted, as shown in Fig.5.24. In the figure, the extreme difference and standard deviation have been reduced, the smallest extreme difference can reach 2.18 μm, and the minimum standard deviation can reach 0.417 μm. The statistical results can show that the general flatness of the variable speed processing in the processing area has been improved.

At the edge of the processing track, the processing effect becomes weak. At the outer edge of the magnetic brush, although the linear velocity is the highest, the driving force of the magnetic brush on the particles is reduced,

and the pressure is also relatively reduced, so the finishing efficiency is also reduced.

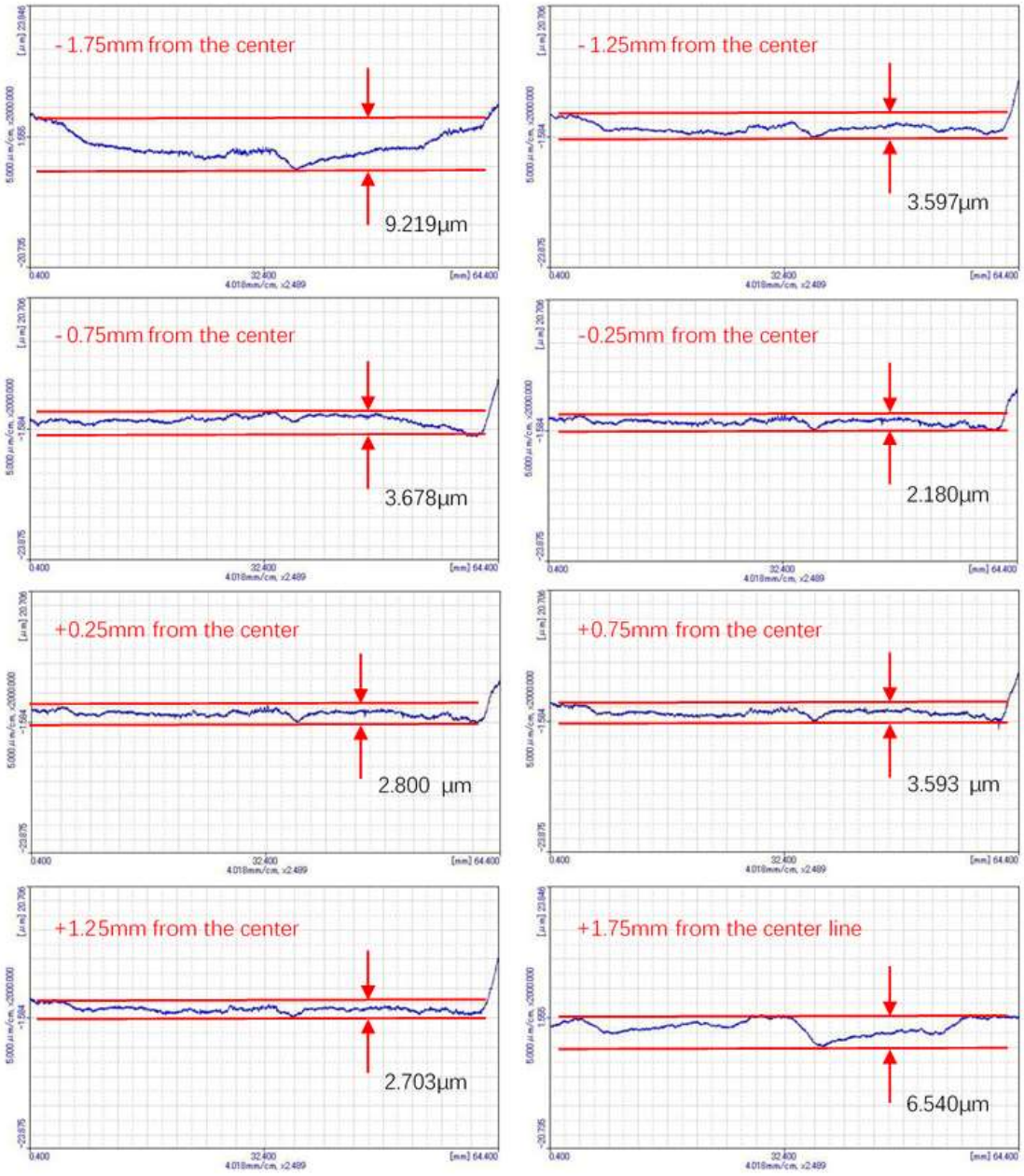

Fig.5. 23 Lateral comparison of workpiece surface after processing

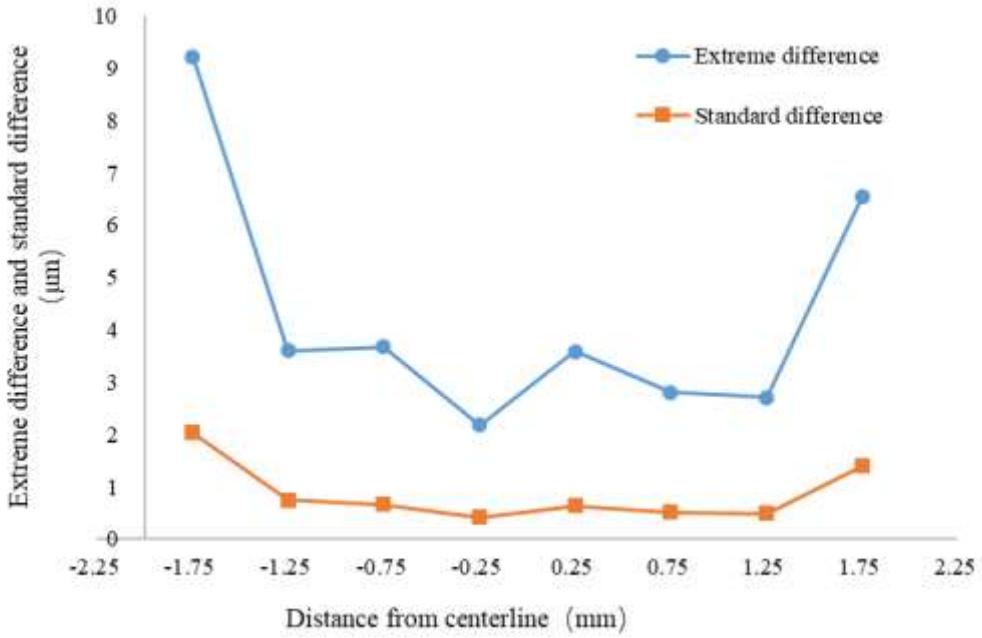

Fig.5. 24 Extreme and standard deviation at different positions

5.8 Conclusions

In this chapter, a processing method for improving the flatness of the workpiece surface through variable-speed finishing is proposed. The processing principle was elaborated in detail. The effectiveness of the method is verified by experiments. Summarized as follows:

(1) Through the magnetic field simulation, it is proved that when the end face diameter of the magnetic pole is reduced, it is conducive to weaken the edge of the magnetic field strength of the cylindrical magnetic pole, and the magnetic pole with end face diameter of 1mm is designed.

(2) Through experimental analysis, considering comprehensive factors such as processing efficiency, processing width, surface roughness, etc., the combination of 0.02g 149 μm iron powder and WA#4000 is more suitable for this process.

(3) Through experimental analysis, the finishing efficiency is 1.88

μm/min when the magnetic pole diameter is 1 mm, the feed speed is 0.5 mm, and the processing length is 6 mm.

(4) The profile correction experiment of the workpiece was implemented using the magnetic pole with the diameter of 1 mm. Measuring the surface curve of the processed workpiece and calculate its range and standard deviation to effectively evaluate the change in surface flatness of the workpiece. The minimum range is 2.18 μm and the standard deviation is 0.417 μm.

(5) Through the comparative experiment of variable speed finishing and uniform speed finishing, it is concluded that variable speed finishing improves surface flatness.

Chapter VI Investigation on correction MAF of plane surface with 1 mm magnetic pole

In order to improve the plane quality of the workpiece surface, a correction abrasive finishing method is proposed. This method is according to the profile of the initial surface to control the effective finishing time of different areas, and to achieve the effect of correcting the workpiece surface, and is extended to larger plane processing. In this paper, the mathematical modeling of the method is presented, and by controlling the feed speed to achieve the change of the effective processing time of different areas. To correct the workpiece more accurately, a magnetic pole with a diameter of 1mm is used in this paper. In addition, some experiments are carried out on the proportion of abrasives and the processing efficiency. Through a series of experiments on SUS304 plates and aluminum plates (A5052), it is proved that the profile of the workpiece surface can be effectively corrected by accurately controlling the feed speed. Under the same processing conditions, this method significantly improves the surface quality compared with uniform feed speed processing. The experimental results show that the extreme difference can be reduced from 4.81 μm to 2.65 μm within the processed area of 30 mm by 10mm after two processing cycles.

6.1 Introduction

With the rapid development of electronic technology, optical technology and aerospace technology, the requirements for workpiece surface accuracy in many fields are higher and higher. For these components, their

surfaces are required to be smooth, low roughness, and high geometric accuracy. Magnetic abrasive finishing (MAF) process is an important non-traditional finishing process [66, 67]. MAF process is using magnetic particles to form a flexible brush structure under the action of magnetic field, and mixing abrasive particles with magnetic particles, and using the motor to drive the magnetic brush to rotate, so as to drive the abrasive particles to move relative to the workpiece and to realize the finishing of the workpiece [10].

Shinmura et al. proposed and designed a plane MAF device, and analyzed the process principle of plane MAF, and discussed the effect of the supply weight of finishing fluid and magnetic abrasive on the finishing depth and surface roughness [17]. Yamaguchi studied the use of magnetic grinding technology to process the inside of the round tube [20]. In order to solve the disadvantage of weak magnetic force when pro0cessing thick tubes, Zou et al. proposed a processing method that can improve the magnetic force, and made it possible to process the inside of thick non-ferromagnetic tubing [68]. Because the magnetic brush formed in the magnetic field has a certain flexibility and can conform to the shape of the workpiece, it is applied to the processing of various irregular shapes, such as the inner and outer surfaces of the tube, irregular surfaces, and so on. In order to improve processing efficiency, researchers combined MAF with other processing methods. Based on the MAF principles, additional ultrasonic vibration is used to achieve high-quality workpiece surface [64, 69]. Mulik et al. employed ultrasonic vibration in the horizontal direction of the workpiece using an ultrasonic power, a piezoelectric transducer, and a horn device [55]. A high frequency electrical signal was generated by the ultrasonic power and transformed into the horizontal mechanical vibration

by the transducer. In order to further improve the processing efficiency of magnetic grinding, Zou et al. made different attempts and proposed a variety of processing methods. They proposed a processing method combining MAF process with electrolytic technology [40, 41, 65], and a processing method combined MAF with fixed abrasive polishing technology [45]. They analyzed the process mechanisms and finishing characteristics, and proved that the purpose of improving processing efficiency can be achieved by these methods through experiments. They also proposed a MAF process using an alternating magnetic field. Compared with static magnetic field, MAF process using alternating magnetic field can achieve higher finishing efficiency and surface quality [53, 58, 70].

With the continuous development and improvement of MAF technology, higher requirements for this technology are put forward. In order to make the magnetic field of fin-ishing tools more uniform, a lot of researches have been done to change the shape of magnetic pole, such as adding grooves and improving finishing tracks and so on. Since the magnetic abrasive finishing process is a finishing process using magnetic brush with flexible finishing behavior, the process can be used to finishing free-form surfaces, and improve surface accuracy without destroying the profile of the workpiece [71, 72, 73]. However, because the magnetic brush is not a uniform finishing tool, further researches are still needed to maintain the geometric accuracy of the workpiece or correct the geometry, which is also the research content of this subject. Zou et al. calculated the trajectory to elevate the surface quality of plane magnetic abrasive finishing. Finishing trajectory could be predicted combining revolution motion of magnetic brush, the pole rotation motion, and linear reciprocating motion of

workpiece to investigate finishing results [49, 50]. They conducted further studied on this method and proved that the revolution radius was an important factor affecting the surface flatness, and proposed an effective method for evaluating the surface topography [51].

Through a series of experiments and theoretical analysis, this research uses magnetic abrasive finishing technology to realize the plane correction of the workpiece. In order to further solve the problem of uniformity of finishing, a method of forming small magnetic brush with small magnetic pole is proposed in this research. According to the initial pro-file of the surface, the finishing at different positions is controlled at different feed speeds. Through the analysis and finishing of the collected surface profile data, and according to the finishing characteristics of the magnetic brush, the feed speed distribution in the finishing process is planned to make the effective finishing time at different positions different, and finally to improve the surface flatness.

6.2 Processing principle

As shown in Fig.6.1, it is a schematic diagram of the finishing trajectory used in this study. The designed processing area has a width of 10 mm and a length of 30 mm. Since the magnetic pole of 1mm is used here, the finishing efficiency is relatively low, so the finishing tool translates in the Y direction once and again. The feed speed control scheme of each track is the same. We call the finishing trace of the tool back and forth at one time as a single finishing trace. Then each single finishing trace should be the same.

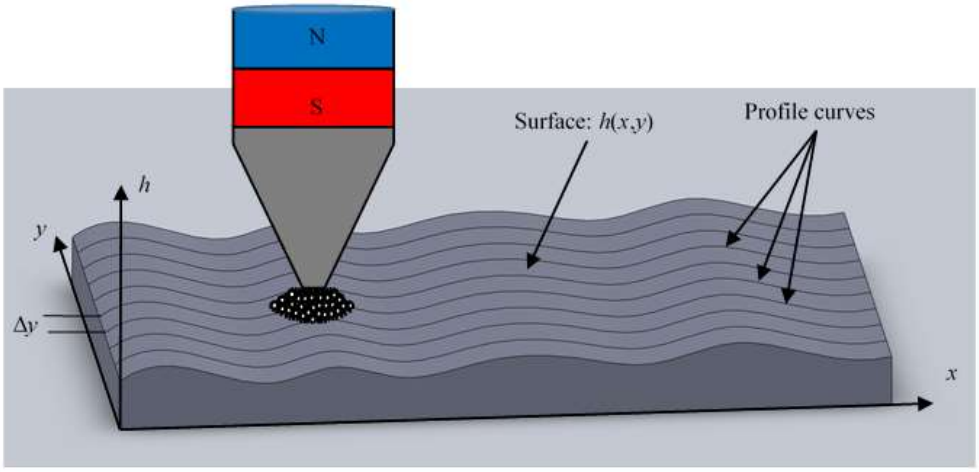

Fig.6. 1 Schematic of finishing principle

Based on Preston's Law (Preston, 1927), the Integrated Material Removal Rate (IMRR) is proportional to the polishing tool pressure on the surface of the workpiece and the relative velocity between the tool and the workpiece [56]. The material removal amount expresses as the following formula:

$$dM_R = kP(x,y)V(x,y)dt \tag{6.1}$$

where, M_R is the amount of material removal, k is the removal factor, (x,y) is the coordinates of a point on the plane. The $P(x,y)$ is the pressure at the point (x,y), and $V(x,y)$ is the resultant velocity of the tool relative to the workpiece, and dt is the finishing time. When the magnetic field strength, the composition of the abrasion liquid, and the working gap etc. are constant, the amount of material removal is depended on $V(x,y)$ and dt [74].

Previous studies have proved that the planar quality of the processed area can be improved by controlling the feed speed of workpiece, but only a single track was finished [75]. Now the finishing area needs to be extended to a larger planar area. Assume that the initial topography of the workpiece is shown in Fig.6.1, and its profile curves are shown as in the figure. Due to the flexibility of the magnetic brush, the workpiece can be finished and

its roughness can be reduced while maintaining the original profile of the workpiece. But if we change the attitude, can we reduce the height difference of the surface and improve its flatness by magnetic abrasive finishing technology? A simple method can easily be thought of, which is to change the processing time or feed speed for different positions. For example, where the surface is high, the feed speed is slower and the processing time is longer. On the contrary, where the surface is low, the feed speed is faster and the processing time is shorter. In other words, the purpose of correcting the plane can be realized by controlling the motion conditions during finishing.

However, for magnetic brush, the processing efficiency of the point with different position from the center point is different. There are many reasons, such as different linear speed of rotation, different magnetic field intensity and many other factors. Therefore, it is not an easy thing to plan the processing speed well. In order to prove the effectiveness of the modified method, theoretical analysis and experimental verification are carried out, and the experiment proves that the surface range can be reduced to 2.18 um [75]. However, previous studies have only carried out single trajectory studies, and further discussion and research are still needed if they are to be extended to the plane range.

At present, the amount of material removal is usually described according to Preston's equation [76]. The Preston equation is related to the pressure, relative velocity and residence time in the contact area [77], as shown in Equation 6.1.

If the density of the workpiece is ρ, the contact area between the workpiece and the magnetic brush is A, and the removal depth of the material is h. Then $M_R = d\rho Ah$, which is substituted into Equation 6.1,

the following equation will be obtained.

$$dM_R = d\rho Ah = \rho Adh = dh = kP(x,y)V(x,y)dt, \qquad (6.2)$$

where dh is the removal depth at (x, y) on the workpiece surface at dt time. dt, k are the dwell time and Preston coefficient respectively. $P(x, y)$, $V(x, y)$ are the pressure applied at point (x, y) and the relative polishing linear velocity. The material removal profile generated after processed time t is expressed as:

$$h(x,y) = \frac{1}{\rho A}\int_0^t kP(x,y)V(x,y)dt \qquad (6.3)$$

In the finishing process, the movement of the particles consists of circular motion and feed motion relative to the workpiece. When the feed speed is very small, the particle velocity can be approximately equal to the linear velocity of circular motion. To simplify the model, in this research, it is considered that the velocity of the particle relative to the workpiece is approximately equal to ωr. Where, ω is the angular velocity of circular motion, r is the distance between the particle and the axis of rotation that is the radius of the circular motion. Therefore, when the angular velocity ω is constant, V is almost unchanged. From Equation (6.2), it can be known that the depth of material removal only depends on the finishing time t. The processing time is inversely proportional to the feed speed v, so the corrective processing of the workpiece can be realized by controlling the feed speed. Then the key is how to calculate the feed speed according to the profile curves.

Then, when Δy is enough small, the finishing amount in the y direction should be uniform. Therefore, only the shape change in the x direction can be corrected by using the correction processing method shown in Fig.6.2. If it is necessary to modify the shape in the Y direction at the same time, it

is necessary to change each single finishing trace for planning. In this study, only one direction of morphology correction is considered.

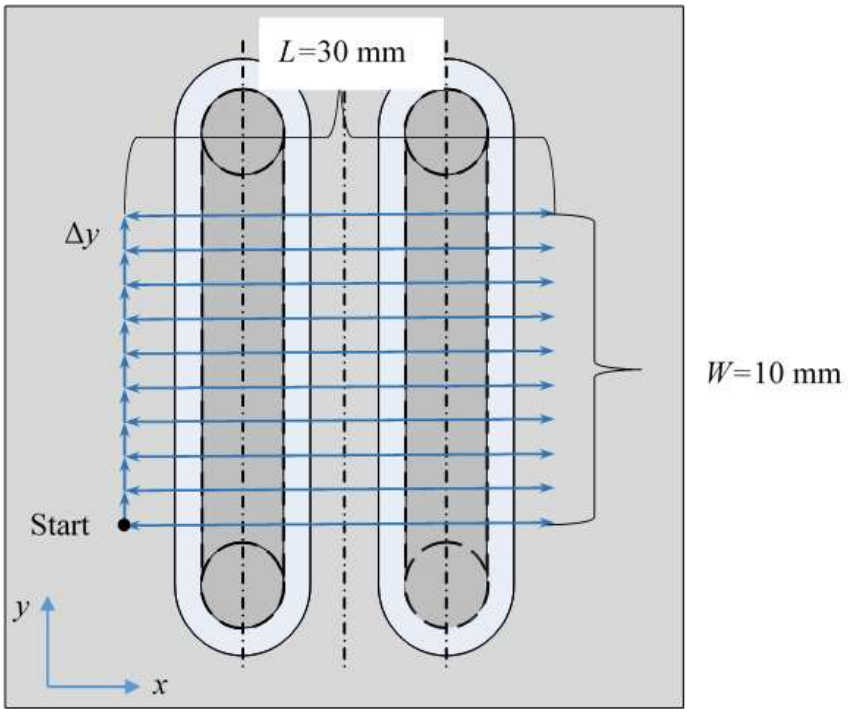

Fig.6.2 Schematic diagram of processing position

6.3 Design of control program for finishing tracks

As shown in Fig.6.3, it is a photo of the STM32 circuit board. It has 5 USART interfaces. Among them USART1, USART2, USART3, USART5 are the electrical interfaces of RS-232. USART4 is an RS-485 interface. USART1 is used to receive the processing parameters sent by the computer. USART5 is used to send commands to the X-Y stage to control the processing position. USART4 is used to send commands to the feed slide motor according to the feed speed curve. There are two 16-bit DACs on the board, and DAC2 is used to control the motor that rotates the magnetic poles. The DIN is the interface of digital inputs, and the DOUT is the interface of digital outputs. They are used to control the feed motor and to confirm its status.

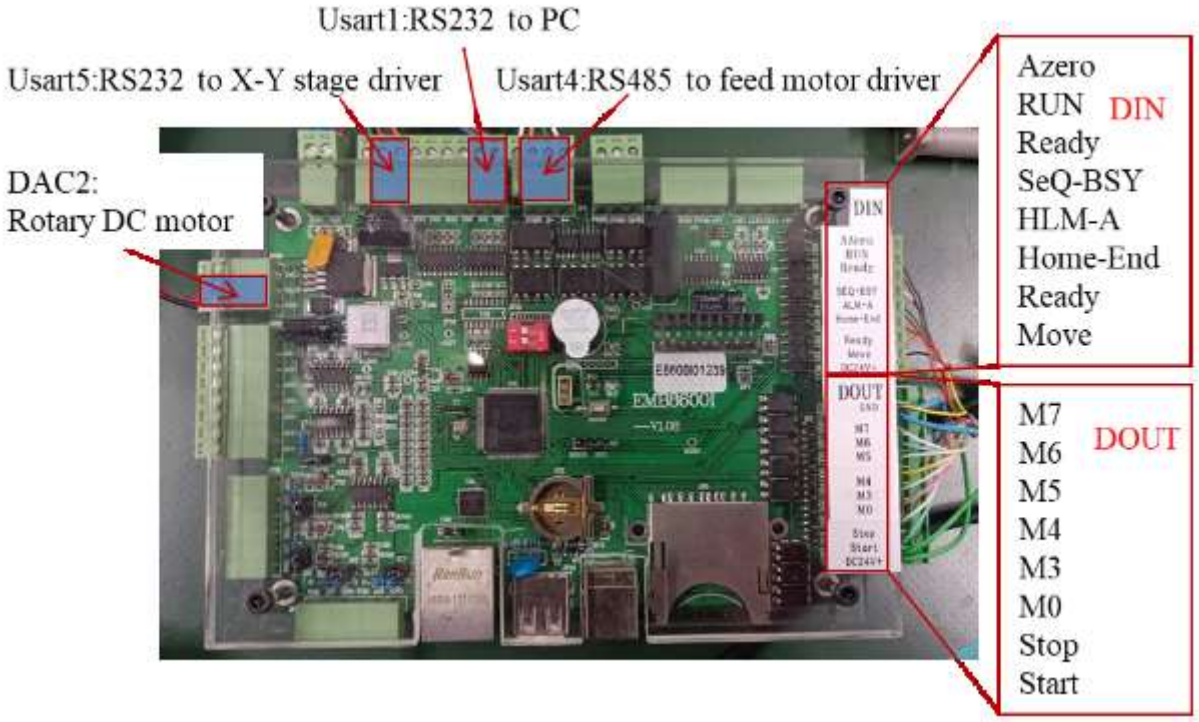

Fig.6. 3 STM32 circuit board

The program is written by C programming language on the basis of μC/OS -II. First, it is necessary to calculate the velocity vector corresponding to each contour curve according to the method in Chapter 2. At present, it is realized by using the data calculation function of Microsoft Excel.

And establishing the data structure as follows:

```
//*************************************************************//
//***       STM32  μC/OS-II
//*************************************************************//
//X-Y stage commands:   X → A,  Y → B, 1 mm↔500 pulses
INT8U     Cmd_XY_test[30]="AGO:A-00006000B-00006000\r\n";
//Feed motor driver commands:       the buffer of array of feed speed
INT8U     Cmd_AZD_byte[50];
//The digital input of feed motor driver: control signal
```

```
INT8U     Cmd_AZD_06[8]={0x01,0x06,0x00,0x7D,0x00,0x00,0x00,0x00};
//The digital output of feed motor driver: the state of the motor
INT8U     Cmd_AZD_03[8]={0x01,0x03,0x00,0x7F,0x00,0x01,0x00,0x00};

INT8U     UART1_ReadBuf[60]; //The buffer of the date received from PC
INT8U     UART5_ReadBuf[30]; //The buffer of the date received from X-Y stage
INT16U    RS485_Buf[16]; //The buffer of the date received from feed motor driver

//The date format received from PC
//"$AllPara#A:+2450,B:-32516,detB:250,Lps:20,RdyP:81RunP:81\r\n";
int Init_A_Pules;        //→A:The X coordinate of the start point.
int Init_B_Pules;        //→B:The Y coordinate of the start point.
int Det_B_Pules;         //→ detB: Δy →  the step of y
int Init_loop_count;     //→Lps: the number of tracks
int Ready_Rotation;      //→RdyP: Rotating speed during preparation
int RUN_Rotation;        //→RunP: Rotating speed during processing
//************************************************************//
```

The program starts by initializing the necessary various data, Such as the magnetic pole rotation speed, the coordinates of the starting point, the number of curves, the value of Δy and so on. In fact, it can be realized by using VC++ or VB to make a program that can interface with the STM32 to transfer these data. However, due to time constraints, this was not done, and I hope this function can be implemented in the future. Now use the STCISP software to transmit a short message. This does not include data for the feed speed curve.

Next, the program needs to wait for the signal of the start button. If the start button is clicked, the X-Y stage will be moved to the position of the

starting coordinate, and then the control data will be sent to the feed motor driver, and the magnetic pole rotation motor will be started at the same time. Then it will start the feed motor to correction process the first curve. After one loop processing, it will adjust the position of the X-Y stage, and to move the Δy distance, and to continue the correction processing of the next curve until all the curves are processed. The program flow chart is shown in Fig.6.4.

As can be seen from Fig.6.4, the data is sent to the feed motor, while the Δy is being adjusted each time. And after the processing is completed, all motors are confirmed having stopped, then the program ends. The program sends data for one feed speed curve at a time, not every time the speed changes. This reduces the amount of data communication and improves the precise correspondence between position and speed. Since that, if you have to send the next speed data at every time, there will be a certain lagging time. This makes the velocity and position do not correspond well.

The time of sending data each time is about 10-20 ms, which means that the motor will stop for about 20ms after each segment. In order to avoid the pause phenomenon caused by data transmission, this paper sends all the data of that track to the driver before each trajectory movement. Then the pulse trigger method is used to send instructions to the driver. The time of a pulse can be microsecond, which minimizes the pause time of the motor.

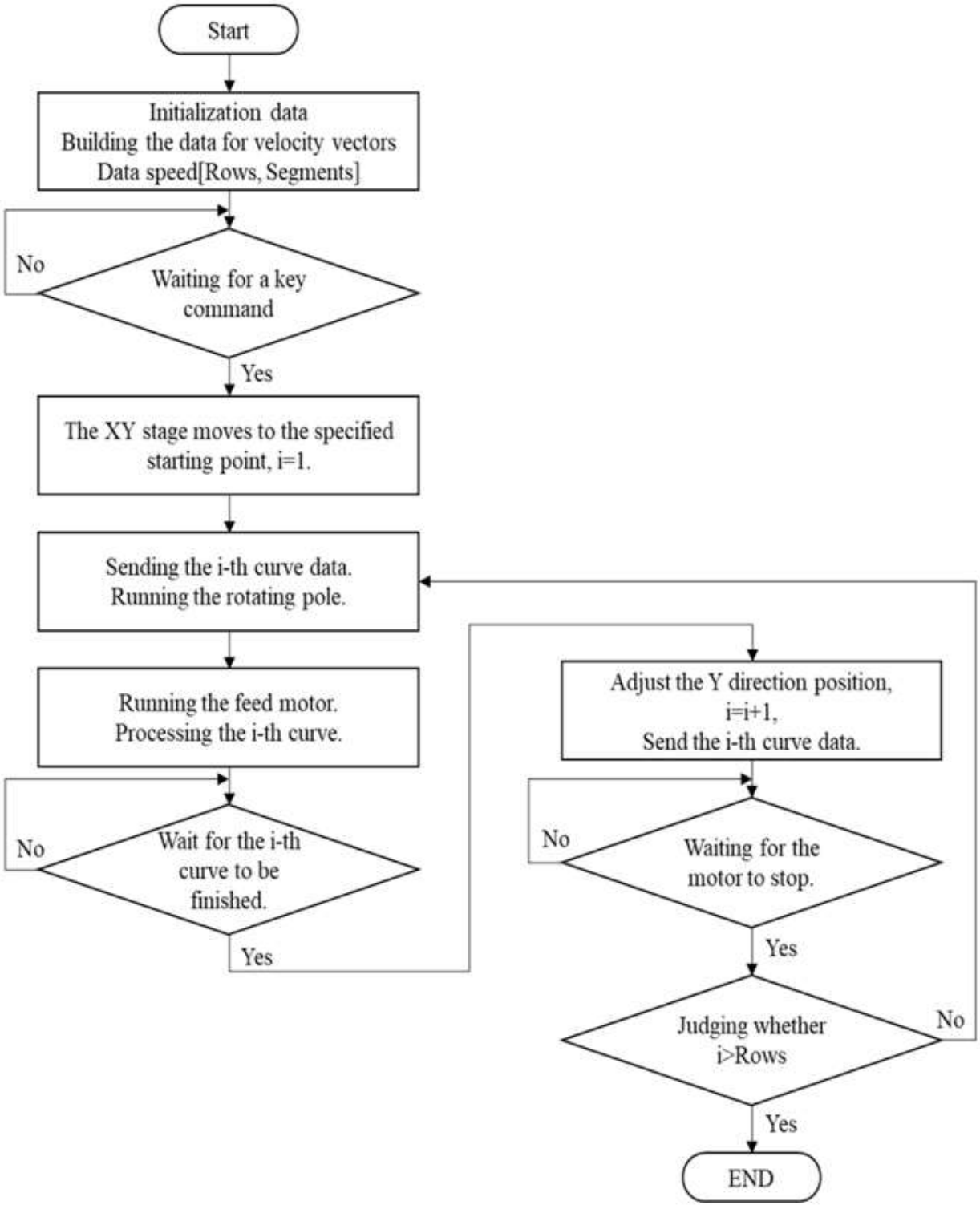

Fig.6. 4 Program block diagram.

6.4 Plane processing experiment

According to previous studies, it is possible to effectively improve the surface morphology of the workpiece and correct the shape of the surface by controlling the feed speed during the finishing process. So can this kind of processing be extended to the plane range? Therefore, we designed the following experiment.

The experimental steps are as follows:

(1) Pre-processing. First process two traces with a magnetic pole with an end face diameter of 3 mm. Fig.6.5 shows a photo of the workpiece after pretreatment. Then the topography of the workpiece is measured along the direction perpendicular to the pretreatment processing. Here a curve is measured every 1mm. The data obtained is used to calculate the speed curve of the correction processing. The processing conditions of the pretreatment are shown in Table 6.1.

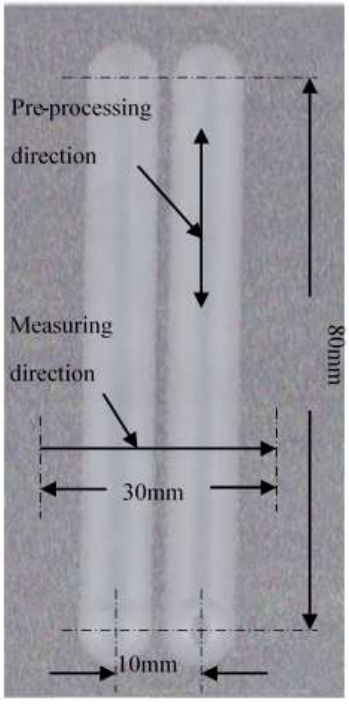

Fig.6. 5 The workpiece after pre-processed

Table 6. 1 Experimental conditions of preparation finishing

Workpiece	A5052 plate (100 mm × 100 mm × 2 mm)
Magnetic pole	Nd-Fe-B rare earth permanent magnet (Φ3×35mm)
Magnetic abrasive	0.5 g of 149 μm iron powder
Abrasion liquid	0.5 mL of oil (Honilo 988) & 1 g of #4000 WA particles
Gap	0.2 mm
Finishing distance	70 mm
Finishing time	20 min
Feed speed	0.5 mm/s
Rotation speed	400 r/min

Figure 6.6 is the measured three-dimensional curved surface with a length of 30mm and a width of 10mm. Fig.6.7 is one of the profile curves.

(2) Calculate the speed curve of each processing track. And program the STM32 controller to realize the processing of the motion trajectory as shown in Fig.6.1. As a comparative experiment, Δy is equal to 0.5mm, 1.0mm, 1.5mm, and 2.0mm for processing.

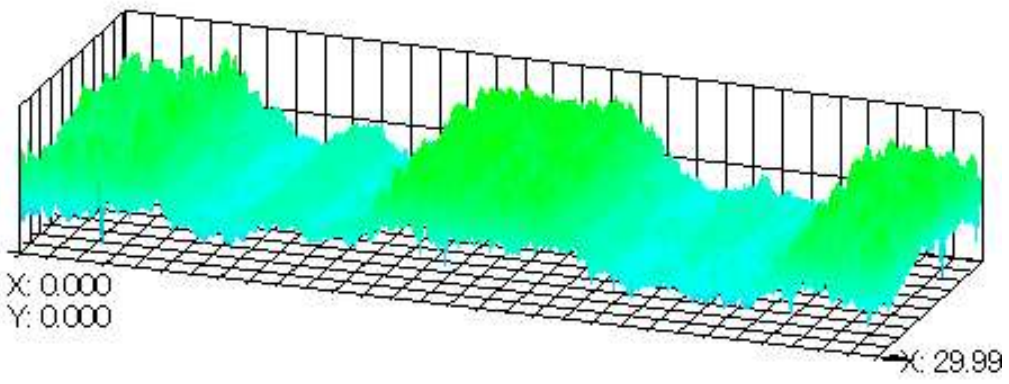

Fig.6. 6 three-dimensional curved surface of processed position

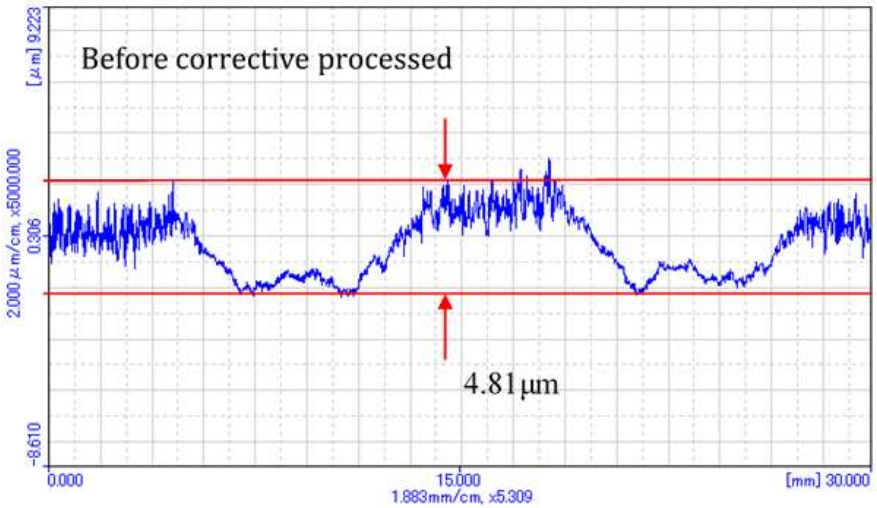

Fig.6. 7 Workpiece surface after pretreatment

(3) Completely process an area of 30mm by 10mm as a stage. When Δy is equal to 2.0mm, 6 tracks need to be processed, when Δy is equal to 1.5mm, 7 tracks need to be processed, when Δy is equal to 1.0mm, 11 tracks need to be processed, and when Δy is equal to 0.5mm, 21 tracks need to be processed Trajectory. Therefore, when Δy is different, the time of a stage is different. After a stage is completed, the surface of the workpiece is measured.

(4) The experimental results are analyzed.

6.5 The results and discussion of the experiments

As shown in the Fig.6.8 is the photo of the processed workpiece. It can be seen from the picture that as the step size of Δy decreases, the surface becomes more uniform. The traces of the transition between the two processing tracks are also reduced. The uniform speed processing also still follows this law. When Δy=0.5, 1.0mm, the difference in appearance is almost not big. But in terms of processing time, the 0.5mm pitch requires longer processing time, so the efficiency is slightly lower.

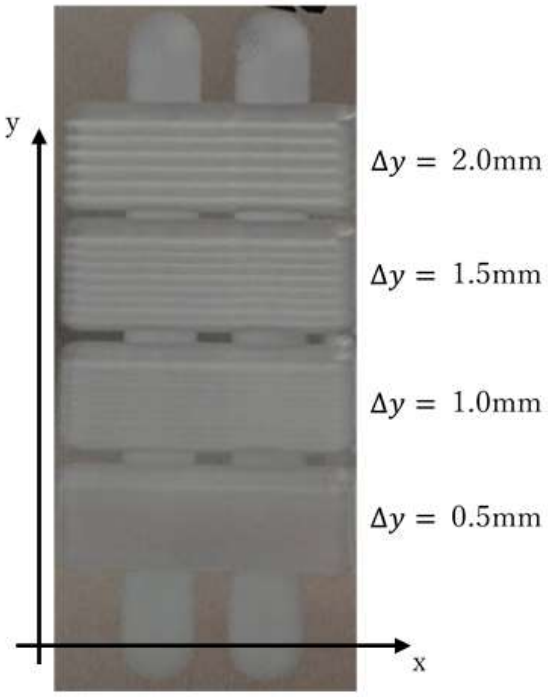

Fig.6. 8 Photograph of the surface of the workpiece after processing

Table 6. 2 Experimental conditions of corrective finishing

Workpiece	A5052 plate (100 mm × 100 mm × 2 mm)
Magnetic pole	Nd-Fe-B rare earth permanent magnet (Φ1×35mm)
Magnetic abrasive	0.5 g of 149 μm iron powder
Abrasion liquid	0.5 mL of oil (Honilo 988) & 1 g of #4000 WA particles
Gap	0.2 mm
Finishing area	30 mm × 10 mm
Feed speed	Speed curve
Rotation speed	400 r/min

Figure 6.9 is a 3D figure of the processed workpiece surface measured by a roughness measuring instrument. The measurement method is to use the roughness to measure a section curve at 0.5mm intervals and draw it into a three-digit image. It can be seen from the figure that when the spacing is 2mm and 1.5mm, there are obvious transition traces. When the

spacing is 1mm and 0.5mm, these traces are not very obvious.

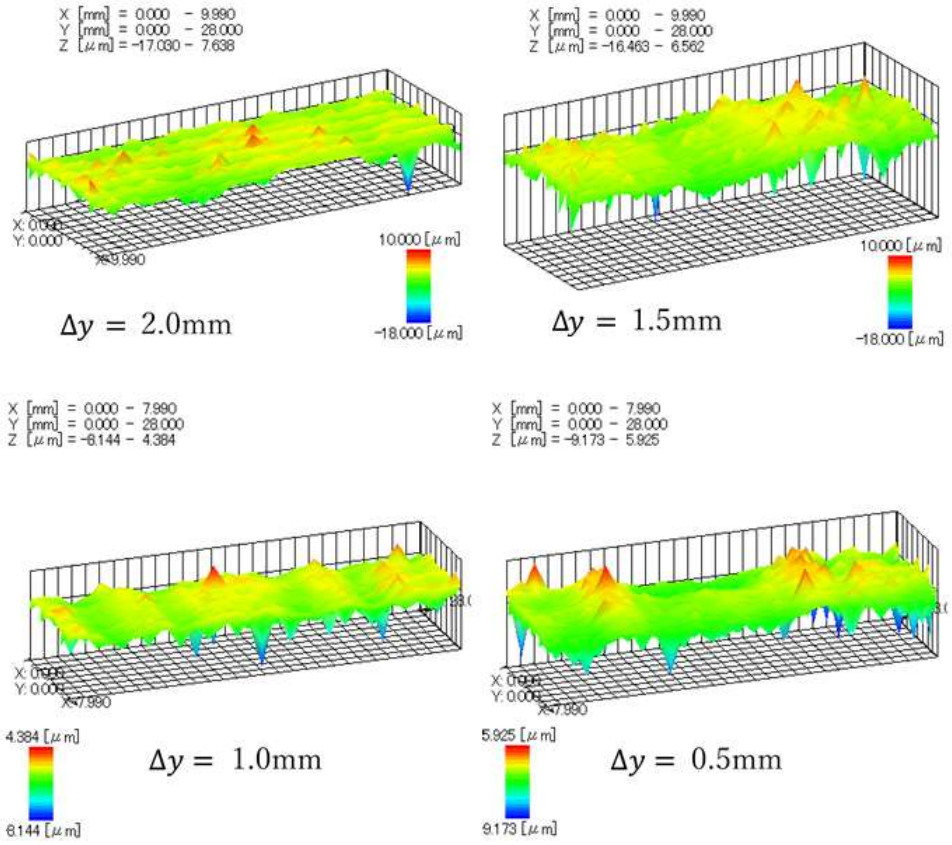

Fig.6. 9 D image of the processed surface before being filtered

In order to be able to see the difference in experimental results more clearly, I measured the cross-sections of the processing area along the X and Y directions. The measurement results are shown in the Fig.6.10 and Fig.6.11.

As shown in Fig.6.10, the x direction is measured along the processing feed direction. It can be seen that the surface has been significantly improved compared with before processing, and the surface of Δy = 1.0mm and 0.5mm is relatively flatness. This is because when Δy is equal to 1.0mm and 0.5mm, the processing time is relatively long, and when Δy is

equal to 1.5mm and 2.0mm, the processing time is relatively short.

The y direction is measured along the translation direction of the trajectory. In this direction, the transition of the processing track during translation can be clearly seen as shown in Fig.6.11. For example, when Δy=2.0 mm, there are 5 obvious transition intervals. When Δy=1.5 mm, there are 6 obvious transition intervals. When Δy=1.0mm and 0.5mm, the transition zone becomes inconspicuous. With the decrease of Δy, the transition is no longer obvious, and the surface is almost flat. This shows that the smaller y is, the better the processing effect is. But when Δy decreases, the time of a processing cycle becomes longer. For example, when Δy = 2.0mm, 6 lines need to be processed. The processing time of each line is about 1min, so a processing cycle is 6 minutes. When Δy = 1.0mm, 11 lines need to be processed, so a processing cycle is 11 minutes. When Δy = 0.5mm, 21 lines need to be processed. The processing time of each line is about 1min, so a processing cycle is 21 minutes.

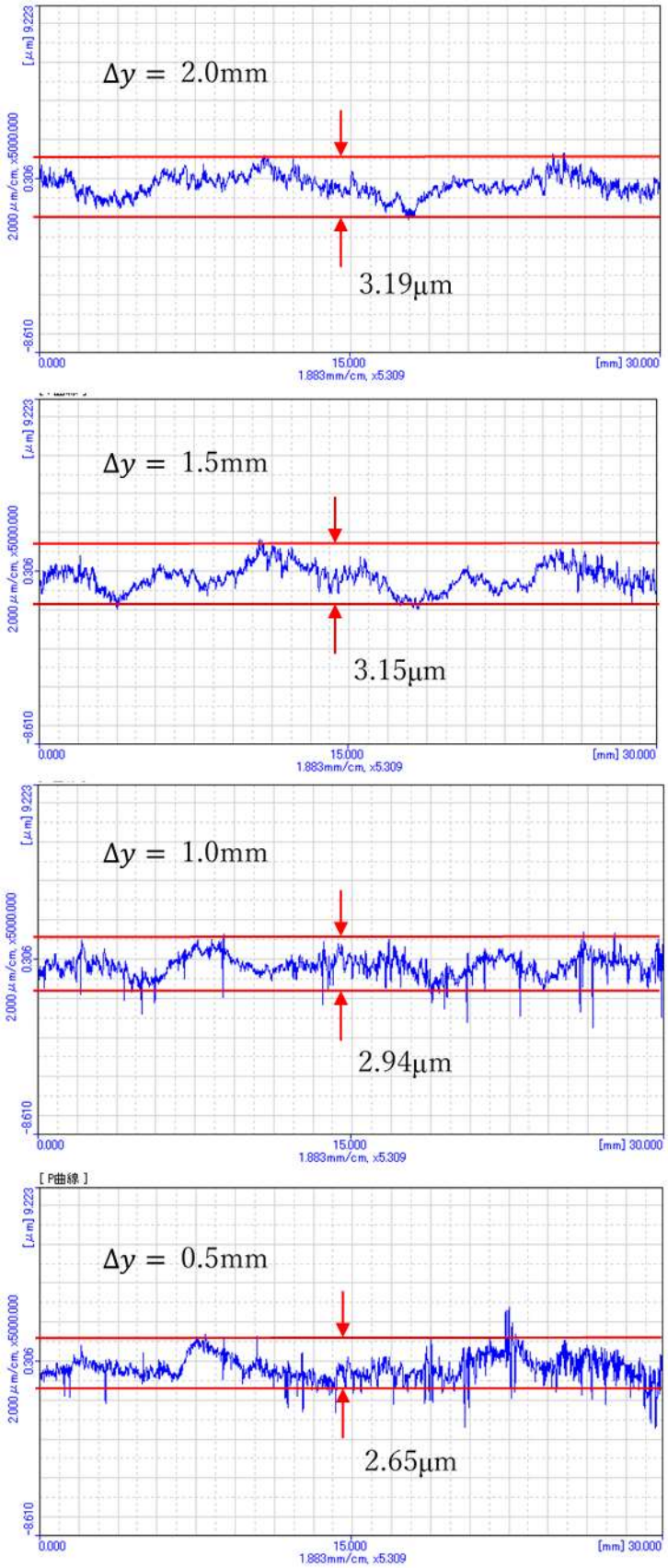

Fig.6. 10 The cross-section curve of the surface along the *x* direction

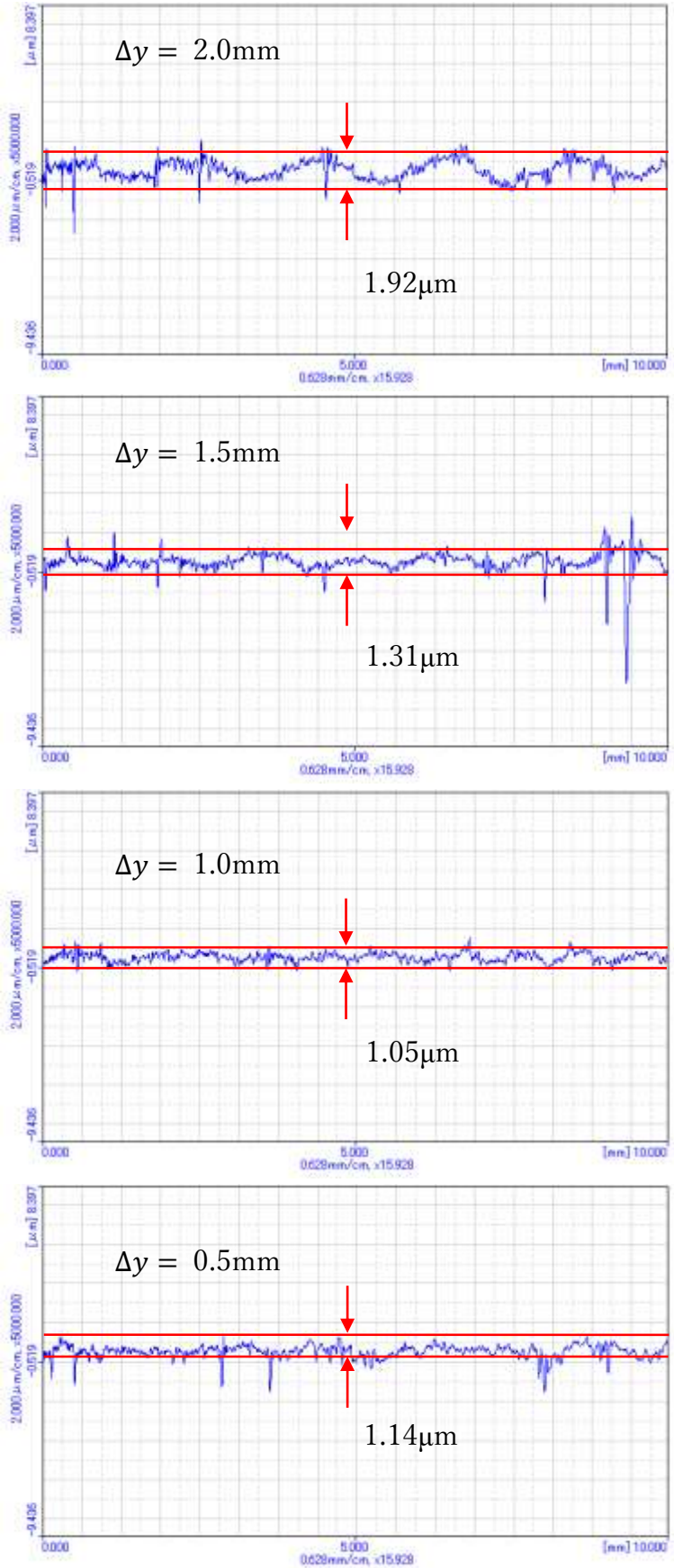

Fig.6. 11 The cross-section curve of the surface along the *y* direction

Figure 6.12 shows the 3D graphics of the workpiece surface after uniform processed at Δy =1.0 mm and 0.5 mm. It can be seen from the figure that in the x direction, the profile of the workpiece does not change much, but there is also no trace of transition in the y direction.

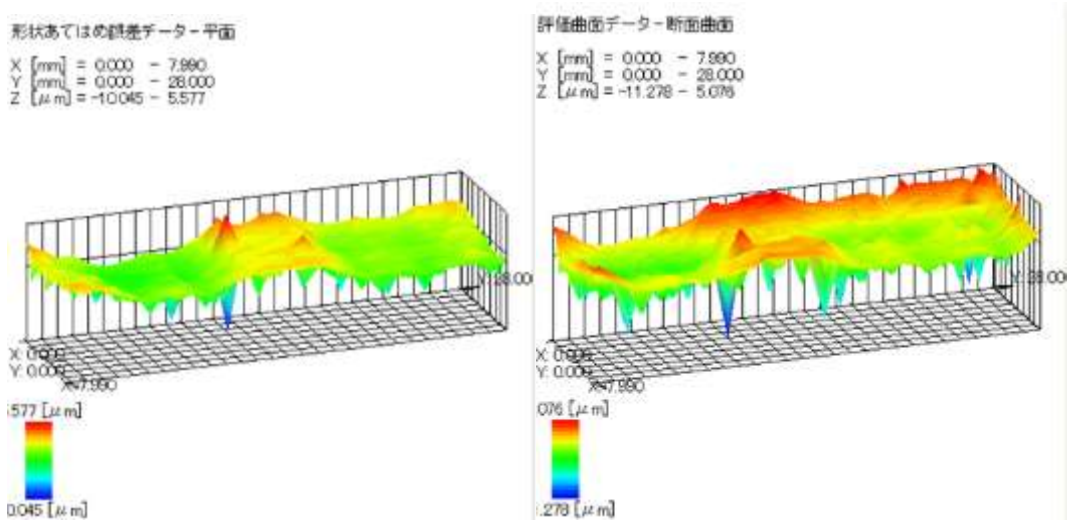

Fig.6. 12 3D image of the processed surface before being filtered

6.6 Conclusions

In this research, a surface modification finishing method is proposed. Summarized as follows:

(1) In this chapter, the feasibility of the speed control method to correct the surface profile of the workpiece is verified.

(2) In the feed direction (direction of x), compared with constant speed finishing, variable speed finishing has obvious effect on surface correction. However, when Δy decreases, the processing time becomes longer, so the correction effect is better.

(3) In variable speed correction finishing, there is a certain correction effect under different Δy conditions, but when Δy is large, it will cause certain damage to the morphology in y direction. When Δy is less than or

equal to 1.0 mm, the damage almost disappears.

(4) When correcting the surface of the workpiece through speed control, the smaller the step of the processing track, the smaller the transition area between the two tracks, but the longer finishing time is required. This experiment proves that the processing effect of 1.0 mm spacing is almost the same as that of 0.5 mm, but the processing time is reduced by half.

(5) Experiments show that the speed control method can be used to correct the surface profile of the workpiece. But its accuracy requires more accurate calculations.

(6) The experimental results show that the extreme difference of the workpiece surface is reduced from 4.8 μm to 2.65 μm.

Chapter VII Conclusions

In order to further solve the problem of processing uniformity, this study proposes a method of the corrective abrasive finishing of workpiece surface using magnetic abrasive finishing process. The process controls the finishing time of different positions at different feed speed according to the initial contour of the surface. Through the analysis and processing of the collected surface profile data, and according to the processing rate characteristics of the magnetic brush, the distribution of the feed speed during the processing is planned, so that the effective processing time at different positions is different, and finally the surface flatness is improved. In this paper, introduced the processing principle of the corrective abrasive finishing. To verify the feasibility of the corrective abrasive finishing method, a comparison between the conventional method and the proposed method was carried out for a finishing path using a 23 mm diameter magnetic pole. In order to improve the correction accuracy, a magnetic pole with a 1mm end face is designed. The magnetic field distribution at the front end of the 1mm magnetic pole and the pressure distribution of the magnetic brush were measured and recorded. The parameters suitable for this process are determined by examining the finishing gap and proportion of abrasive. Moreover, the feasibility of this process to correct a wide range of plane areas is investigated. The influence of the translation step length on the plane quality and processing efficiency is discussed. The main research contents and conclusions of each chapter are as follows.

7.1 Conclusions of each chapter

This thesis discusses the corrective abrasive finishing of workpiece surface using magnetic abrasive finishing process. The conclusions of each

chapter of the paper is as follows:

Chapter 1

In chapter 1, the research background on MAF process are introduced. In addition, the research purpose of this article is explained.

Chapter 2

In chapter 2, first introduced the processing principle of traditional MAF. Secondly, the processing principle of the corrective abrasive finishing is introduced. In addition, the method and steps of data processing are also given out.

Chapter 3

In chapter 3, the experimental setup is described in detail. Firstly, the block diagram of the system is described. The connection mode and control mode of the electrical control part are introduced. Secondly, the mechanical structure is introduced. Finally, the structure of magnetic poles used in this system are introduced.

Chapter 4

In chapter 4, the investigation on correction MAF with 23 mm magnetic pole application of aluminum alloy plate is discussed. By comparing the results of three finishing methods: constant speed finishing, segmentation fixed-point unequal time finishing and segmentation variable speed finishing, the effectiveness of segmentation variable speed finishing method is verified, and the feasibility of correction MAF is proved. However, due to the edge characteristics of the magnetic field distribution of the magnetic pole, the correction effect is obvious at the upper and lower edges of the finishing track. The closer to the middle line of the trajectory, the worse the effect of correction.

Chapter 5

In chapter 5, the investigation on correction MAF with 1 mm magnetic pole application of aluminum alloy plate is discussed. In order to overcome the disadvantage of the marginalization of the magnetic field strength of the large magnetic pole, the magnetic pole is redesigned. Firstly, different magnetic poles are simulated by simulation software. It is concluded that when the end face diameter is reduced, it is conducive to weaken the disadvantage of magnetic field marginalization. Therefore, a magnetic pole with an end face diameter of 1mm is designed. Secondly, using the new magnetic pole, the proportion, quality and different finishing gaps of finishing materials are tested, and the appropriate magnetic brush is selected for subsequent experiments. Thirdly, the routine processing and correction processing experiments of 5052 aluminum alloy plate are carried out, and the experimental results are measured. Finally, the experimental results are analyzed and discussed to prove the feasibility and effectiveness of the correction process.

Chapter 6

In chapter 6, the investigation on correction MAF of plane surface with 1 mm magnetic pole application of aluminum alloy plate is discussed. First design the processing trajectory and program the control circuit board. Then carry out processing experiments according to different moving steps. The influence of the translation step length on the plane quality and processing efficiency is discussed, and the optimal processing method is obtained. The experimental results show that under different Δy conditions, the modified finishing method can correct the workpiece morphology in the x direction (feed direction). However, when the Δy is large, it will leave traces of excessive trajectory in the y direction. When the Δy is reduced to

1mm, there is almost no trace of this excess. But the processing time becomes longer.

Third, compare with the experimental results of conventional processing. The experimental results are analyzed and discussed from different angles. It is proved that this method can correct the workpiece in the plane range.

Chapter 7

In chapter 7, the main conclusions of this thesis are summarized.

7.2 Prospects

Through the research of this subject, it has been proved that magnetic abrasive finishing technology can realize the profile correction of workpiece surface. By controlling the feed speed of the workpiece, the correction finishing of the plane workpiece can be effectively realized. However, this technology still needs to be improved. The processing characteristics of the magnetic brush can be further refined to the processing efficiency of each point on the magnetic brush, the non-uniformity of the magnetic brush can be quantified, and a more accurate model can be established, so as to effectively predict the processing results. Moreover, the real-time monitoring module of workpiece morphology can also be added to effectively monitor the surface changes after finishing and correct the finishing parameters in time. In addition, this research only realizes the correction finishing by controlling the feed speed. In the future research, we can further control the rotation speed and finishing gap of the magnetic pole, and even control multiple parameters at the same time to realize more accurate contour and morphology correction finishing, and also realize the correction finishing of complex surfaces.

References

Chapter 1

[1] Im, I. T.; Mun, S. D.; Oh, S. M.: Micro machining of an STS 304 bar by magnetic abrasive finishing.: Journal of Mechanical Science and Technology. 2009, 23(7), 1982–1988

[2] Sumit, Y.; Chhikara, G.: Modern magnetic abrasive finishing process. International Journal of Enhanced Research in Science Technology & Engineering. 2014, 3(6), 460–462.

[3] Kanish TC, Narayanan S, Kuppan P, Ashok SD (2017) Investigations on the finishing forces in magnetic field assisted abrasive finishing of SS316L. Procedia Eng 174:611–620.

[4] Ganguly V, Schmitz T, Graziano A, Yamaguchi H (2013) Force measurement and analysis for magnetic field–assisted finishing. J Manuf Sci Eng 135(4):041016.

[5] Houshi M N. A comprehensive review on magnetic abrasive finishing process[C]//Advanced Engineering Forum. Trans Tech Publications Ltd, 2016, 18: 1-20.

[6] Kumar H, Singh S, Nanak G, et al. Magnetic abrasive finishing-a review[J]. 2013.

[7] Shinmura T. Study on magnetic-abrasive finishing (1st report)[J]. J. of JSPE, 1986, 52(5): 851.(in Japanese)

[8] Shinmura T.,Takazawa K.,Hatano E.,Aizawa T., 1986, Study on Magnetic Abrasive Finishing(2nd Report) -Finishing Characteristics, J. of JSPE. 52, 10: 1761-1767. (in Japanese)

[9] Shinmura T., Takazawa K., Hatano E., 1986, Study on Magnetic Abrasive Finishing(3rd Report) -Finishing Characteristics of Non-ferromagnetic Substances, J. of JSPE, 53, 9:1440-1446.(in Japanese)

[10] Shinmura T, Takazawa K, Hatano E, et al. Study on magnetic abrasive finishing[J]. CIRP annals, 1990, 39(1): 325-328.

[11] Song J, Shinmura T, Mun S D, et al. Micro-Machining characteristics in high-speed magnetic abrasive finishing for fine ceramic bar[J]. Metals, 2020, 10(4): 464.

[12] Heng L, Kim J S, Tu J F, et al. Fabrication of precision meso-scale diameter ZrO2 ceramic bars using new magnetic pole designs in ultra-precision magnetic abrasive finishing[J]. Ceramics International, 2020, 46(11): 17335-17346.

[13] Yin C, Wang R, Kim J S, et al. Ultra-high-speed magnetic abrasive surface micro-machining of AISI 304 cylindrical bar[J]. Metals, 2019, 9(5): 489.

[14] Shinmura T. Development of plane magnetic-abrasive finishing apparatus and its finishing performance[J]. J. Jpn. Soc. Precis. Eng., 1986, 52(6): 1080.

[15] Shinmura T, Aizawa T. Development of Plane Magnetic Abrasive Finishing Apparatus and its Finishing Performance (2nd Report, Finishing Apparatus Using a Stationary Type Electro-magnet)[J]. Journal of Japan Society of Precision

Engineering, 1988, 54(5): 928-933.

[16] Shinmura T. Study on plane magnetic abrasive finishing (3rd report on the finishing characteristics of non-ferromagnetic substance)[J]. J. Jpn. Soc. Prec. Eng, 1989, 55(7): 1271-1276.

[17] Shinmura, T.; Aizawa, T. Study on magnetic abrasive finishing process-development of plane finishing apparatus using a stationary type electromagnet. Bull Jpn Soc Precis Eng 1989, 23(3):236–239.

[18] Zou Y, Shinmura T. Study on a new plane magnetic abrasive finishing process by application of a constant-pressure magnetic brush[J]. Journal of the Japan Society for Abrasive Technology, 2009, 53(1): 31-34..

[19] Shinmura T, Yamaguchi H. Study on a new internal finishing process by the application of magnetic abrasive machining: internal finishing of stainless steel tube and clean gas bomb[J]. JSME international journal. Ser. C, Dynamics, control, robotics, design and manufacturing, 1995, 38(4): 798-804.

[20] Yamaguchi H, Shinmura T. Study of an internal magnetic abrasive finishing using a pole rotation system: Discussion of the characteristic abrasive behavior. Precision Engineering 2000;24:237–244.

[21] Yamaguchi H, Shinmura T. Internal finishing process for alumina ceramic components by a magnetic field assisted finishing process[J]. Precision Engineering, 2004, 28(2): 135-142.

[22] Yamaguchi, H.; Shinmura, T.; Takenaga, M.: Development of a new precision internal machining process using an alternating magnetic field, Precision Engineering. 2003, 27, 51–58.

[23] Zou Y H, Shinmura T. Study on internal magnetic field assisted finishing process using a magnetic machining jig[C]//Key Engineering Materials. Trans Tech Publications Ltd, 2005, 291: 281-286.

[24] Zou Y H, Shinmura T. A new internal magnetic field assisted machining process using a magnetic machining jig-machining characteristics of inside finishing of a SUS304 stainless steel tube[C]//Advanced Materials Research. Trans Tech Publications Ltd, 2009, 69: 143-147.

[25] Zou Y H, Liu J N, Shinmura T. Study on internal magnetic field assisted finishing process using a magnetic machining jig for thick non-ferromagnetic tube[C]//Advanced Materials Research. Trans Tech Publications Ltd, 2011, 325: 530-535.

[26] Kim J S, Chanchamnan S, Heng L, et al. Development of an Inner Finishing Method for Brass Cone Pipe via a Movable Manual Electromagnet in a Magnetic Abrasive Finishing Process[J]. Metals, 2021, 11(9): 1379.

[27] Yoon S, Tu J F, Lee J H, et al. Effect of the magnetic pole arrangement on the surface roughness of STS 304 by magnetic abrasive machining[J]. International journal of precision engineering and manufacturing, 2014, 15(7): 1275-1281.

[28] Yin C, Heng L, Kim J S, et al. Development of a new ecological magnetic abrasive tool for finishing bio-wire material[J]. Materials, 2019, 12(5): 714.

[29] Kim J S, Heng L, Chanchamnan S, et al. Machining the Surface of Orthopedic Stent Wire Using a Non-Toxic Abrasive Compound in a Magnetic Abrasive

Finishing Process[J]. Applied Sciences, 2021, 11(16): 7267.

[30] Kim J D, Kang Y H, Bae Y H, et al. Development of a magnetic abrasive jet machining system for precision internal polishing of circular tubes[J]. Journal of Materials Processing Technology, 1997, 71(3): 384-393.

[31] Kim J D. Polishing of Ultra-clean Inner Surfaces Using Magnetic Force[J]. International Journal of Advanced Manufacturing Technology, 2003, 21(2).

[32] Shinmura T. Study on Free Form Surface Finishing by Magnetic Abrasive Finishing Process: 1st Report, Fundamental Experiments[J]. JSME international journal: bulletin of the JSME, 1987, 30(267): 1513.

[33] Sathua C S, Jain V K, Ramkumar J, et al. Analysis of forces and surface roughness in magnetic abrasive finishing with a ball-end tool[J]. International Journal of Precision Technology, 2013, 3(2): 131-142.

[34] Jain, V. K.: Magnetic field assisted abrasive based micro-/nanofinishing. Journal of Materials Processing Technology. 2009, 209, 6022–6038.

[35] Jain, V. K.; Kumar, P.; Behera, P. K.; Jayswal, S. C.: Effect of working gap and circumferential speed on the performance of magnetic abrasive finishing process. Wear. 2001, 250, 384–390.

[36] Wu J, Zou Y, Sugiyama H. Study on ultra-precision magnetic abrasive finishing process using low frequency alternating magnetic field[J]. Journal of Magnetism and Magnetic Materials, 2015, 386: 50-59.

[37] Wu, J.; Zou, Y.: Study on mechanism of magnetic abrasive finishing process using low-frequency alternating magnetic field. International Conference on Electromechanical Control Technology and Transportation (ICECTT 2015). 2015, 395, 985–989.

[38] Xie H, Zou Y. Investigation on finishing characteristics of magnetic abrasive finishing process using an alternating magnetic field[J]. Machines, 2020, 8(4): 75.

[39] Xie H, Zou Y. Study on the magnetic abrasive finishing process using alternating magnetic field—discussion on the influence of current waveform variation[J]. The International Journal of Advanced Manufacturing Technology, 2021, 114(7): 2471-2483.

[40] Zou Y, Xing B, Sun X. Study on the magnetic abrasive finishing combined with electrolytic process—Investigation of machining mechanism[J]. The International Journal of Advanced Manufacturing Technology, 2020, 108(5): 1675-1689.

[41] Sun X, Zou Y. Development of magnetic abrasive finishing combined with electrolytic process for finishing SUS304 stainless steel plane[J]. The International Journal of Advanced Manufacturing Technology, 2017, 92(9): 3373-3384.

[42] Xing B, Zou Y. Study on the magnetic abrasive finishing combined with electrolytic process Investigation on Processing Stability[C]//Proceedings of JSPE Semestrial Meeting 2020 JSPE Autumn Conference. The Japan Society for Precision Engineering, 2020: 168-169.

[43] Xu J, Zou Y. Development of a new magnetic abrasive finishing process with renewable abrasive particles using the circulatory system[J]. Precision Engineering, 2021, 72: 417-425.

[44] Xu J, Zou Y, Xie H. Investigation on the Finishing Characteristics of a Magnetic Abrasive Finishing Process with Magnetic Abrasive Slurry Circulation System[J]. Machines, 2021, 9(9): 195.

[45] Zou Y, Satou R, Yamazaki O, et al. Development of a New Finishing Process Combining a Fixed Abrasive Polishing with Magnetic Abrasive Finishing Process[J]. Machines, 2021, 9(4): 81.

[46] Jain V K, Jayswal S C, Dixit P M. Modeling and simulation of surface roughness in magnetic abrasive finishing using non-uniform surface profiles[J]. Materials and manufacturing processes, 2007, 22(2): 256-270.

[47] Madhab G B, Jain V K, Dixit P M. On simulation of magnetic abrasive finishing process for plane surfaces using FEM[J]. International Journal of Machining and Machinability of Materials, 2006, 1(2): 133-165.

[48] Kim J D, Choi M S. Simulation for the prediction of surface-accuracy in magnetic abrasive machining[J]. Journal of materials processing technology, 1995, 53(3-4): 630-642.

[49] Zou Y H, Jiao A Y, Aizawa T. Study on plane magnetic abrasive finishing process-experimental and theoretical analysis on polishing trajectory[C]. Advanced materials research. Trans Tech Publications Ltd, 2010, 126: 1023-1028.

[50] Jiao A Y, Quan H J, Li Z Z, et al. Study on improving the trajectory to elevate the surface quality of plane magnetic abrasive finishing[J]. The international journal of advanced manufacturing technology, 2015, 80(9): 1613-1623.

[51] Zou Y, Xie H, Zhang Y. Study on surface quality improvement of the plane magnetic abrasive finishing process[J]. The International Journal of Advanced Manufacturing Technology, 2020, 109(7): 1825-1839.

[52] Jain N K, Jain V K, Jha S. Parametric optimization of advanced fine-finishing processes[J]. The International Journal of Advanced Manufacturing Technology, 2007, 34(11): 1191-1213.

[53] Xie H, Zou Y, Dong C, et al. Study on the magnetic abrasive finishing process using alternating magnetic field: investigation of mechanism and applied to aluminum alloy plate[J]. The International Journal of Advanced Manufacturing Technology, 2019, 102(5): 1509-1520.

[54] Gupta, Bhavesh, et al. "Effects of process parameters on the surface finish of flat surfaces in magnetic assist abrasive finishing process." Materials Today: Proceedings 5.9 (2018): 17725-17729.

[55] Mulik, Rahul S., and Pulak M. Pandey. "Ultrasonic assisted magnetic abrasive finishing of hardened AISI 52100 steel using unbonded SiC abrasives." International Journal of Refractory Metals and Hard Materials 29.1 (2011): 68-77.

[56] Preston F W. The theory and design of plate glass polishing machines[J]. Journal of Glass Technology, 1927, 11(44): 214-256.

[57] Zou Y H, Jiao A Y, Aizawa T. Study on plane magnetic abrasive finishing process-experimental and theoretical analysis on polishing trajectory[C]//Advanced materials research. Trans Tech Publications Ltd, 2010, 126: 1023-1028.

[58] Zou Y, Xie H, Dong C, et al. Study on complex micro surface finishing of alumina ceramic by the magnetic abrasive finishing process using alternating magnetic

field[J]. The International Journal of Advanced Manufacturing Technology, 2018, 97(5): 2193-2202.

[59] Bagehorn S, Wehr J, Maier HJ. Application of mechanical surface finishing processes for roughness reduction and fatigue improvement of additively manufactured Ti-6Al-4V parts. Int J Fatigue 2017;102:135–142.

[60] Shinmura T, Takazawa K, Hatano E, Aizawa T. Study on magnetic-abrasive finishing (2nd Report) Finishing characteristics. J Jpn Soc PrecEng 1986;52(10):1761–1767 (in Japanese).

[61] Yin SH, Shinmura T. Vertical vibration-assisted magnetic abrasive finishing and deburring for magnesium alloy. Int J Mach Tool Manuf 2004;44:1297–1303.

[62] Yin SH, Shinmura T. A comparative study: polishing characteristics and its mechanisms of three vibration modes in vibration-assisted magnetic abrasive polishing. Int J Mach Tool Manuf 2004;44:383–390.

[63] Mulik RS, Pandey PM. Experimental investigations and optimization of ultrasonic assisted magnetic abrasive finishing process. Proceedings of the Institution of Mechanical Engineers, Part B: Journal of Engineering Manufacture 2011;225(8):1347–1362.

[64] Misra A, Pandey PM, Dixit US. Modeling of material removal in ultrasonic assisted magnetic abrasive finishing process. International Journal of Mechanical Sciences 2017;131:853–867.

[65] Xing B, Zou Y. Investigation of finishing aluminum alloy A5052 using the magnetic abrasive finishing combined with electrolytic process[J]. Machines, 2020, 8(4): 78.

[66] Patil, M.G.; Chandra, K.; Misra, P.S. Magnetic abrasive finishing–A Review. Advanced Materials Research. Trans Tech Publications Ltd 2012, 418: 1577-1581.

[67] Qian, C.; Fan, Z.; Tian, Y.; et al. A review on magnetic abrasive finishing. The International Journal of Advanced Manufacturing Technology 2020, 112(3): 619-634

[68] Zou Y. A new internal magnetic deburring process using a magnetic machining jig-Precise deburring of a drilled hole on the inside of a SUS304 stainless steel tube[J]. J. Jpn. Soc. Abras. Technol., 2007, 51(12): 696.

[69] Qu S, Wang Z, Zhang C, et al. Material removal profile prediction and experimental validation for obliquely axial ultrasonic vibration-assisted polishing of K9 optical glass[J]. Ceramics International, 2021, 47(23): 33106-33119.

[70] Wu J, Zou Y, Sugiyama H. Study on finishing characteristics of magnetic abrasive finishing process using low-frequency alternating magnetic field[J]. The International Journal of Advanced Manufacturing Technology, 2016, 85(1): 585-594.

[71] Lin C T, Yang L D, Chow H M. Study of magnetic abrasive finishing in free-form surface operations using the Taguchi method[J]. The International Journal of Advanced Manufacturing Technology, 2007, 34(1): 122-130.

[72] Zhang M D, Lv M, Chen H L. Theoretical research on polishing free-form surface with magnetic abrasive finishing[C]//Key engineering materials. Trans Tech

Publications Ltd, 2009, 392: 404-408.

[73] Maksarov V V, Keksin A I. Technology of magnetic-abrasive finishing of geometrically-complex products[C]//IOP Conference Series: Materials Science and Engineering. IOP Publishing, 2018, 327(4): 042068.

[74] Oh J H, Lee S H. Prediction of surface roughness in magnetic abrasive finishing using acoustic emission and force sensor data fusion[J]. Proceedings of the Institution of Mechanical Engineers, Part B: Journal of Engineering Manufacture, 2011, 225(6): 853-865.

[75] Zhang, Y.L.; Zou, Y.H. Study of corrective abrasive finishing for plane surfaces using magnetic abrasive finishing processes. Nanotechnology and Precision Engineering 2021, 4(3): 033001.

[76] Kim, D.W.; Kim S.W. Static tool influence function for fabrication simulation of hexagonal mirror segments for extremely large telescopes, Opt Express 2005, 13(3): 910-917.

[77] Michaeli, W.; Heßner, S.; Klaiber, F.; Forster, J. Geometrical accuracy and optical performance of injection moulded and injection-compression moulded plastic parts. CIRP annals 2007, 56(1): 545-548.

Acknowledgement

I am grateful to those who have offered me encouragement and support over the past several years. It would be impossible to accomplish this work without the kindhearted help and full-hearted support of many people.

First and foremost, I express my deepest gratitude to my advisor, Associate Professor Yanhua Zou, for her consistent and illuminating instruction. Through countless discussions and daily work with her, I have not only learned a lot about the magnetic abrasive finishing process but also her rigorous attitude towards scientific research will provide guidance for the rest of my life and future research work.

I would like to express my heartfelt gratitude to Professor Katsutoshi Yoshida, Professor Ryunosuke Sato, Associate Professor Yoshimasa Takayama and Professor Koichi Ozaki for their willingness to serve as members of my thesis defense committee.

I would like to express my sincere gratitude to Professor Yukitoshi Otani, Associate Professor Takahiro Yajima, whose courses have expanded my knowledge.

The gratitude is also extended to some supports from Creative Department for Innovation (CDI) of Utsunomiya University and mechanical processing factories of Utsunomiya University for this research.

Last but not least, I want to express my special gratitude to my wife (Ms. Li Xu) and family for their loving considerations and great confidence in me all through these years. I also owe my sincere gratitude to my friends and my fellow classmates who gave me their help and time in listening to me and helping me work out my problems during the difficult course of the thesis.

Contributed papers related to this study

Articles

1. Zhang Y, Zou Y, Xie H. Study on Plan Magnetic Abrasive Finishing-Discussion on Processing Methods for Improving Flatness. Materials Science Forum. 2021, 1018: 123-128.
2. Zhang Y, Zou Y. Study of corrective abrasive finishing for plane surfaces using magnetic abrasive finishing processes. Nanotechnology and Precision Engineering, 2021, 4(3): 033001.
3. Zhang Y, Zou Y. Study on Corrective Abrasive Finishing for Workpiece Surface by Using Magnetic Abrasive Finishing Processes. Machines. 2022; 10(2):98.

Domestic conference

1. 張 玉龍, 鄒 艶華, 平面磁気研磨法の平面品質を改善に関する研究, 2020 年度精密工学会秋季大会学術講演会, 8 月, 2020.
2. 張 玉龍, 鄒 艶華, 磁気研磨法による工作物表面の修正研磨に関する研究, 2021 年度砥粒加工学会学術講演会, 9 月, 2021.

Appendix A: ABBREVIATIONS

AFF	Abrasive flow finishing
AFM	Abrasive flow machining
AVG	Average
CBN	Cubic boron nitride
CMP	Chemical mechanical polishing
CNTs	Carbon nanotubes
DAC	Digital to analog converter
ECP	Electrolytic and chemical polishing
EMM	Elastic emission machining
EMAF	Electrolytic magnetic abrasive finishing
FMAB	Flexible magnetic abrasive brush
MAF	Magnetic abrasive finishing
MAAF	Magnetic abrasive flow finishing
MAPs	Magnetic abrasive powders/particles
MDIF	Magnetically driven internal finishing
MFAF	Magnetic field-assisted finishing
MFP	abrasive flow polishing
MR	Material removal
MRAFF	Magnetorheological abrasive flow finishing
MRAH	Magnetorheological abrasive honing
MRF	Magnetorheological finishing
MRFF	Magnetorheological flow finishing
MRJF	Magnetorheological jet finishing
MRR	Material removal rate
USART	Universal asynchronous receiver transmitter

Appendix B: LIST OF FIGURES

签。

Appendix C: LIST OF TABLES